10/10/15/91 gm (1)

9/17/91

CONTRACTOR REPORT

SAND91—7007
Unlimited Release
UC—237

Design of the Support Structure, Drive Pedestal, and Controls for a Solar Concentrator

Vernon R. Goldberg
John L. Ford
Arnold E. Anderson
WG Associates
6607 Stonebrook Circle
Dallas, TX 75240

Prepared by Sandia National Laboratories Albuquerque, New Mexico 87185
and Livermore, California 94550 for the United States Department of Energy
under Contract DE-AC04-76DP00789

Printed August 1991

Issued by Sandia National Laboratories, operated for the United States Department of Energy by Sandia Corporation.

Available to DOE and DOE contractors from
Office of Scientific and Technical Information
PO Box 62
Oak Ridge, TN 37831

Prices available from (615) 576-8401, FTS 626-8401

Available to the public from
National Technical Information Service
US Department of Commerce
5285 Port Royal Rd
Springfield, VA 22161

NTIS price codes
Printed copy: A06
Microfiche copy: A01

SAND--91-7007

DE92 000604

SAND91-7007
Unlimited Release
Printed August 1991

DESIGN OF THE SUPPORT STRUCTURE, DRIVE PEDESTAL AND CONTROLS FOR A SOLAR CONCENTRATOR

Vernon R. Goldberg
John L. Ford
Arnold E. Anderson

WG Associates
Dallas, Texas

Sandia Contract 42-9815

ABSTRACT

The glass/metal McDonnell-Douglas dish is the state-of-the-art of parabolic dish concentrators. Because of the perceived high production cost of this concentrator, the Department of Energy's Solar Thermal Program is developing stretched-membrane technology for large (75 kWt) solar concentrators for integration with receivers and engines in 25 kWe dish-Stirling systems. The objective of this development effort is to reduce the cost of the concentrator while maintaining the high levels of performance characteristic of glass/metal dishes. Under contract to Sandia National Laboratories, Science Applications International Corporation, Solar Kinetics Inc. and WG Associates are developing a faceted stretched-membrane dish concentrator based on successful stretched-membrane heliostat technology. This design will result in a low-risk, near-term concentrator for dish-Stirling systems.

WG Associates has designed the support structure, drives and tracking controls for this dish. The structure is configured to support 12 stretched-membrane, 3.5-meter diameter facets in a shaped dish configuration. The dish design is sized to power a dish-Stirling system capable of producing 25 kW (electric).

In the design of the structure, trade-off studies were conducted to determine the "best" facet arrangement, dish contour, dish focal length, tracking control and walk-off protection. As part of the design, in-depth analyses were performed to evaluate pointing accuracy, compliance with AISC steel design codes, and the economics of fabrication and installation. Detailed fabrication and installation drawings were produced, and initial production cost estimates for the dish were developed. These issues, and the final dish design, are presented in this report.

CONTENTS

LIST OF FIGURES

LIST OF TABLES

1.0 INTRODUCTION

This report documents the trade-off studies, analysis, and design of the support structure, drive pedestal, and control system for a faceted, stretched-membrane solar concentrator. The configuration is similar to a conventional point focus system with a 10-to-11 meter diameter parabolic reflector except that the continuous parabolic reflector is replaced with 12 facets. The 12 facets are stretched membranes with an active surface diameter of 3.5 meters each. When attached to the structure, the facets can be aimed so that 12 sun images are at the same focal point. The dish is designed to provide about 75 kWt of thermal power to a receiver-Stirling engine-generator located at the focal point of the dish. The electrical output of the dish-Stirling system is about 25 kWe. The faceted dish-Stirling system is illustrated by the artist concept shown in Figure 1.0-1.

This report covers the design of the prototype support structure and drive pedestal illustrated in the figure, and the system to control collector pointing.

The project objectives included designing a prototype concentrator that would meet all of the requirements of the Statement of Work (SOW) while reducing fabrication and installation costs below those of the glass-metal dish. Where choices were made between added cost to insure performance and economy with the potential of compromising performance, priority was placed on meeting performance objectives without "gold plating" the design. Thus, the design objectives have been approached conservatively. If the prototype proves to have performance in excess of the requirements, economies readily can be achieved for future models. Similarly, with large-volume production, design adjustments, and production tooling, changes can be made to yield significant per unit cost savings. This report includes production cost estimates based on the current conservative prototype design.

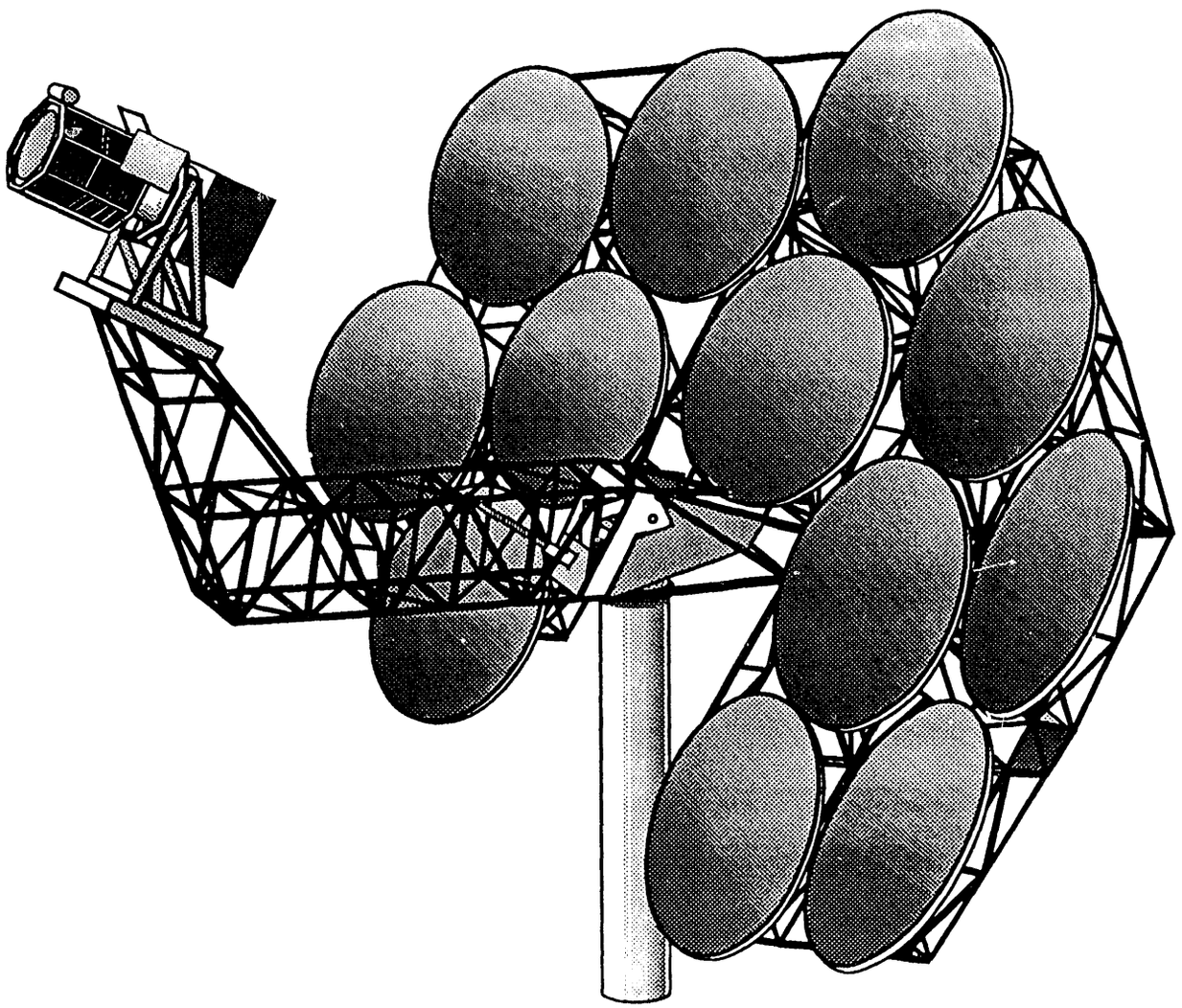

Figure 1.0-1 Faceted Stretched-Membrane Dish Concentrator

1.1 Summary of Dish Design Requirements

The requirements that the facet support structure (FSS) and drive pedestal must meet are defined in the SOW for Contract No. 42-9815 and subsequently modified by program management directive. They are categorized for ease of reference and summarized below.

1.1.1 Configuration Requirements

- Axis Configuration - Elevation over azimuth
- Number of Facets - 12
- Diameter of Facets - 3.5 m (11.5 ft.)
- Facet Mounting - 3 points, approximately equally spaced
- Receiver/Engine/Generator Weight - 1500 lb.
- Dish f/D, nominal - 0.6
- Control System - 2-axis ephemeris tracker using off-the-shelf components

1.1.2 Environmental Requirements

Operating

- Temperature: -30 deg. to +50 deg.C (-22 deg. to +122 deg.F)
- Humidity: 0 to 100% RH
- Wind: 27 mph (including gusts) - full performance
  35 mph (including gusts) - degraded performance

Survival

- Temperature: -30 deg. to +50 deg.C (-22 deg. to +122 deg.F)
- Humidity: 0 to 100% RH
- Wind: 50 mph (including gusts) - dish at any attitude
  90 mph (including gusts) - dish at stow position
- Seismic: Per Unified Building Code, Zone "Z"
- Snow and Ice: 10 psf on upward-facing surfaces, stow position (not concurrent with 90 mph wind)

1.1.3 Performance Requirements

- Structural Deflection: 1.0 mr, one sigma, relative to receiver
- Tracking System Error: 0.6 mr, one sigma
- Sky Coverage: Zenith to both horizons anywhere in Continental U.S. and Hawaii

1.1.4 Miscellaneous

The design must provide for:

- ground-level access to receiver/engine, and
- protection of structure from beam walk-off due to loss of power.

1.2 Project Results

The result of this project is a complete set of fabrication and assembly drawings for the faceted dish, including pedestal, drives, FSS, controls, etc. These drawings have been reviewed by potential vendors; prototype pricing has been developed and is included in this report. The faceted collector support structure and pointing controls built to these drawings will meet or exceed the requirements stated in Section 1.1 without significant risk and without excessive cost. There is a high probability that further economies can be achieved through design modifications after the prototype has been fabricated and fully evaluated.

1.3 Report Organization

Trade-off studies conducted early in the program and their results are described in Section 2 of this report. The design of the FSS, the azimuth and elevation drives, and the pedestal are described in Section 3. Also in Section 3 the structural analysis is discussed, and its results are summarized. Section 4 contains the control system description. In Section 5 the pointing error budget for the dish is re-developed. In Section 6 production cost methodology is presented, and costs are developed for several levels of production effort. A summary of the project is contained in Section 7. Section 8 is a glossary of terms used in this report. Finally, Appendix A contains the details of the structural analysis.

2.0 DESIGN TRADE-OFFS

Before design of the faceted dish could start, it was necessary to resolve a number of open issues. These issues were related to the integration of the facets and the configuration of the FSS. Tasks were assigned by project management to evaluate various concepts of facet arrangement, support structure contour and collector focal length. Other study tasks involved collector operational considerations such as windmilling and solar walk-off protection. In each of these studies the impacts of various design options on system performance, design risk and cost were evaluated.

Descriptions of these trade-off studies and the results are presented in this section.

2.1 Facet Arrangement

Several geometric arrangements of the 12 stretched-membrane facets were considered in developing an efficient FSS design. All arrangements had similar performance levels; the two most viable options were selected for evaluation based on apparent simplicity and practicality of fabrication. These two candidate configurations, designated 4INLINE and 2TOP respectively, are shown in Figure 2.1-1. Both arrangements were analyzed and compared for structural weight, wind load effects on a drive system, facet interface requirements, power conversion assembly (PCA) support structure interface, and ease of fabrication.

A graphic design was made of each of the configurations using comparable outline geometry and nominal assembly focal lengths. The structural elements - vertical trusses, horizontal trusses, diagonal beams, etc. - were defined and positioned to provide appropriate mounting facilities and load paths for the facet mounting. The weights and center of gravity (CG) of all of the elements were determined, and a composite support structure CG was calculated. This data was the basis for comparison of the two arrangements.

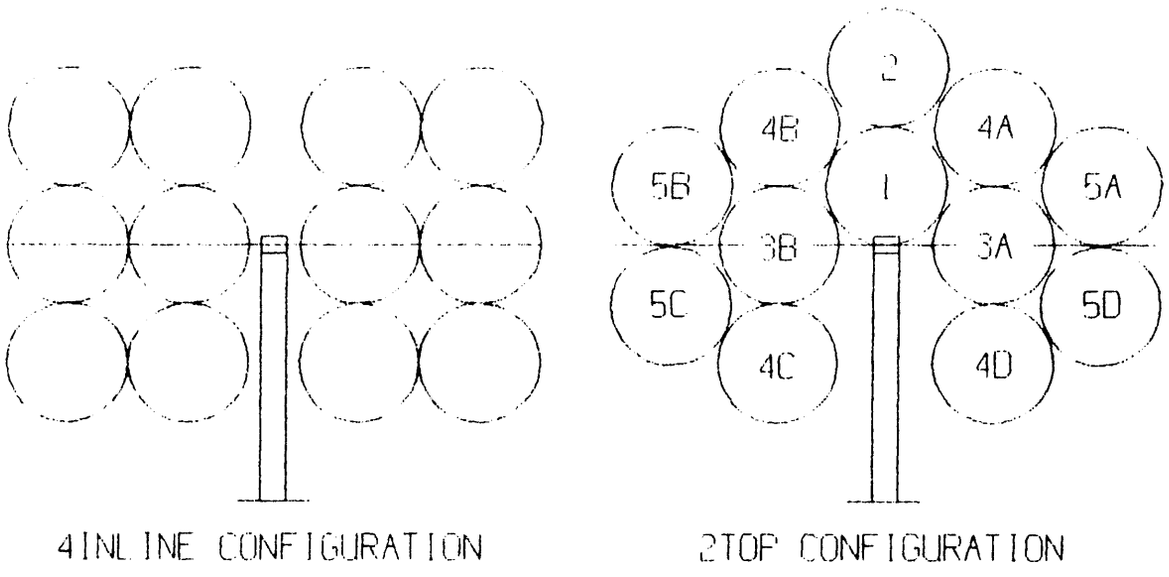

Figure 2.1-1 Alternate Facet Arrangement

The 2TOP configuration was found to be lighter than the 4INLINE, primarily because it has a shorter total length of all trusses. The difference, however, is so slight that this effect alone is considered of no consequence to the design.

Geometry considerations disclose wind load and inertia differences. The horizontal chord length of the 2TOP is about 5% greater than that of the 4INLINE, due primarily to the larger "gap" at the drive interface. On the other hand, the 4INLINE arrrangement, with 3 facets at the extreme radius versus 2 for the 2TOP, has a greater area and weight concentration at the maximum moment arm. The chord length and area distribution differences tend to cancel each other relative to wind-caused yaw effects. But the attendant weight concentration at the extremities of the 4INLINE result in it having a somewhat higher mass moment of inertia. Therefore, the 4INLINE requires sightly more azimuth drive power.

The vertical height of the 2TOP is about 14% greater than the 4INLINE. But again, the area distribution tends to reduce the difference between the two designs. Nevertheless, the 2TOP wind-induced overturning moments are somewhat greater than the 4INLINE. Therefore, the 2TOP requires slightly greater azimuth bearing capacity and elevation drive power than the 4INLINE configuration.

To evaluate the interface of the PCA Support Structure, including the transition, it was assumed that the horizontal chord of the 4INLINE would be held to a minimum to reduce wind and inertia effects. Since, in this arrangement, no facets are on the vertical centerline, the gap, or clearance, about the drive and pedestal is limited only by the diameters of those elements and/or the width of the transition. In the 2TOP arrangement the gap is dictated by the mounting provisions for the centerline facets. The relatively large, unused lateral space in the gap area of the 2TOP allows abundant room for diagonal bracing of the transition structure. This space does not exist on the 4IN-LINE. Therefore, the 2TOP arrangement results in a significantly stiffer assembly.

With regard to economy of fabrication, the 4INLINE structure is symmetrical about both the X and Y axes. The 2TOP is symmetric only about the Y axis. Thus, it is reasonable to conclude that the 4INLINE, with fewer different parts, has a potential cost advantage.

Other less important factors were considered such as shear loads, axial loads, facet mounting facilities, factory/field assembly, and alignment. But in each of these, the differences between the two configurations were too slight to have impact.

In consideration of the above, the 2TOP arrangement was selected for the faceted dish design because its interface assembly is stiffer. As a result, the 2TOP configuration has a higher system resonant frequency, better tracking accuracy and, ultimately, better system performance than the 4INLINE configuration.

2.2 Parabolic vs. Spherical Facet Support Contour

Optical studies conducted by Sandia showed that the contour of a facet array support structure has little impact on concentrator optical/thermal performance. However, at the outset of this contract, it had not been fully determined that readily adjustable stretched membrane facets were practical with focal length to diameter (f/D) ratios in the range of 2.2 to 3.0. It was not clear that elastically-formed membranes could be made at all in this range. On the other hand, plastically-formed membranes, which can be made in this f/D range, may not be readily adjustable. Since facets of both forming methods were being considered for the dish, it was desirable to devise a single structural contour with an f/D that could accommodate both facet designs.

Three basic structural configurations were considered initially: flat, spherical and parabolic. It was immediately obvious that a flat structure would require facets with a larger f/D range than either the parabolic or spherical contour structure. Since there was no significant optical, structural or economic advantage to a flat structure, it was eliminated from further consideration.

A comparison was made between a spherically-contoured structure and one that is parabolically contoured. Two dish focal lengths were investigated for each contour. For the first, the focal length of the outermost facet was set to 25 ft.; and, for the second, the length was set to 34.5 ft. Only a single facet diameter of 11.5 ft. was considered.

Both contours were shown to have problems. In the spherical arrangement, the vertex of each facet is on a spherical surface; and all facets have the same focal length. However, as illustrated by Figure 2.2-1, the difference between adjacent facet edges in the line-of-sight (Z axis) direction ("Z offset") is about 29 in. for a facet No. 5 focal length of 34.5 ft. The Z offset for a No. 5 focal length of 25 ft. is about 3.5 ft. An offset this large increases the complexity of the facet mounting pads and could compromise the integrity of the

structure design. The excessive length of the "standoffs" add weight and cost to the design, and can also contribute significantly to the overall structural deflection error.

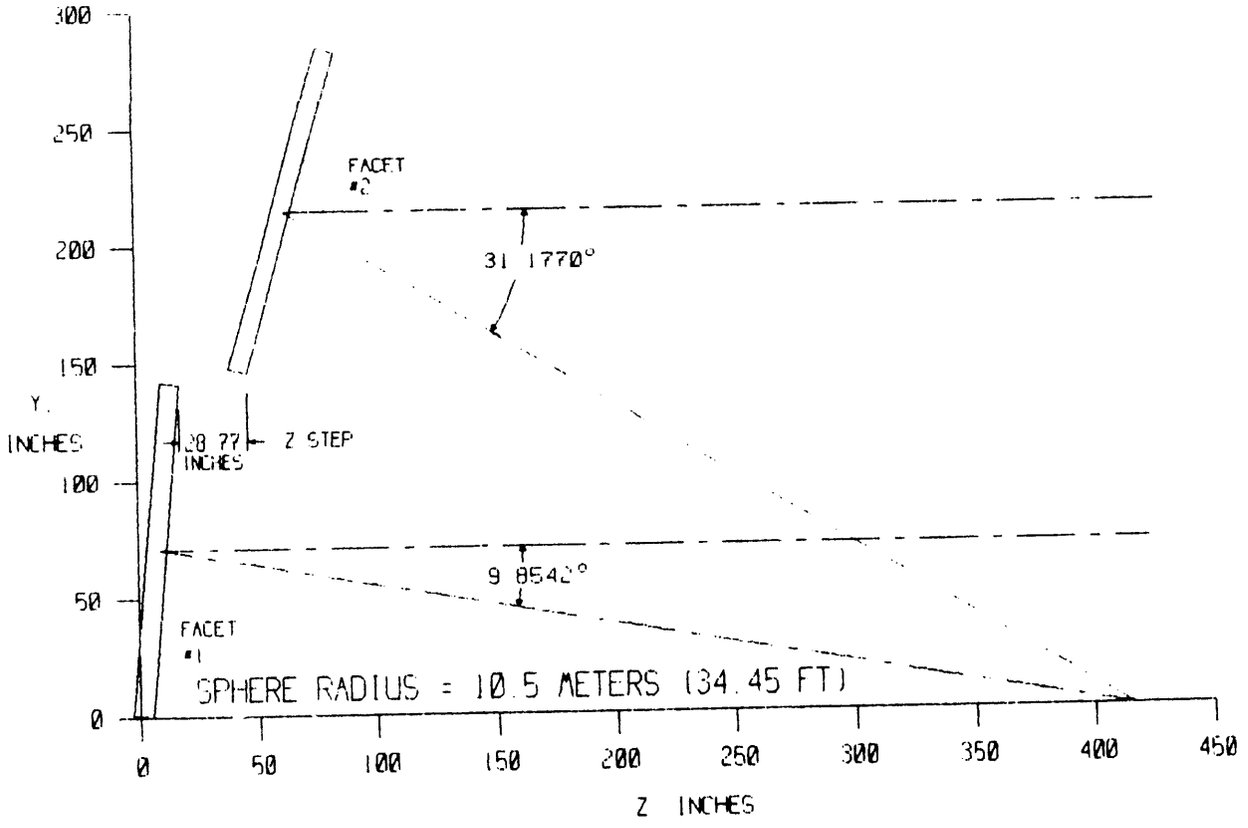

Figure 2.2-1 Facets on a Spherical Contour

With a parabolic contour, the facet Z offsets are considerably reduced for the case where the No. 5 focal length is 34.4 ft.; i.e., they are essentially planar as shown in Figure 2.2-2. Thus they require little or no intermediate structure for attachment to the backup structure. However, the focal lengths of the facets around a system centerline of symmetry vary significantly.

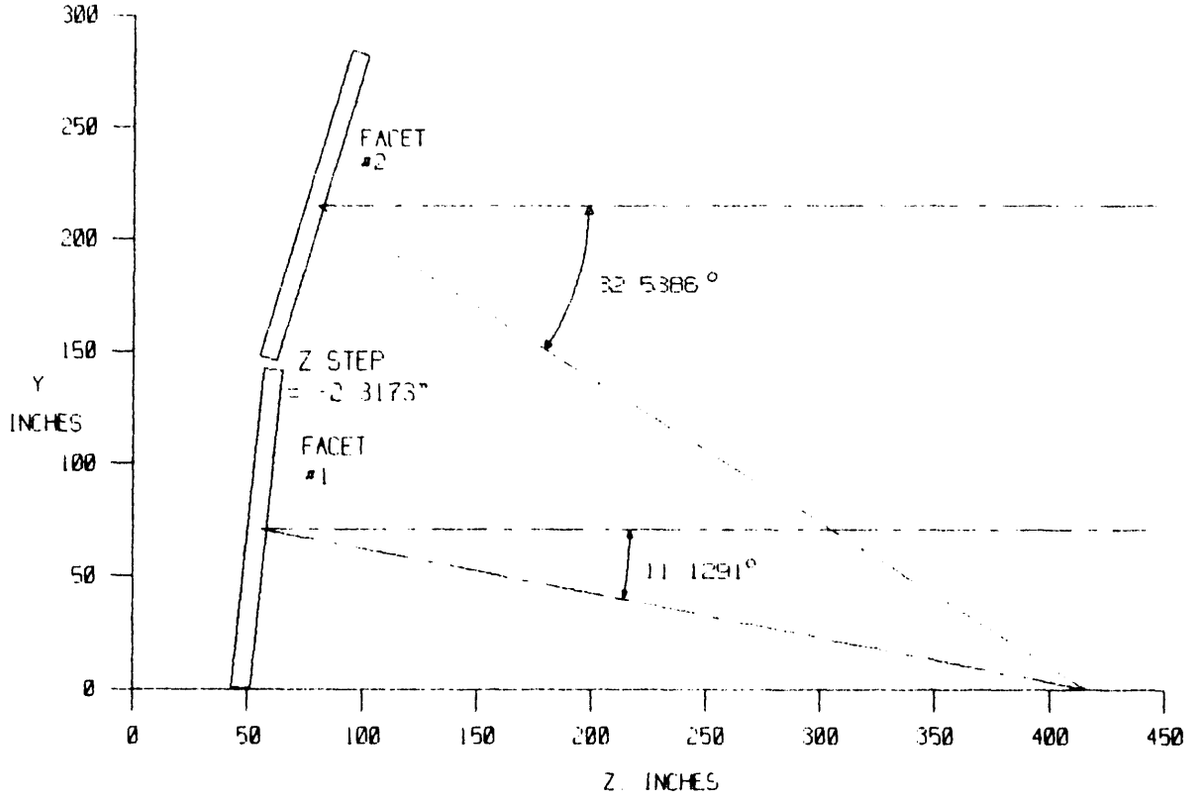

Figure 2.2-2 Facets on a Parabolic Contour

In Figure 2.2-3, the variation of facet focal lengths is shown for two parabolic contour focal lengths of 30.7 ft and 25 ft. In the first case, the focal length of facet No. 5 is 34.5 ft., and the difference in focal length between facet Nos. 1 and 5 is 41.1 in. In the second case, the focal length of facet No. 5 is 29.6 ft., and the focal length difference between facet Nos. 1 and 5 is 51.5 in. Therefore, unless the facets have a large range of focal length adjustment, it probably will be necessary to manufacture facets with different focal lengths. The attendant cost increases in the fabrication of facets with different focal lengths is not insignificant.

Both the spherical and the parabolic dish contours offer optimum optical performance characteristics, but neither is a good choice for different reasons. It was concluded that a compromise configuration with greater overall cost effectiveness was needed. The new configuration would be an uncomplicated structure that would minimize the facet focal length variations.

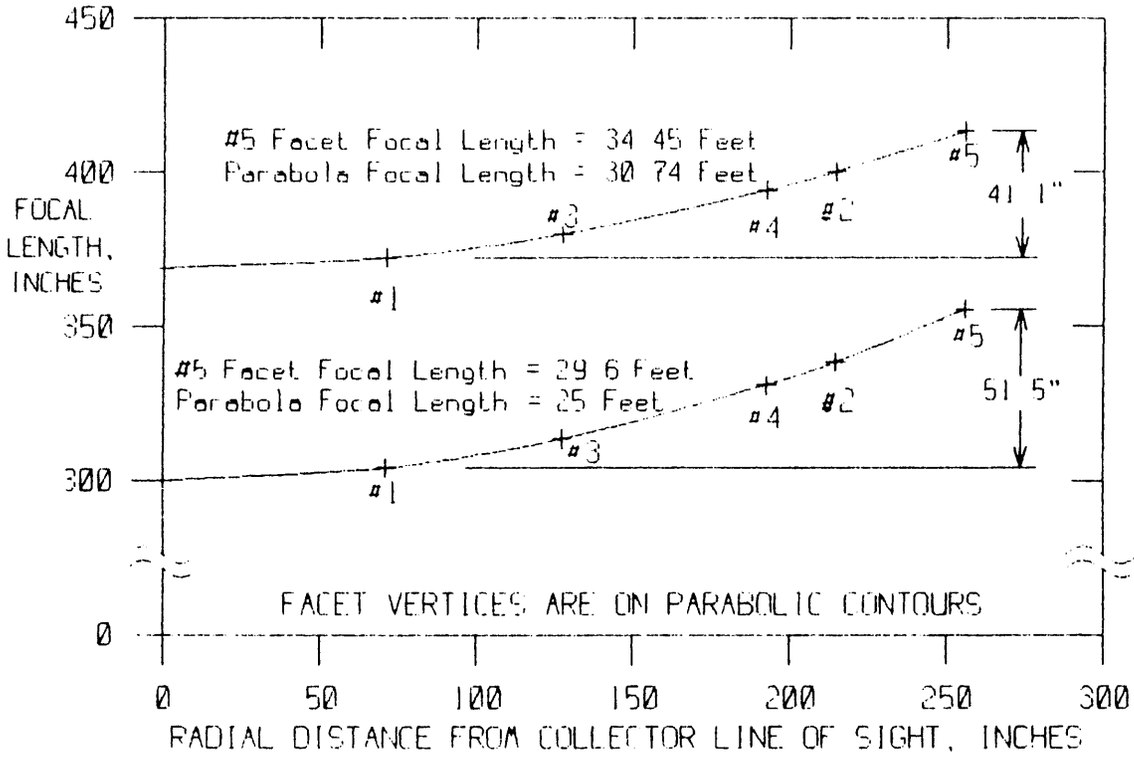

Figure 2.2-3 Facet Focal Lengths on Parabolic Contours

To this end, two structure contours, falling between the spherical and parabolic, were considered. As shown in Figure 2.2-4, contour No. 1 maintains the outermost facets, No's. 5A, 5B, 5C, and 5D (see Figure 2.1-1 above), on a spherical radius. The remaining facets are moved off the spherical radius closer to the focal point. In contour No. 2, the inner facets are moved toward the focal point as in contour No. 1. However, the outer facets are also moved off the spherical radius but away from the focal point. Since the outer facets, with their large off-axis aberrations, strongly influence the size of the image, it became immediately apparent that the defocussing of outer facets in contour No. 2 would serve to increase the size of the receiver with an attendant loss of efficiency. Therefore, contour No. 2 was dropped from further consideration, and contour No. 1 was selected as the starting compromise contour for the FSS.

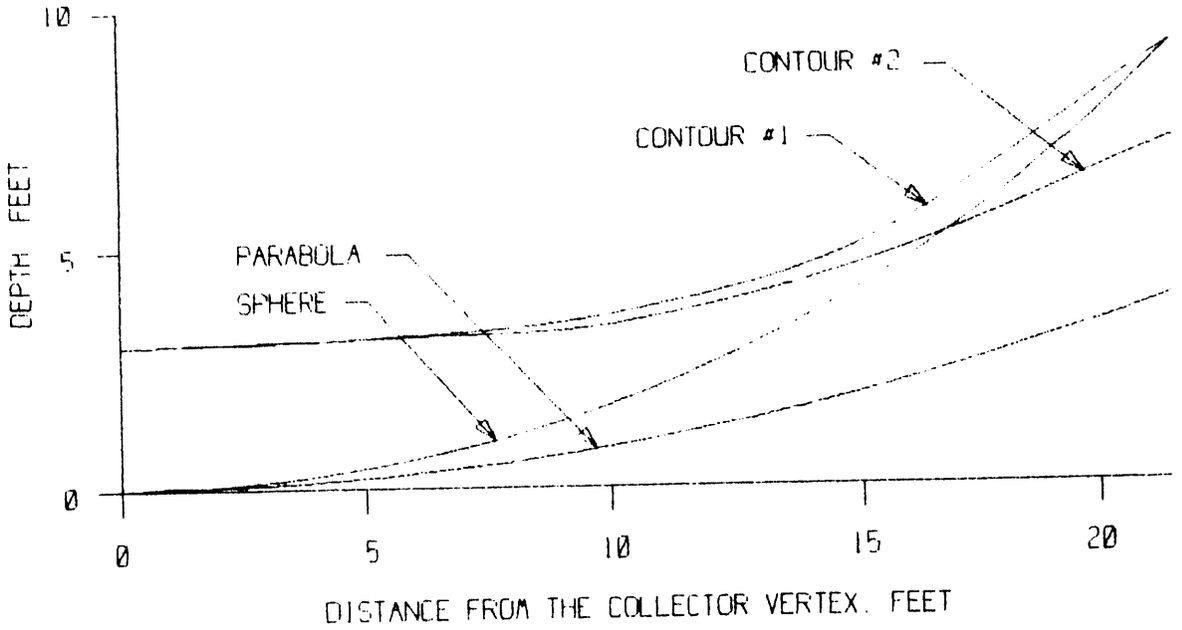

Figure 2.2-4 Contour Comparison, F = 29.9 ft.

A computer routine was developed to define the geometry of the facet locations relative to the vertex of the dish (X = 0, Y = 0, Z = 2.8 in.) of a spherical contour of f = 34.5 ft. The routine calculates the Z offsets, facet interference points, and the facet bolt circle geometry.

If the facet focal length and the radial distance of the facets from the dish vertex are varied, the facets can be positioned to achieve a reasonable compromise between the Z offsets and the f/D variations while providing appropriate rim-to-rim clearances. Analysis of sequential runs with selected input parameters enabled optimization of the facet locations.

Table 2.2-I shows the facet focal lengths for the selected dish contour. It also shows the position of the facet vertices, the radial distance in the XY plane of the vertices from the X = 0, Y = 0 point (DistFrmXY), the angle in the XY plane of the facet vertices from the X axis, the tilt of the facet relative to the XY plane (RotateAng), and

the minor axis of the projection of the facet into the XY plane (Radius InXY).

As shown in Table 2.2-I, the maximum facet f/D variation is approximately 0.3 (from 2.7967 to 3.0911). This is equivalent to a facet focal length variation of 39.4 in.

The resultant compromise contour is within the adjustment range of both the plastically-formed and the elastically-formed facets while having little or no effect on the thermal/optical performance of the dish. The Z offsets are minimized so that the facet mounting pads are in close proximity to the backup structure and, thus, make negligible contribution to deflection errors. Both of these factors represent significant cost savings by limiting fabrication to only a single facet configuration and by reducing the amount and complexity of structure, respectively.

2.3 Focal Length

Prior studies [Ref. 1] indicate that, at a dish f/D of about 0.6, the optical efficiency is almost independent of support structure contour. In this case, structural considerations, such as simplicity of design, commonality of parts, system inertia, etc., are more significant. The drive system is of particular interest since it is sensitive to load changes, and such sensitivity could impact the cost of the dish. Therefore, a study was initiated to determine how changes in the dish focal length, within a limited range, impact the drive system. In this study, certain parameters were held fixed while others were varied. The effect of any given parameter was then plotted to establish trends and to ascertain its effect on design.

Both spherical and parabolic support structure configurations were examined. Fixed parameters, established by directive, included a collector focal-length range from 25 ft. to 34.5 ft. and a dish populated with twelve facets, each of 11.5-ft. diameter. The 2TOP configuration defined the dish size of about 47 ft. x 40 ft.

Table 2.2-I

FINAL FACET VERTEX LOCATIONS

COORDINATE DATA FOR THE SANDIA 12 FACET COLLECTOR
WITH THE 2TOP CONFIGURATION, Page 1
RUN AT 09:32:34 ON 02-10-1991

DEFAULT FILE: ADJMOUNT.DFT, ENTITLED: FINAL DESIGN

FOCAL POINTS @ X = 0, Y = 0, & Z = 10.57112 Meters or 416.1859 Inchs

Facet Number	Facet Focal Dist. Meters	Inchs	F/D	Offset Adjust
1	9.5000	374.0157	2.7967	0.5000
2	10.2000	401.5748	3.0028	5.0000
3	9.6000	377.9528	2.8262	5.8000
4	10.0000	393.7008	2.9439	4.0000
5	10.5000	413.3858	3.0911	1.0000

Facet 4 Angle From X Axis Multiplier = 1.0185
Reflector Radius = 1.6984 Meters or 66.86614 Inchs
Facet Radius = 1.8 Meters or 70.86614 Inchs
Mounting Bolt Radius = 1.851 Meters or 72.87402 Inchs
Facet Front To Nominal Mounting Surface = 10 Inchs

THE FOLLOWING IS THE LOCATION OF THE FACET VERTICES

The units are inchs and degrees.

Number	X, Inchs	Y, Inchs	Z, Inchs	Vertex Depth
1	0.0000	71.0429	48.9786	-2.9886
2	0.0000	214.6533	76.7937	-2.7835
3A	127.6805	0.0000	60.4522	-2.9574
4A	126.5884	144.9751	72.7342	-2.8391
5A	246.1739	70.8661	91.7391	-2.7039
3B	-127.6805	0.0000	60.4522	-2.9574
4B	-126.5884	144.9751	72.7342	-2.8391
5B	-246.1739	70.8661	91.7391	-2.7039
4C	-126.5884	-144.9751	72.7342	-2.8391
5C	-246.1739	-70.8661	91.7391	-2.7039
4D	126.5884	-144.9751	72.7342	-2.8391
5D	246.1739	-70.8661	91.7391	-2.7039

Number	DistFrmXY	AngleFrmX	RotateAng	RadiusInXY
1	71.0429	90.0000	5.4746	66.5611
2	214.6533	90.0000	16.1558	64.2255
3A	127.6805	0.0000	9.8720	65.8761
4A	192.4641	48.8734	14.6325	64.6974
5A	256.1710	16.0595	19.1465	63.1673

With reference to Figure 2.3-1, the weight of the structure was found to remain virtually unchanged as the dish focal length changes from 25 ft. to 34.5 ft. As the focal length increases, however, the CG of the dish assembly moves toward the focal point (see Figure 2.3-2), moving the "balance" point, or elevation axis, of the assembly in the same direction. This causes the center of pressure of the reflector to move relatively further from the elevation axis, increasing the wind torque loading on the azimuth drive. At the same time, the mass moment of inertia of the assembly (the drive inertia) increases slightly, as shown in Figure 2.3-3, causing an increase in inertial (acceleration) loading of the drive.

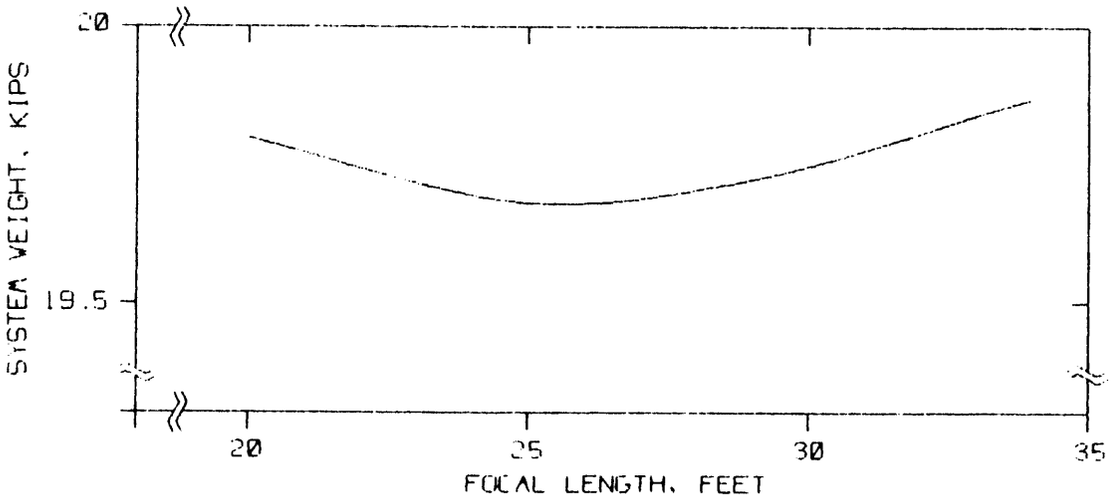

Figure 2.3-1 System Weight vs. Focal Length

The increased system inertia tends to reduce the natural resonance, or control frequency, of the system. The natural resonance is a function of the stiffness of the drive, which in turn is defined as the spring rate. Two load conditions must be considered when determining spring rate requirements - inertial loads and wind loads. Each of these is represented by a different spring rate. In the case of inertial loads, the resonant frequency of the system is a function of the drive spring rate. For wind loads, the angular deflection, or

rotation, of the drive is a function of drive spring rate. Since the two spring rates are derived from unrelated load factors, the largest, or most dominant, spring rate drives the design.

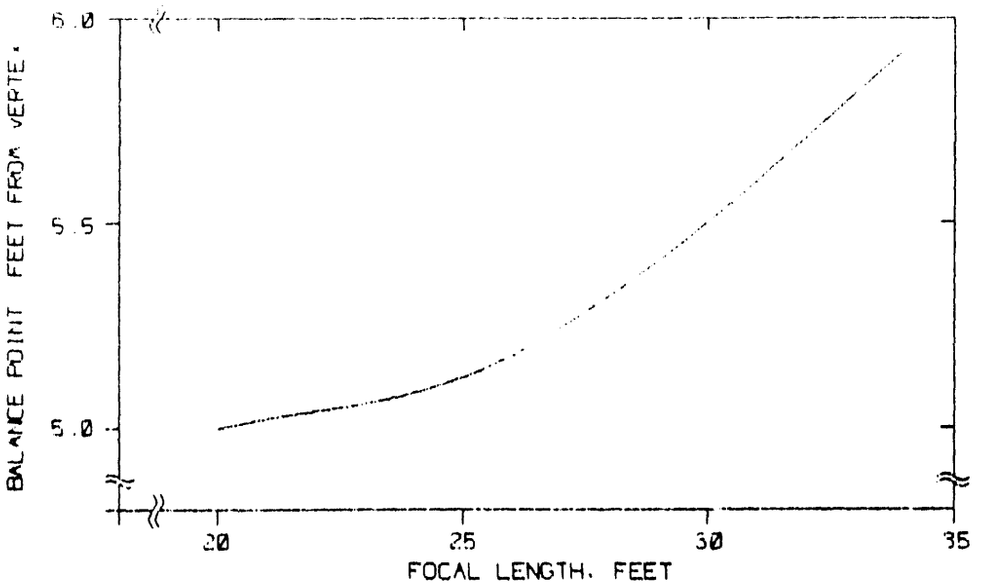

Figure 2.3-2 Balance Point vs. Focal Length

In the faceted dish, the resonant frequency can be as little as 1 Hz and still be fully compatible with control system capabilities. The inertial spring rate required to maintain a 1 Hz resonance is shown in Figure 2.3-4 as a function of dish focal length. It shows that, for a fixed resonance, the required spring rate must increase by about 50% when the focal length increases from 25 ft. to 34.5 ft.

To hold structural deflections at operating wind conditions within specified limits, a spring rate 2-1/2 times the inertial spring rate is required. Preliminary calculations indicate that the deflection spring rate should be on the order of 1.75 x 10E08 in-lb/radian. Thus, the wind loads, requiring the largest spring rate of the two, define the minimum stiffness of the drive.

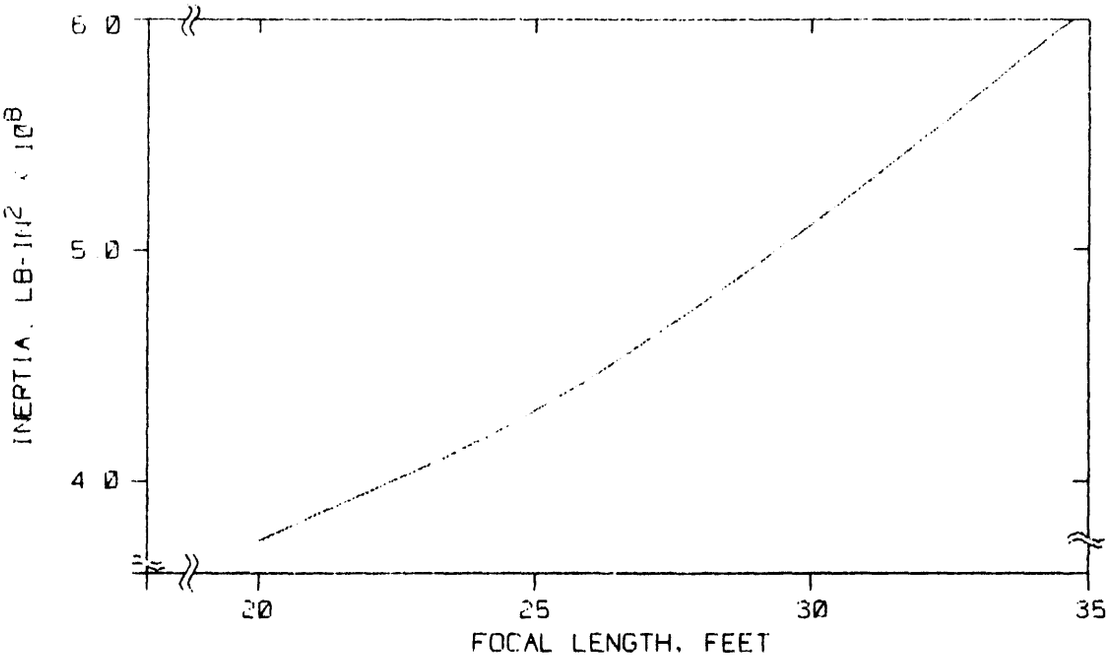

Figure 2.3-3 Drive Inertia vs. Focal Length

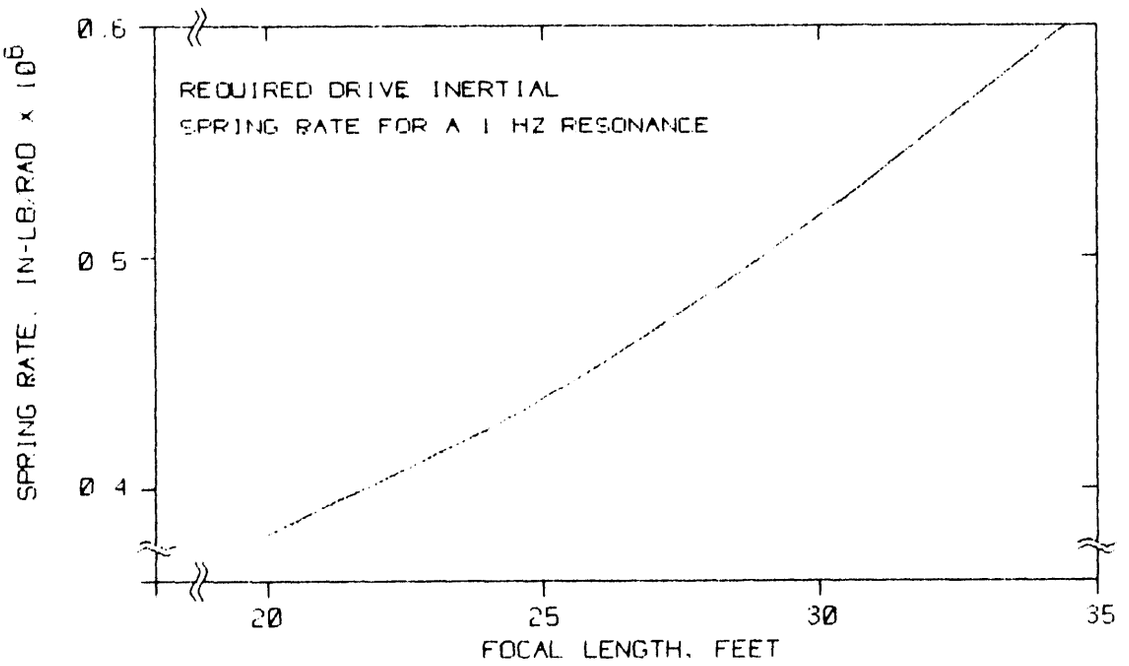

Figure 2.3-4 Required Drive Inertial Spring Rate vs. Focal Length

The inertia and wind loading tend to increase as the dish focal length increases in the range from 25 to 34.5 ft. In turn, these cause increases in drive loading and stiffness requirements as the focal length increases. However, the magnitude of these increases is slight.

In summary, although drive loads are greater at a focal length of 34.5 ft. than at a focal length of 24 ft., the difference is slight and has little impact on drive system design. Since the longer focal length favors facet manufacturing, and since it causes no significant drive disadvantage, it was decided that the dish focal length would be designed to accommodate a maximum facet focal length of 34.5 feet.

2.4 Windmill Option

Wind loads on full-motion concentrating dishes can be reduced by allowing the dish the freedom to seek the position of least resistance when at stow. The availability of this option, called "windmilling", was examined for applicability to the faceted dish.

Windmilling serves to minimize the projected area of the faceted dish at stow relative to the wind. Since the total wind force is proportional to the projected area, both unbalanced azimuth torque and overturning moment are positively affected.

The windmilling option is available only when the dish is in a "power off" mode. This condition exists

1. when the dish is at 0 deg. elevation (Mode 1) awaiting morning start-up or evening go-to-stow signals, or
2. when the dish is at 90 deg. elevation in stow mode (Mode 2), or
3. when a power failure occurs (Mode 3), which can happen at any look angle.

Moreover, windmilling can only be available about the azimuth axis since the elevation drive must always be in a locked position when the power is off. Therefore, it can be reasonably concluded that the

prime beneficiary of windmilling is azimuth torque and gear tooth loading.

Examination of each of the three power-off modes disclosed the following:

- Mode 1 - 0 deg. elevation
  The dish is in this position only if wind conditions are favorable for start-up, i.e., under 35 mph. If, after reaching this position, the wind exceeds 35 mph, then a go-to-stow signal is transmitted to the drives and the dish immediately proceeds under power to the zenith position. Thus, the dish never sees winds above 35 mph in this mode. Since the driving design loads occur at wind velocities of 50 mph at any dish attitude, the loads at 35 mph are not critical and windmilling offers no advantage.
- Mode 2 - 90 deg. elevation
  At this position, the dish presents minimum projected area at all azimuth angles. Therefore, the windmilling option is a non-issue.
- Mode 3 - Power Failure
  Since power failure can occur at any dish orientation, the dish could experience survival-level wind loads well in excess of the design criteria. In this mode the capability of windmilling allows the dish to feather, thus presenting a minimum area to the wind and reducing wind loading.

The windmilling option was examined for compatibility with the two candidate drive systems - the Winsmith azimuth drive and a conventional spur-gear/pinion-type drive. This option, however, is available only on a drive train that can freewheel in both clockwise and counter-clockwise directions. The Winsmith drive is non-backdriving, and thus it is incapable of windmilling by virtue of a 460:1 primary stage gear reducer. (For a differential planetary reducer, ratios greater than 400:1 are considered to be self-locking.) The conventional drive train is capable of windmilling only if it has no directly coupled worm gear or equally inefficient stage. However, to achieve

the overall reduction desired in the azimuth drive of about 30,000:1, a gear train without one or more worm gear stages would be too massive and costly for use on the faceted concentrator. It is conceivable that the last stage of this type drive could be clutch-coupled so that, in a power-off condition, the clutch would release and allow the dish to windmill. But the added complexity and cost of such an approach would not be justified by the advantages of windmilling.

In summary, the following conclusions and recommendations were reached:

1. Only in case of power failure does the windmilling option have a significant advantage.
2. Neither of the two candidate drive systems, in consideration of practicalities, can windmill.
3. Since the windmilling option is not available, three alternatives have been considered.
   - An emergency power source will be provided to drive the dish to stow in case of power failure.
   - The probability of power failure occurring at a worst case attitude of the dish is assumed to be too low for consideration.
   - The design criteria must be changed to include the power failure mode.

The approach taken in the parabolic dish concentrator development task was to provide an uninterruptable power source. This approach will also be used in the faceted dish.

2.5 Solar Walk-Off Protection

The SOW for the Faceted Dish Project requires that the structure be provided with walk-off protection, or a "safe" path, when the concentrated solar beam is acquiring the sun, when it is leaving the receiver, or when beam walk-off results from loss of power. A safe path can be provided by passive means such as placing insulation on

the structural elements over which the concentrated beam would pass. This appears to be the most practical solution to a loss-of-power situation. However, at the outset of the design it was believed that, under operational conditions, quick engagement or disengagement by a relatively high-speed drive was a more positive solution.

The critical operational condition occurs when emergency defocussing is required. Assuming a 16-in. diameter concentrated beam image at the receiver, and a receiver structure diameter of 36 in., the beam must be moved 26 in. to be totally clear of the receiver structure. With a 34.5 ft. (414 in.) nominal dish focal length this represents an angular change of 3.6 deg.

The on-sun, off-sun capability at high elevation angles requires use of the elevation plane of motion since, at high elevation angles, azimuth motion is ineffective at moving the concentrator image. Two methods for achieving the requisite elevation motion were investigated. One method entailed articulating the PCA support structure. The other approach was to design the elevation drive so that it has adequately high output speed to move the image off of the receiver.

An articulated PCA support structure had the potential advantage of accommodating both emergency defocussing and receiver/engine maintenance. By pivoting the truss at or near the "elbow", one could lower the outboard section to near ground level, as shown in Figure 2.5-1, using a linear actuator screw jack as the driving element. The same drive could also be used to move the receiver/engine out of the concentrated focal point image. However, it was found that these two functions were very different.

For emergency defocus, the receiver must be moved out of the concentrated solar image quickly. In the maintenance mode, it can be lowered at a very slow rate. Therefore, the size and cost of the motor required for adequate defocussing is significantly greater than is required for the maintenance function.

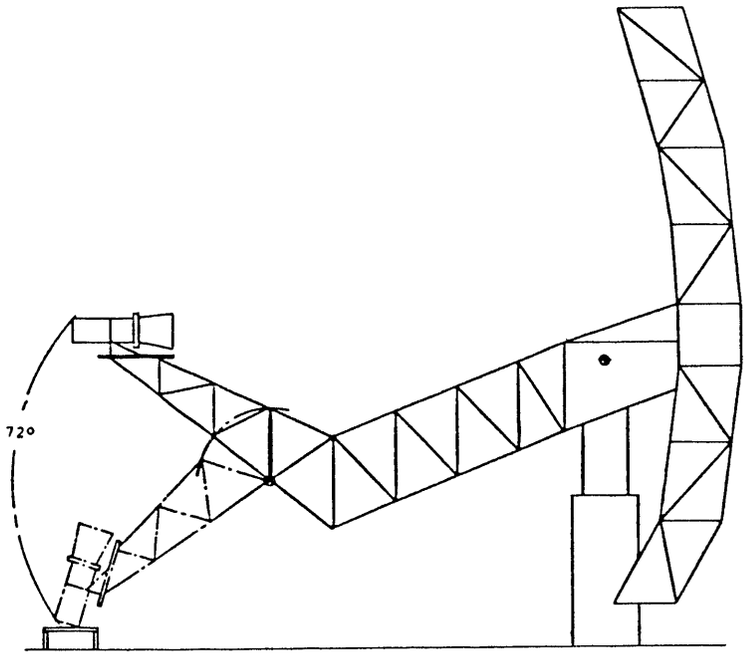

Figure 2.5-1 Articulated PCA Support Structure

It was determined that the planned elevation drive could provide sufficiently rapid movement for tracking the image off of the receiver without a significant cost penalty. Further, a relatively inexpensive cable winch could be used to meet the maintenance requirement of lowering the receiver/engine assembly. Therefore, the use of the articulation for the walk-off requirement was not employed in this design.

The elevation drive design moves the dish at an average rate of 9 deg./min. with the drive motor operating at its rated speed of 1140 RPM. Thus, the elevation drive alone will move the concentrated beam off the structure in about 24 seconds. The control system has the capability of driving the motor at twice its rated speed for a limited period of time. A speed of 2300 RPM is required for 12 seconds for the image to be clear of the structure. This is within the capability of the motor and the motor controller. The control system will use this high-speed mode to acquire and move off the sun, for example, in an emergency or upon receiving an appropriate signal from the fault alarm on the receiver/Stirling engine.

Other factors can help reduce the time required to move the image off the structure. The 36-in. diameter receiver/engine mount is an estimate based on the preliminary design of the heat-pipe receiver and the Stirling engine. If the Stirling engine package designated for the faceted collector is foot mounted, as opposed to radially mounted, the 36-in. dimension could be reduced. Further, as the dish drives off target, the images from the facets start to separate; and the heat energy is less concentrated as a function of the off-track angle. Finally, the above discussion is based on a high dish elevation angle. At lower elevation angles, simultaneous azimuth motion is available to further reduce the time required to move the concentrated image.

In summary, the designed elevation drive can operate for a limited period of time at twice rated speed. This capability facilitates moving the receiver/Stirling engine and its support structure off sun in about 12 seconds. Thus, in worst-case conditions of high elevation pointing angles, the elevation drive accommodates the SOW requirements for walk-off protection.

2.6 Tracking Error Considerations

The project SOW defines the required pointing error for the concentrator in terms of the contribution of three sources. First, the allowable facet slope error is less than 2.5 mr, 1 standard deviation. Second, the support structure shall have a maximum error no greater than 1.0 mr. Third, the control system shall have a standard deviation error of no greater than 0.6 mr.

The portion of the project covered by this report includes design of the control system and the support structure up to the facet mounting interface. Facet design is treated in reports by SAIC [Ref. 2] and SKI [Ref. 3]. As a result, this report neglects any error in the line-of-sight of the facets relative to the facet mountings on the support structure. Deflections of the support structure that cause movement of the facet mounts are included.

The proper allocation of the support system individual error sources to either the structure or control system depends on the system configuration. As a result, it was decided to combine the structure and control system errors into an overall error. This overall error (excluding facet errors) is referred to below as the collector system error.

If the maximum structural error is taken to be equivalent to a three sigma error, the SOW requirement for the one sigma collector system pointing error is 0.69 mr (.039 deg.).

While this accuracy is within reach with proper implementation, it appeared that it might be more demanding than could be justified. Consequently, a trade-off study of several alternate control system designs was undertaken.

2.6.1 Active versus Passive Track

The SOW required that the system would "... have a closed-loop, aperture feedback control ...". This is referred to below as "active track". The specified accuracy could be achieved with relative ease using active tracking. In this case, the term "active track" is taken to mean that the collector position control loop would be closed through a sun-direction sensor. The sun sensor would be mounted on the collector structure. The sensor error output would be used to drive the collector so that the sensor would be on the line-of-sight to the sun.

To test this, an estimated error budget was developed. In this budget, each of the error source values is an ESTIMATED peak value for the conditions stated, except for the effect of the backup structure and PCA dead weight deflections. The error of the line-of-sight of the sun sensor relative to the line-of-sight of the collector caused by these two sources is used at 20% of their estimated peak value. It was estimated that these error sources would be corrected to within 20% of their actual value by causing the program to insert bias in the error output of the sensor. The wind-induced deflections

of the backup structure, the engine, and the control system are not similarly reduced since they cannot be predicted easily. It should be noted that these estimates were made before the structure was designed or analyzed and, therefore, the values used here are not the same as the final values for the structure reported in Section 5.0.

In order to evaluate the configuration promising the most accuracy, linear drives were used, e.g., silicon-controlled rectifier motor controllers driving DC servo motors inside torque and velocity loops. Such drives have small errors under the conditions expected here.

The resulting error budget is shown in Table 2.6-I. The errors, as shown in the table, include the composite deflections of the structure and, therefore, the facet mounts, due to gravity and wind relative to the sun position sensor. They do not include deflections of the facet mountings relative to each other.

The pointing error for this case is well within the one sigma error specification of 0.69 mr. However, due to the problems that had been experienced with previous sun sensors, the project manager made the decision to use passive tracking in lieu of active tracking even though the errors would be larger.

In this case, passive tracking is taken to mean that the position loops would be closed using the error between the calculated sun position and the collector position as reported by position sensors coupled directly to the collector axes.

With passive tracking, the errors caused by backup structure deflection, pedestal deflections, and collector axis misalignments are greater than for active tracking since the errors of concern are the deflections relative to the earth-based coordinate system used to calculate the position of the sun. Some of these errors can be partially corrected, but the residual errors will still appear. In the active case, only deflections of the collector relative to the sun sensor mounting are of primary concern.

Table 2.6-I Pointing Error W/Linear Drive and Sun Tracker

COLLECTOR SYSTEM POINTING ERROR ESTIMATES
USING A CONTROL SYSTEM WITH LINEAR DRIVE AND A SUN TRACKER

ERROR SOURCE	16.8 MPH WIND		27 MPH WIND	
3 SIGMA OR PEAK VALUES	AZIMUTH	ELEVATION	AZIMUTH	ELEVATION
	Millirad	Millirad	Millirad	Millirad
Backup Struct Gravity X.2	.00	.15	.00	.15
Engine Dead Weight X.2	.00	.08	.00	.08
Backup Structure Wind Def.	.25	.25	.65	.65
Engine Wind Deflection	.01	.01	.01	.01
Linear Servo Wind Error	.01	.01	.01	.01
Linear Servo Limit Cycle	.02	.02	.03	.03
Sun Sensor Error	.10	.10	.10	.10
RSS AXIS RESULT	.27	.32	.66	.68
RSS TOTAL		.42		.95

NOTES: The individual errors are estimated peak errors except those marked X.2 which are 20% of estimated peak errors.
The errors in each axis are combined by an RSS calculation for each axis. The values for the axis total are also the result of an RSS calculation.
Thus, it can be expected that, for a 16.8 mph wind gusting to 27 mph, the result of the 16.8 mph case represents a reasonable estimate of the probable error (one sigma). The result of the 27 mph case represents a reasonable estimate of the three sigma error for the 16.8 mph wind gusting to 27 mph condition.

The sun position calculation will have some small error due to incomplete algorithm implementation, calculation errors, incorrect time, etc. The error due to a time error can affect either or both axes depending on the sun position. In this analysis, all the estimated time error was arbitrarily taken to be in the azimuth budget.

Finally, the axis position sensors have errors that must be included. At the time, the availability of reasonable cost encoders with

sufficient accuracy was not known, so it was assumed that two-speed resolvers would be used to close the control loops.

An error budget for this case is shown in Table 2.6-II.

Table 2.6-II Pointing Error W/Linear Drive and Resolvers

COLLECTOR SYSTEM POINTING ERROR ESTIMATES
USING A PASSIVE CONTROL SYSTEM W/LINEAR DRIVE AND RESOLVERS

ERROR SOURCE	16.8 MPH WIND		27 MPH WIND	
3 SIGMA OR PEAK VALUES	AZIMUTH	ELEVATION	AZIMUTH	ELEVATION
	Millirad	Millirad	Millirad	Millirad
Backup Struct Gravity X.2	.00	.30	.00	.30
Engine Dead Weight X.2	.00	.08	.00	.08
Backup Structure Wind Def.	.50	.50	1.30	1.30
Engine Wind Deflection	.01	.01	.01	.01
Pedestal Wind Deflection	.14	.14	.36	.37
Ped & El Axis Align X .2	.20	.20	.20	.20
Linear Servo Wind Error	.01	.01	.01	.01
Linear Servo Limit Cycle	.02	.02	.03	.03
Prediction Error w/o time	.20	.20	.20	.20
Time Error (5 Seconds)	.40	.00	.40	.00
Resolver Error	.30	.30	.30	.30
RSS AXIS RESULT	.77	.73	1.47	1.45
RSS TOTAL		1.07		2.06

NOTES: The notes for Table 2.6-I also apply to this table.

The resultant estimated system error of 1.07 mr is in excess of the specified allowable error, but as a result of a study [Ref. 4], the error requirements were re-evaluated. It was decided that the error requirement would be relaxed and that passive tracking would be used for the faceted dish.

2.6.2 Control System Configuration Study

Table 2.6-II is not supported by existing solar control systems, and it is relatively expensive because of the linear drives and the resolver position sensors. Accordingly, a cost and performance trade-off study was performed with regard to these two components.

2.6.2.1 Collector Drive Considerations

The linear drives used for the estimates in Tables 2.6-I and 2.6-II would be relatively expensive regardless of the type of linear drive used. The three drive configurations examined included only four-quadrant controllers that would provide good performance under gusting wind loads. One type used silicon-controlled rectifiers to drive DC servo motors. Another type used pulse-width modulation to drive DC servo motors. Both of these would be operated inside torque and velocity loops. The third type considered utilized four-quadrant, flux-vector controllers with a full set of features driving standard 3-phase AC induction motors.

All three of these configurations would provide error performance near to that shown in Tables 2.6-I and 2.6-II. Any of these configurations would, however, cost more than two thousand dollars per axis for the two-HP systems thought to be needed at the time the estimate was made.

A more economical drive method uses a "bang-bang" approach where drives with appropriate gear ratios and motor size for the drive-to-stow situation are pulsed to produce tracking motion. This is done either with multiple short pulses or with pulse-width modulation. The pulsing is done in a manner that attempts to move the collector axis the correct amount to eliminate the detected error. The pulses normally have an amplitude equal to the full voltage rating of the motor. If the motor is an AC motor, the applied frequency normally is the line frequency. This yields positioning with considerably greater error than is achieved with a linear drive. The additional error arises from the controller dead band, varying friction, backlash, etc. If the

resultant error and intermittent application of power is acceptable, the method yields an effective, relatively low cost drive.

An error budget for this case is shown in Table 2.6-III.

Table 2.6-III Pointing Error W/"Bang-Bang" and Resolvers

COLLECTOR SYSTEM POINTING ERROR ESTIMATES
USING A PASSIVE CONTROL SYSTEM W/BANG-BANG DRIVE

POSITION FEEDBACK - RESOLVERS

ERROR SOURCE 3 SIGMA OR PEAK VALUES	16.8 MPH WIND AZIMUTH	16.8 MPH WIND ELEVATION	27 MPH WIND AZIMUTH	27 MPH WIND ELEVATION
	Millirad	Millirad	Millirad	Millirad
Backup Struct Gravity X.2	.00	.30	.00	.30
Engine Dead Weight X .2	.00	.08	.00	.08
Backup Structure Wind Def.	.50	.50	1.30	1.30
Engine Wind Deflection	.01	.01	.01	.01
Pedestal Wind Deflection	.14	.14	.36	.37
Ped & El Axis Align X .2	.20	.20	.20	.20
Bang-Bang Dead Band & OS	1.00	1.00	1.00	1.00
Prediction Error w/o Time	.20	.20	.20	.20
Time Error (5 Seconds)	.40	.00	.40	.00
Resolver Error	.30	.30	.30	.30
RSS AXIS RESULT	1.26	1.24	1.78	1.76
RSS TOTAL		1.77		2.50

NOTES: The notes for Table 2.6-I also apply to this table.

The only difference between the error sources in Table 2.6-III and Table 2.6-II is that the errors due to the "bang-bang" full power method have replaced the errors due to the linear drive. The drive errors are labeled "bang-bang" dead band & OS (Over Shoot). A "bang-bang" drive must be pulsed for a period long enough to develop enough torque to overcome both maximum friction losses and the maximum load

that can oppose the desired motion; if the pulse duration is not enough, no motion of the load will occur. Then, when less loss and/or load is present, the motion that results is usually larger than desired. This happens because the excess velocity achieved by the long pulse must be absorbed by a smaller load that may actually be in the direction of the motion. The result is that the system will substantially overshoot the zero error point when the drive is lightly loaded. If the overshoot triggers a reverse correction, back-and-forth motion about zero error (hunting) can result. To prevent hunting, an error threshold must be used to prevent drive operation when the detected error is less than the threshold. This results in a dead band error equal to twice the value of the threshold. The value of one mr error used for each axis is somewhere between realistic and quite optimistic. This value is probably very optimistic for the elevation axis where the gravity load is high at both low and high elevation angles but with a reversal at about 35 deg. elevation.

The resultant RMS error of about 1.8 mr was higher than desired. This was felt to be particularly true with the possibility that this value might be optimistic for practical drives. This result led to a decision to use drives other than full power, rated frequency, "bang-bang" drives even though they may be useful in the future. The controllers ultimately chosen are such that they can be set to simulate the full-power pulsing so that this method can be tested when the system is operated.

One requirement of the SOW was that the control system design be based on existing and proven designs. However, none of the existing and proven solar collector controllers could control linear drives. As a result, it was decided to use motor controllers that will allow use of a "soft bang-bang" system. The controllers would be flux vector controllers but without the complexity and cost of those used with a fully linear control system.

The controllers selected are two-quadrant inverters from Polyspede Electronics Corporation; Dallas, Texas. This inverter generates

synthesized, 3-phase, AC power at any of four preselected frequencies between 0.5 and 132 Hz. Nearly full torque can be developed for any frequency. This means that the tracking command frequency can be set at 1 Hz and nearly full torque developed, but the motor velocity will not exceed 1/60th of rated speed. The consequence of using a two-quadrant inverter is that when the command to drive is removed, the controller does not aid in the deceleration of the motor. Under light load conditions, the coast-down travel is less than with a full power "bang-bang" system since the speed is less. The result is that the overshoot in light load conditions is considerably less than if the normal 60 Hz is applied and the motor allowed to accelerate for the total pulse duration and then coast down from the higher speed.

The error budget shown in Table 2.6-IV applies for this case. Everything is the same except for the amount allocated to the "bang-bang" errors. This factor was reduced from 1.0 mr to 0.5 mr. While this is not a large reduction, there is considerably more confidence that this value is achievable with the flux vector controller.

2.6.2.2 Collector Position Sensor Considerations

In all the above error budgets, a resolver with a total one sigma error of 0.3 mr was assumed. This requires a two-speed resolver since a single-speed resolver and a resolver-to-digital converter together have errors greater than 0.3 mr peak. Even though incremental encoders with sufficient accuracy and lower cost than a two-speed resolver were later found, the use of motor revolution counters was considered for position sensing since they are still less expensive.

Table 2.6-IV, modified by eliminating the resolver error and adjusting the other errors to account for using motor counters, resulted in Table 2.6-V, which shows the effect of using motor counters. The direct errors in the motor counters themselves are neglected.

The two new error sources are drive backlash and the drive deflections due to wind loads. The two new error sources must be included

since they affect the relation between the position of the motors and the collector axes. Compensation for these changes cannot be made by biasing the control system.

Table 2.6-IV Pointing Error W/"Soft Bang-Bang" & Resolvers

COLLECTOR SYSTEM POINTING ERROR ESTIMATES
USING A PASSIVE CONTROL SYSTEM W/SOFT BANG-BANG DRIVE

POSITION FEEDBACK - RESOLVERS

ERROR SOURCE	16.8 MPH WIND		27 MPH WIND	
3 SIGMA OR PEAK VALUES	AZIMUTH	ELEVATION	AZIMUTH	ELEVATION
	Millirad	Millirad	Millirad	Millirad
Backup Struct Gravity X.2	.00	.30	.00	.30
Engine Dead Weight X .2	.00	.08	.00	.08
Backup Structure Wind Def.	.50	.50	1.30	1.30
Engine Wind Deflection	.01	.01	.01	.01
Pedestal Wind Deflection	.14	.14	.36	.37
Ped & El Axis Align X .2	.20	.20	.20	.20
Bang-Bang Dead Band & OS	.50	.50	.50	.50
Prediction Error w/o Time	.20	.20	.20	.20
Time Error (5 Seconds)	.40	.00	.40	.00
Resolver Error	.30	.30	.30	.30
RSS AXIS RESULT	0.92	0.89	1.55	1.53
RSS TOTAL		1.28		2.18

NOTES: The notes for Table 2.6-I also apply to this table.

As can be seen in Table 2.6-V, the use of motor counters in place of resolvers results in significantly larger errors. The size of the errors led to a decision to use the resolvers (later replaced by encoders).

Table 2.6-V Pointing Error W/Motor Revolution Counters

COLLECTOR SYSTEM POINTING ERROR ESTIMATES
USING A PASSIVE CONTROL SYSTEM W/SOFT BANG-BANG DRIVE

POSITION FEEDBACK - MOTOR COUNTERS

ERROR SOURCE	16.8 MPH WIND		27 MPH WIND	
3 SIGMA OR PEAK VALUES	AZIMUTH	ELEVATION	AZIMUTH	ELEVATION
	Millirad	Millirad	Millirad	Millirad
Backup Structure Gravity X.2	.00	.30	.00	.30
Engine Dead Weight X .2	.00	.08	.00	.08
Backup Structure Wind Def.	.50	.50	1.30	1.30
Engine Wind Deflection	.01	.01	.01	.01
Pedestal Wind Deflection	.14	.14	.36	.37
Drive Wind Deflection	.44	.50	1.16	1.29
Drive & Ped. Wind Total	.58	.64	1.52	1.66
Drive Backlash	1.38	1.00	1.38	1.00
Ped & El Axis Align X .2	.20	.20	.20	.20
Bang-Bang Dead Band & OS	.50	.50	.50	.50
Prediction Error w/o Time	.20	.20	.20	.20
Time Error (5 Seconds)	.40	.00	.40	.00
RSS AXIS RESULT	1.72	1.45	2.53	2.42
RSS TOTAL		2.25		3.50

NOTES: The notes for Table 2.6-I also apply to this table. Also, The Pedestal Wind Deflection and the Drive Wind Deflection are directly added since they are always in the same direction.

The use of motor counters to replace the encoders may eventually prove to be acceptable if the actual errors are less than the requirement that exists at the time. The electronics as designed will be capable of utilizing motor counter pulses without hardware, firmware, or software modification. Also, the motors selected have rear

ware, or software modification. Also, the motors selected have rear shaft extensions so that motor counters can easily be installed for test.

2.6.3 Control System Selection Summary

In summary, the trade-off studies resulted in selecting a control system with the following characterestics for the faceted dish:

1. Passive tracking utilizing a modified solar collector controller.
2. "Soft bang-bang" motor controller operation utilizing flux vector controllers.
3. Position feedback from the collector axes utilizing incremental encoders.
4. Static structure errors compensated by the control system.

3.0 STRUCTURE DESIGN

The design of the faceted, stretched membrane dish concentrator builds on the successful stretched membrane heliostat program. It integrates a reflective surface consisting of 12 stretched-membrane facets with a full-motion tracking structure capable of providing full hemisphere coverage. The tracking structure is a kingpost type in which the FSS and the power conversion assembly are balanced about the elevation axis.

The decisions impacting the structure, reached as a result of the studies described in Section 2.0, are incorporated in the design, as listed below.

- The facets are arranged in the 2TOP configuration.
- The facet vertices are on a compromise contour, between parabolic and spherical.
- The nominal focal length is 34.5 ft.
- The elevation drive provides adequate walk-off protection.

The concentrator structure, as shown in Figures 1.0-1 and 3.0-1, consists of a FSS, a power conversion assembly (PCA), a transition assembly, a pedestal, and a drive system. The facets, each nominally 11.5 ft. in diameter, are positioned on the FSS in the 2TOP arrangement, as shown in Figure 3.0-2. The facet numbers and the coordinate axes used in the design, and referenced in subsequent paragraphs, are shown in Figure 3.0-2.

The FSS is a structural space frame with the primary function of providing the facets with a mounting base sufficiently stiff to maintain facet alignment within specified limits. The PCA support structure is a cantilevered space-frame beam that supports the PCA (receiver, engine and generator) at the focal point of the dish with minimum deflections. The transition assembly interfaces the FSS and the PCA support structure with the elevation axis and the azimuth drive. All moving structure loads are transmitted through the

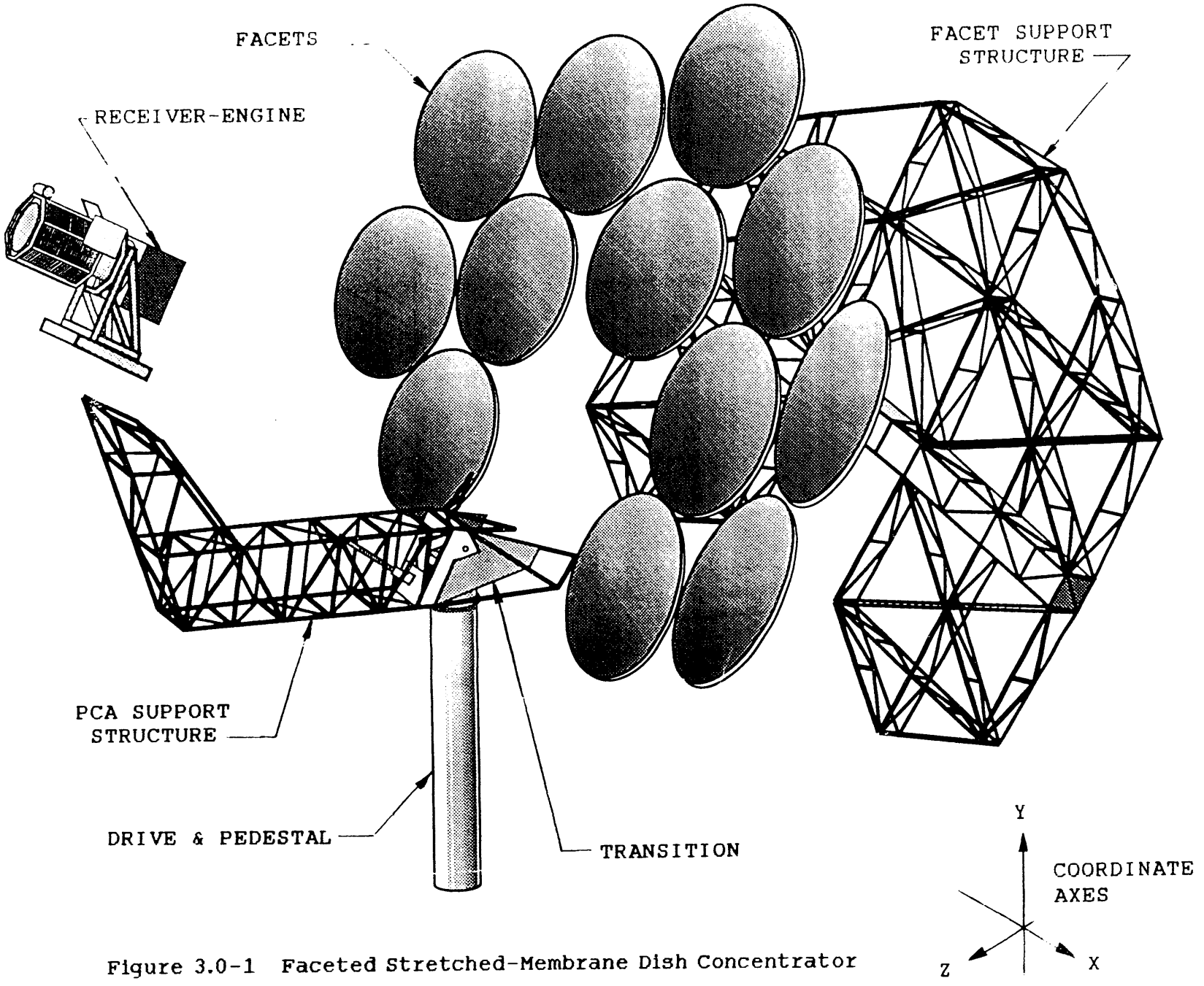

Figure 3.0-1 Faceted Stretched-Membrane Dish Concentrator

transition, into the drive assembly and thence to the pedestal and foundation.

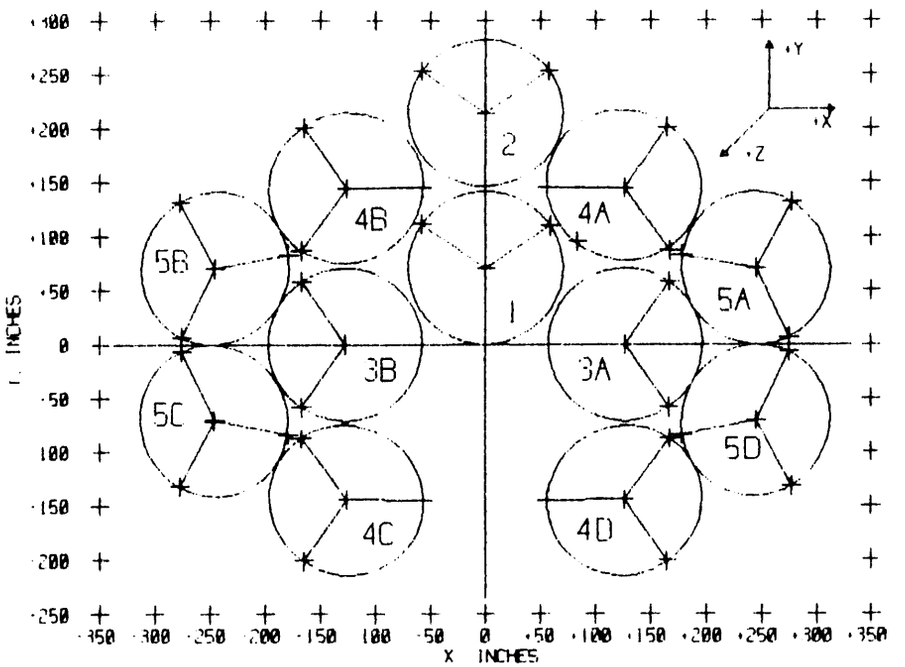

Figure 3.0-2 2TOP Collector Configuration

The drive assembly consists of elevation and azimuth drives. The elevation axis is mounted at the top of the azimuth drive so that all loads from the moving structure are reacted by the azimuth drive. The elevation drive rotates with the azimuth drive but is independently controlled. The drive assembly bolts to the collector pedestal interfacing the moving structure with the foundation. The pedestal is a large-diameter structural steel tube designed for minimum deflection under normal dish operating conditions.

The prototype design meets the requirements delineated in Section 1.1. The support structure is designed for low risk and near term-availability. The structure is designed for ease of fabrication using conventional shop equipment and tooling and for quick field assembly and installation. Facet adjustments are readily accessed, and the PCA maintenance can be performed at ground level. The prototype

design employs standard structural steel shapes and fasteners, as well as off-the-shelf components such as drives, bearings, and motors.

The design was driven by four key considerations:

1. The geometry of the FSS was determined by two critical factors, the location of the elevation axis and the positioning of the vertical trusses. The elevation axis is between the facets and the focal point, relatively close to the boresight axis (Z axis) of the dish. When the structure rotates up in elevation, the lower half of the FSS straddles the pedestal. Thus, it was necessary to build a gap in the lower half of the FSS to clear the pedestal. It was also necessary to position the vertical trusses so that the facets, each with 3 mounting points, would interface with mounting facilities at hard points on the trusses.
2. Static and dynamic imbalance about the elevation axis could not be eliminated because of the lack of symmetry about the X (horizontal) axis; it could only be minimized. This caused the overturning moment to be greater than originally calculated, and impacted the design of the drives and the pedestal.
3. The relatively high loads experienced by the drives, the expressed requirement for a low-risk configuration, and cost factors led to the selection of the proven Winsmith azimuth drive. This had significant impact on the design of the transition assembly.
4. The requirement for ground-level access for maintenance of the PCA led to the decision to articulate the PCA support structure. This favorably impacted the elevation drive design by eliminating the need to rotate the concentrator assembly below 0 deg. elevation.

A number of other factors contributed to design decisions but, for the most part, their impact on the structure was localized and had lesser effect on the overall design.

The structure was designed to meet the required deflection criteria and then analyzed for stress compliance with the AISC codes. Assem-

blies and individual elements such as plates, angles, tee's, etc., were selected to insure operational stiffness. After meeting the deflection criteria, the individual structural elements were checked for conformance under worst-case conditions with AISC codes for buckling and stress limits. As a result of the deflection design and this process, stresses throughout the structure are low.

3.1 Facet Support Structure (FSS)

The FSS, as shown in Figure 3.1-1, is a rectangular grid, triangulated space frame configured symmetrically about the X axis. The structure is designed to meet deflection requirements and to be low weight. It comprises a horizontal box section spine truss; segmented vertical flat trusses attached perpendicularly to the spine; and flat horizontal, diagonal and ring trusses to support and stabilize the vertical beams. Facet mounting pads are welded to the primary beams. The trusses are fully welded assemblies and are made exclusively from standard structural steel shapes. For ease of fabrication, assembly and economy of manufacture, they are of constant depth.

3.1.1 Spine Truss

The spine truss is the main load-bearing member in the FSS. It is a 48-in.-square space-frame beam designed for torsional and bending stiffness. It reacts all wind and gravity loads transmitted by the vertical trusses and is the primary load path from the facets to the elevation axis. The spine truss is made in three sections, a center section and two mirror-image outer sections. The three sections bolt together at installation.

Analysis indicated that, to meet deflection requirements, the center section of the spine truss must be stiffer in torsion than the two outer sections. It also indicated that excessive point loads were likely at the corners of the center section frame. To solve both problems the center section is fully covered with a sheet metal web. With the web the center section becomes an effective torque box. The web also serves to distribute the loads uniformly into the transition assembly shear plates, thereby eliminating the point loading and

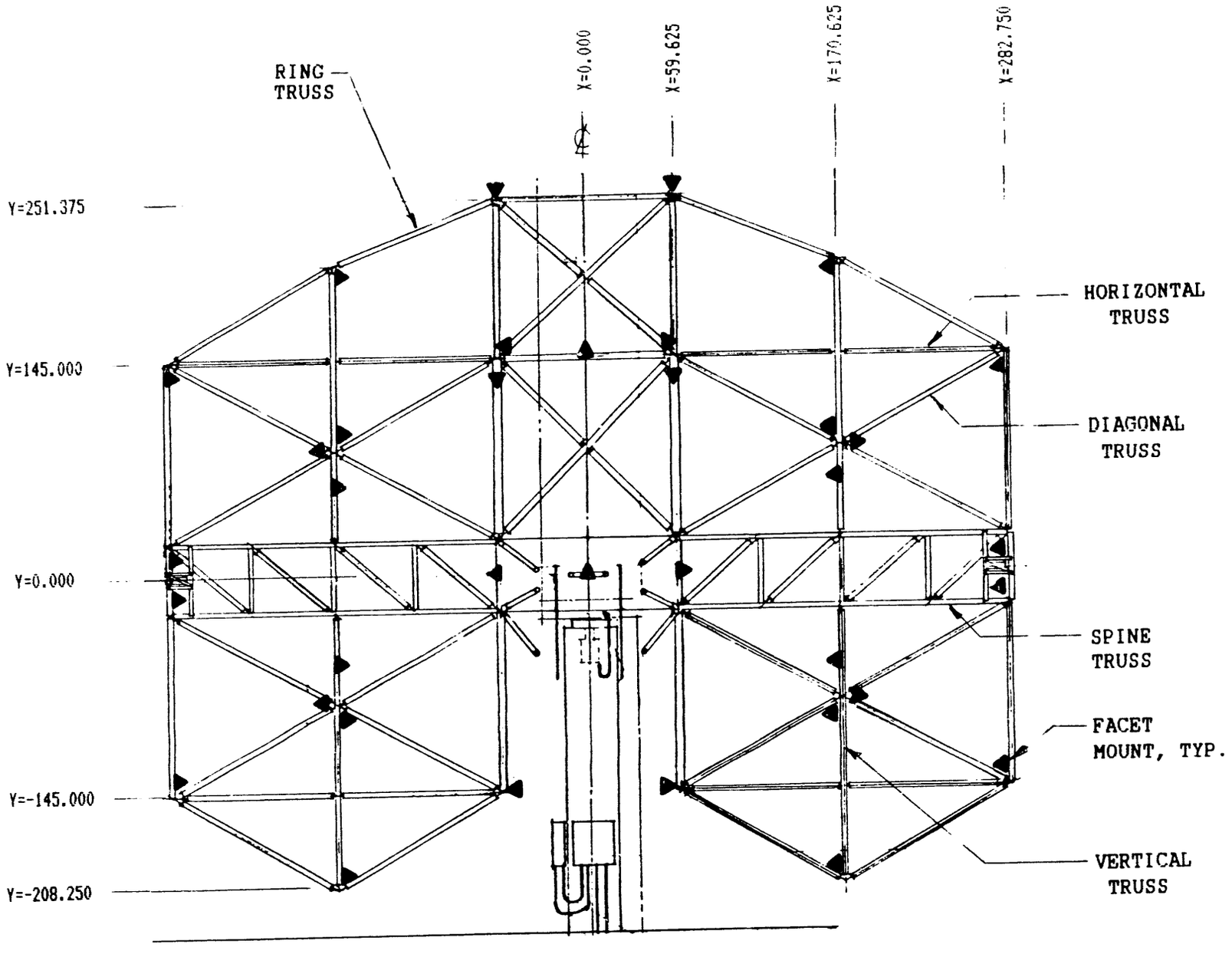

Figure 3.1-1 Facet Support Structure

potential local buckling. The center section is notched on the bottom surface to allow the tracking structure to nest with the pedestal at high elevation angles.

The outer sections of the spine truss are open space frames. Analysis showed that these sections need not be true torque tubes for the structure to meet the specified deflection criteria. Although the outer two sections would be stiffer if webbed, the reduction in deflection does not justify the increased weight and cost.

3.1.2 Trusses

Vertical trusses are bolted orthogonally to the spine truss, symmetrical about the X axis, as shown in Figure 3.1-1. Horizontal and diagonal trusses in each bay stabilize the vertical beams. Peripheral beams form a circumferential, or ring, beam integrating the truss structure to react torsional loads. All of the trusses experience load reversals with changes in dish elevation angle and with changes in the wind direction. Therefore, all members are designed to sustain maximum compression loads without buckling.

The vertical trusses are the major load-bearing trusses in the FSS. Most of the facet mounts are located on vertical trusses, as shown in Figure 3.1-1. (Seven mounts are on the spine truss, and one is on a secondary beam.) These facet loads are dumped directly into the vertical trusses. To minimize local deflections at the facet mounts, the mounts are positioned at or near "hard" points. A "hard" point is a location on the truss that has three-dimensional support. The vertical trusses are split into upper and lower sections that are attached to the spine truss at assembly. They are welded, flat trusses, as shown in Figure 3.1-2, designed for simplicity of fabrication fixturing. The trusses are 48 in. deep, as determined by deflection analysis. The chord members, or caps, are sized for compatibility with deflection requirements and with the AISC code for buckling constant (L/r) limits. The two inner vertical trusses at X = ±59.625 in. are more highly loaded than the other vertical trusses; thus, their cap sections are heavy-duty structural tee's. The

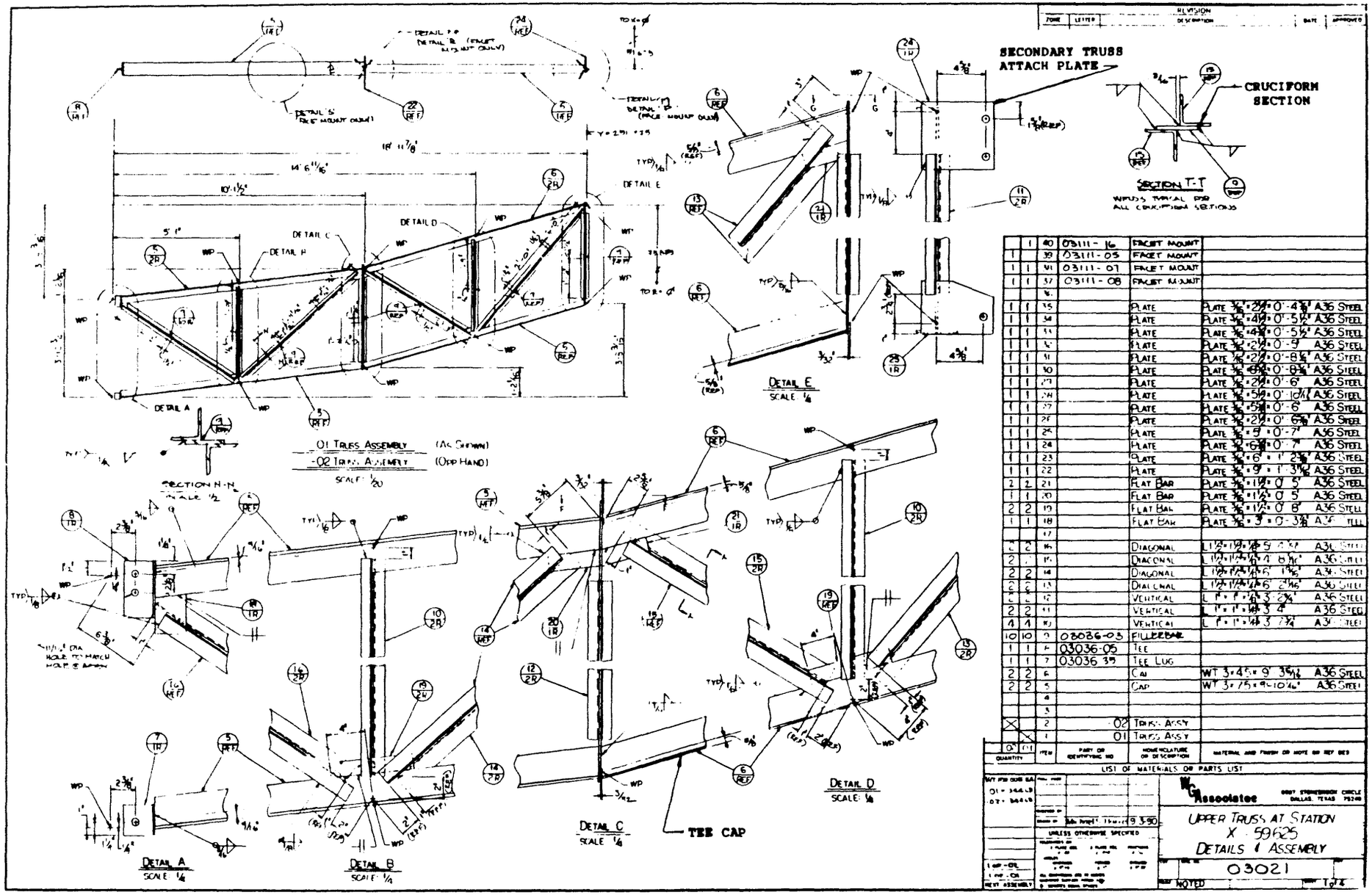

Figure 3.1-2 Vertical Truss

intermediate vertical trusses at X = ±170.625 in. are made with a comparably sized tee that has a smaller section modulus. The outer vertical trusses at X = ±282.75 in. are capped with an inverted structural angle. The material weight saved by "stepping" the vertical trusses in this manner and the lower drive inertial loading, justifies the slightly higher cost of fabrication associated with these members.

The secondary members of the vertical trusses are small structural angles arranged as shown in Figure 3.1-2, Section T-T. The "cruciform" cross-section is similar in section modulus to the more conventionally used back-to-back angle section. The cruciform has the singular advantage of affording complete accessibility for post-fabrication painting, whereas the back-to-back angles invariably are difficult to finish and corrosion-proof.

The horizontal, diagonal and ring beams are, like the vertical trusses, 48-in., constant-depth, welded, flat trusses. Their function is to stabilize the vertical trusses. Therefore, they are relatively lightly loaded in both tension and compression. Common materials are used for the cap members, vertical and diagonal members, and the end fittings of these trusses, with cost advantages accruing from quantity purchase. Only the arrangement of the members is varied to accommodate length and slope angle differences. Thus, economical tabletop fixtures, with pre-set clip locations for the various sized trusses, can be used for fabrication.

A typical secondary truss is shown in Figure 3.1-3. These trusses efficiently meet stiffness requirements due to the use of inverted structural angles for cap members. The angle is weakest about its diagonal centroidal, or Z, axis. In this truss design, the cap angle is rotated so that its Z axis is perpendicular to the plane of the truss. Thus, the vertical center support shortens the effective length of the cap so that its L/r meets the AISC code. The L/r ratio in the unsupported plane is fully compatible with AISC code. The stiffness

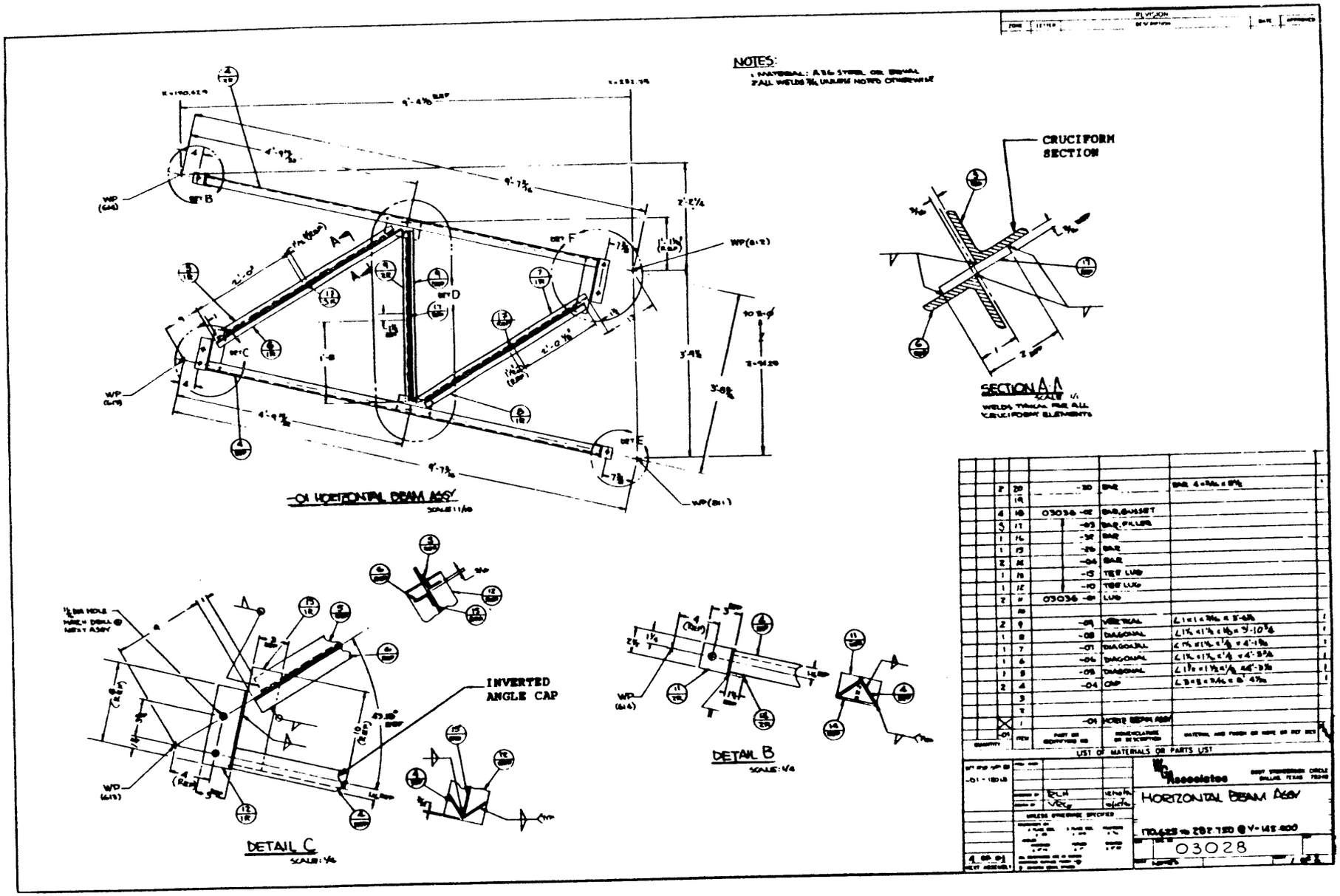

Figure 3.1-3 Secondary Truss

requirements could be met more easily using standard structural tee caps, but only with a significant weight penalty.

The cost effectiveness of using tubular secondary members in the trusses was compared against the cost of structural shapes with equivalent section properties. Tubular members are more efficient, i.e., their stiffness-to-weight ratio is higher than structural shapes. However, tubing material costs are much higher and, even though the actual material weight of shapes is greater, the cost is less. Moreover, tube members require more fabrication processing for attachment than structural shapes, which also increases the cost of piece parts. Finishing of tubular members also has cost impact since the tube ends must be capped or the parts must be dip-galvanized to prevent corrosion. As a result, the decision was made to employ structural shapes throughout the FSS.

The FSS is designed to accommodate the pedestal clearance gap in the lower half. The ring beams integrate the two halves of the FSS into a single rigid structure. They also help minimize the in-plane torsional deflections. The vertical truss matrix and the spine are designed so that no Z deflections can be attributed to the gap.

3.1.3 Facet Mounts

The 12 facets are mounted in the 2TOP arrangement on the support structure. Each facet has 3 mounting studs nominally equally spaced on a 72.87-in. radius about the center of the 70.87-in. radius facet ring. The studs are double-nutted to facilitate axial adjustment . A mounting pad for each stud is permanently installed on the structure at the nominal centerline of the facet stud.

The spacing of the studs is based on a best-fit analysis for attaching the mounting pads to structure. Ideally, for deflection considerations, each of the pads would be installed directly over the intersection of a vertical truss and a horizontal or diagonal truss. However, this is impractical because the nesting of facets in the 2TOP arrangement would require a spacing of as little as 60 deg.

between mounting points, creating an unstable condition. From a manufacturing perspective, it would be economical if the facet mounts were equally spaced at 120 deg., since symmetry is desirable. This is also impractical because it would require some of the pads to be so far offset from the hard points that supplemental structure would be required to prevent excessive deflections. Therefore, various combinations of facet mount spacing and location relative to hard points were evaluated, to find a compromise solution for all of the facet mounting points.

The analysis resulted in angular spacing of the studs around the facet at 0 deg., 125 deg. and 250 deg. on each facet. The orientation of the facet mounts is shown in Figure 3.1-2. To accommodate this solution, some of the facet mounts are offset a relatively short distance from the hard points in the X and Y directions. Also, the height, or Z dimension, of the facet mounts varies with location on the structure. In summary, to realize maximum economy, the relatively costly facets are identical while the less costly facet mount configurations vary with location on the structure.

The mounting pads are designed to provide maximum latitude for facet adjustment without adding significantly to their deflection error. They are configured to allow full accessibility to the adjustment nuts using standard tools. The pads are designed for compatibility with two installed conditions. In one, the pad is directly on a truss cap member. In the other, the pad is offset from the cap.

Figure 3.1-4 shows typical facet mounts. In Detail S, the facet mount is directly over the truss cap member. The pad is made from a 4-in.-square tube, cut and installed so that the mounting surface is perpendicular to the facet line-of-sight. A 1.25-in. diameter hole in the mounting surface provides for radial adjustment of the 0.75-in. diameter mounting stud. At the centerline of the hole, the mounting surface is typically 3.50 in. above the cap member. This provides for ±.75 in. axial adjustment of the stud for alignment. The mounting hole

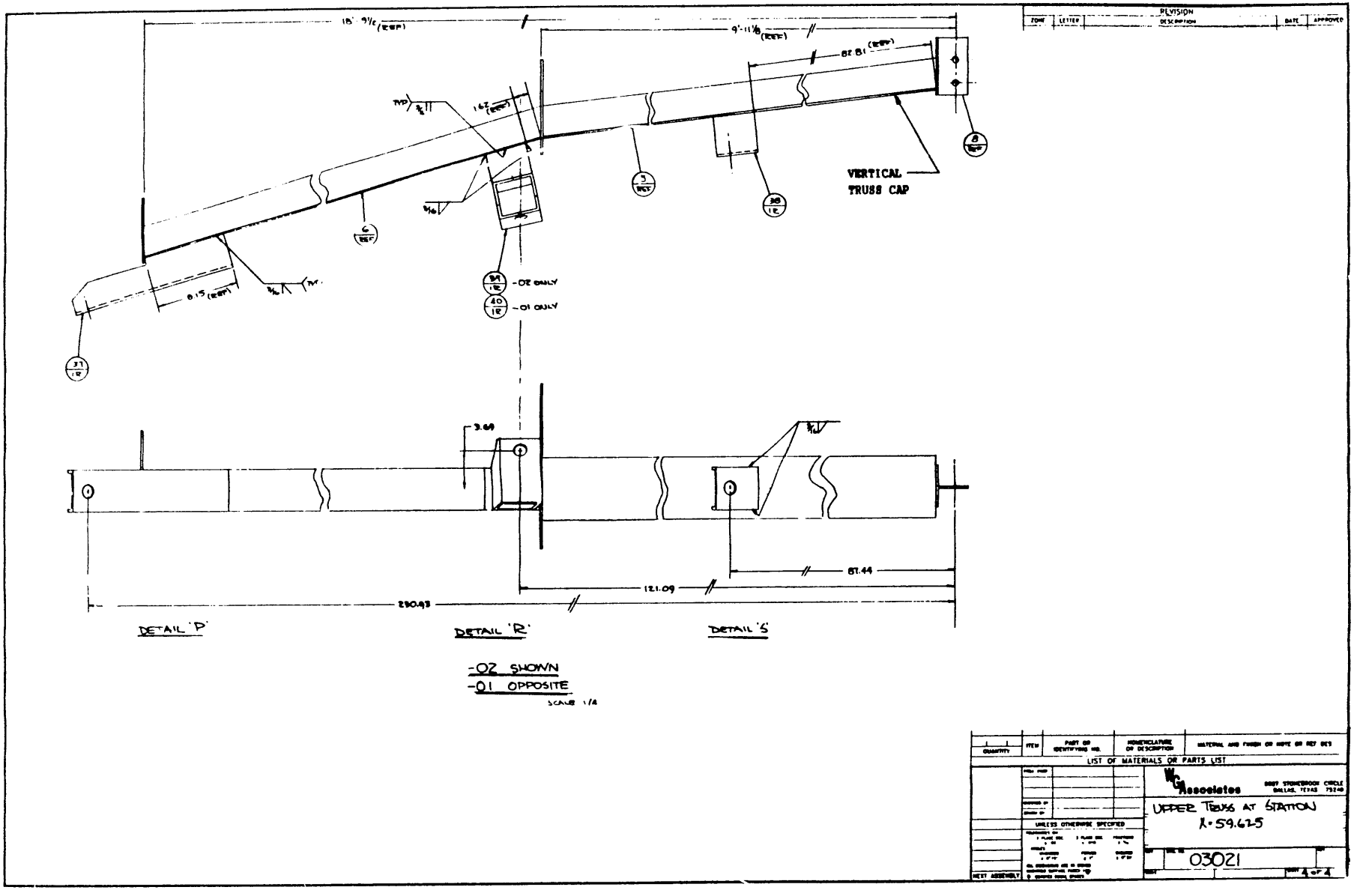

Figure 3.1-4 Facet Mounts

is positioned on the pad so that the adjustment nut on the underside can be accessed easily with a standard open-end wrench.

Two typical offset pads are shown in Details P and R. These pads are also made from 4-in.-square tube. However, they require some minor supplemental structure for proper positioning of the mounting pad and for load path development. These pads allow access to the adjustment nuts with a socket wrench because there is no interfering structure on the underside.

The coordinates of the mounting pad centerlines correspond to the mounting bolt centers shown in Table 3.1-I. With the facets installed on these centers, the clearances between facets at their closest proximity, or interference points, are shown in Table 3.1-II.

3.2 Transition Assembly

The transition assembly has two primary functions. First, it structurally joins the FSS and the PCA support structure, integrating them into a single rigid body called the tracking structure. Second, it interfaces the tracking structure with the elevation axis which is integral with the drive assembly. Thus, all gravity and wind loads acting on the moving structure are transmitted by the transition assembly to the drive assembly.

The transition assembly is shown in Figure 3.2-1. It consists of the center section of the spine truss, two shear plates installed perpendicular to the spine, an elevation axis beam on each shear plate, the PCA support mount, and appropriate support trusses. The spine center section, as discussed earlier, is fully webbed over a structural frame for torsional rigidity. It is notched on the bottom so that it nests with the pedestal at high elevation angles. The shear plates are factory-welded to the frame of the center spine truss on the sides of the notch. The PCA structure mount is a factory-welded frame that bolts to the outer ends of the shear plates. Each of the elevation axis beams consists of two structural "hat" sections bolted together with the shear plate sandwiched between them to form

Table 3.1-I Mounting Bolt Centers

COORDINATE DATA FOR THE SANDIA 12 FACET COLLECTOR
WITH THE 2TOP CONFIGURATION, Page 4
RUN AT 09:34:12 ON 02-10-1991

DEFAULT FILE: ADJMOUNT.DFT, ENTITLED: FINAL DESIGN

FOCAL POINTS @ X = 0, Y = 0, & Z = 10.57112 Meters or 416.1859 Inchs

Facet Number	Facet Focal Dist. Meters	Inchs	F/D	Offset Adjust
1	9.5000	374.0157	2.7967	0.5000
2	10.2000	401.5748	3.0028	5.0000
3	9.6000	377.9528	2.8262	5.8000
4	10.0000	393.7008	2.9439	4.0000
5	10.5000	413.3858	3.0911	1.0000

Facet 4 Angle From X Axis Multiplier = 1.0185
Reflector Radius = 1.6984 Meters or 66.86614 Inchs
Facet Radius = 1.8 Meters or 70.86614 Inchs
Mounting Bolt Radius = 1.851 Meters or 72.87402 Inchs
Facet Front To Nominal Mounting Surface = 10 Inchs

FOLLOWING IS FOR THE MOUNTING BOLT CENTER

Number	X, Inchs	Y, Inchs	Z, Inchs	DistFrmXY
1	0.0000	71.7118	41.9991	71.7118
2	0.0000	216.6613	69.8622	216.6613
3	128.8880	0.0000	53.5139	128.8880
4	127.7782	146.3378	65.8056	194.2731
5	248.4735	71.5281	84.8467	258.5640

FOLLOWING IS FOR THE BOLT CENTER COORDINATES

Angle	X, Inchs	Y, Inchs	Z, Inchs
For Facet # 1			
35.0	59.6949	113.3200	45.9869
145.0	-59.6949	113.3200	45.9869
270.0	-0.0000	-0.8298	35.0467
For Facet # 2			
35.0	59.6949	256.8094	81.4927
145.0	-59.6949	256.8094	81.4927
270.0	-0.0000	146.6652	49.5849
For Facet # 3			
55.0	170.0679	59.6949	60.6802
180.0	57.0930	0.0000	41.0199
305.0	170.0679	-59.6949	60.6802
For Facet # 4			
55.4	167.6148	204.5541	84.0956
180.4	55.9367	147.0094	53.6007
305.4	170.3550	87.3509	61.5163
For Facet # 5			
60.6	281.4865	134.2221	101.8827
170.6	180.0757	84.4372	63.2662
295.6	279.3193	5.6231	88.8082

Table 3.1-II Facet Clearances

COORDINATE DATA FOR THE SANDIA 12 FACET COLLECTOR
WITH THE 2TOP CONFIGURATION, Page 3
RUN AT 09:32:39 ON 02-10-1991

DEFAULT FILE: ADJMOUNT.DFT, ENTITLED: FINAL DESIGN

FOCAL POINTS @ X = 0, Y = 0, & Z = 10.57112 Meters or 416.1859 Inchs

Facet Number	Facet Focal Dist. Meters	Inchs	F/D	Offset Adjust
1	9.5000	374.0157	2.7967	0.5000
2	10.2000	401.5748	3.0028	5.0000
3	9.6000	377.9528	2.8262	5.8000
4	10.0000	393.7008	2.9439	4.0000
5	10.5000	413.3858	3.0911	1.0000

Facet 4 Angle From X Axis Multiplier = 1.0185
Reflector Radius = 1.6984 Meters or 66.86614 Inchs
Facet Radius = 1.8 Meters or 70.86614 Inchs
Mounting Bolt Radius = 1.851 Meters or 72.87402 Inchs
Facet Front To Nominal Mounting Surface = 10 Inchs

FOLLOWING IS FOR THE FRONT FACET RIM INTERFERENCE POINTS

Facets	X, In.	Y, In.	Z, In.	Gap, In.	Z Step, In.
1 - 2	0.0000	141.3007	58.7144		
2 - 1	-0.0000	145.8113	59.7487	4.5106	1.0342
1 - 3	61.9263	36.4599	48.6664		
3 - 1	66.1642	34.4550	52.7488	4.6882	4.0824
1 - 4	61.1896	106.3416	55.3639		
4 - 1	66.3600	110.3292	58.5121	6.5294	3.1482
2 - 4	62.0774	181.0468	69.9561		
4 - 2	64.3610	178.9852	71.6712	4.5952	1.7151
3 - 4	126.6627	70.8643	63.2770		
4 - 3	127.7666	74.8664	62.0828	4.1516	-1.1942
3 - 5	187.1009	36.3588	73.7946		
5 - 3	188.1356	35.3104	71.8225	1.4730	-1.9721
4 - 5	186.1212	106.8451	78.3928		
5 - 4	187.6005	108.6571	78.6886	2.3392	0.2958
5 Down	246.3638	0.0547	87.8636	0.1093	0.0000

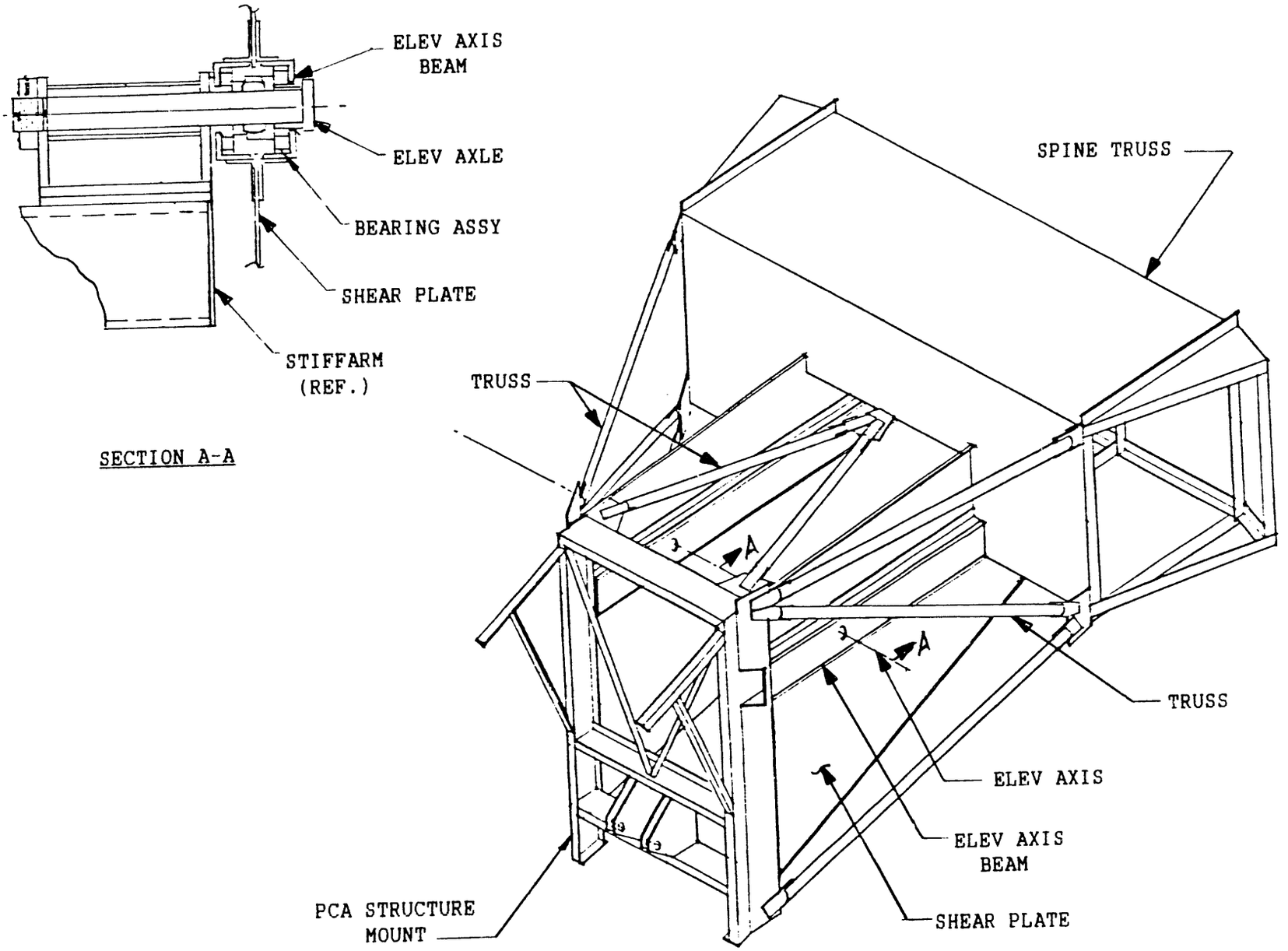

Figure 3.2-1 Transition Assembly

a high-strength box beam, as shown in Section A-A of Figure 3.2-1. The elevation bearing is installed in the box beam, as shown in Section A-A. Tubular trusses between the PCA structure mount and the spine center section stabilize the assembly in torsion and lateral bending.

The dominant loads in the transition assembly are due to dead-weight shear, with wind loads contributing to the total. The most effective method of transferring shear loads is with a plate. With the unitized configuration of the spine center section and the shear plates, the shear loads in the center section are uniformly distributed into the shear plates. Similarly, the PCA support structure introduces additional shear loads into the opposite end of the plates. The shear plates react all of these in-plane loads. The shear plates are capped and beaded to minimize potential local buckling.

High load concentrations exist at the interface of the transition assembly with the elevation bearings and axle. The box beams distribute these loads so that local stresses in the shear plates are reduced to allowable levels. The box beams also react side or out-of-plane loads caused by off-axis winds.

The elevation axis is located near the top of the transition assembly which straddles the pedestal, as shown in Figure 3.2-2. To accommodate 90 deg. elevation movement of the tracking structure, the bottom of the transition assembly is open; i.e., it is free of any structure that could interfere with the pedestal within the confines of the tracking arc. To develop torsional stability around the open section, trusses are installed on either side and in the top plane of the assembly. As shown in Figure 3.2-1, the trusses triangulate the PCA structure mount, the shear plates and the spine center section to re-establish the load path normally existing in a closed section. Thus, the trusses are the primary load path for out-of-plane loads and help provide the torsional rigidity necessary to meet deflection requirements of the structure.

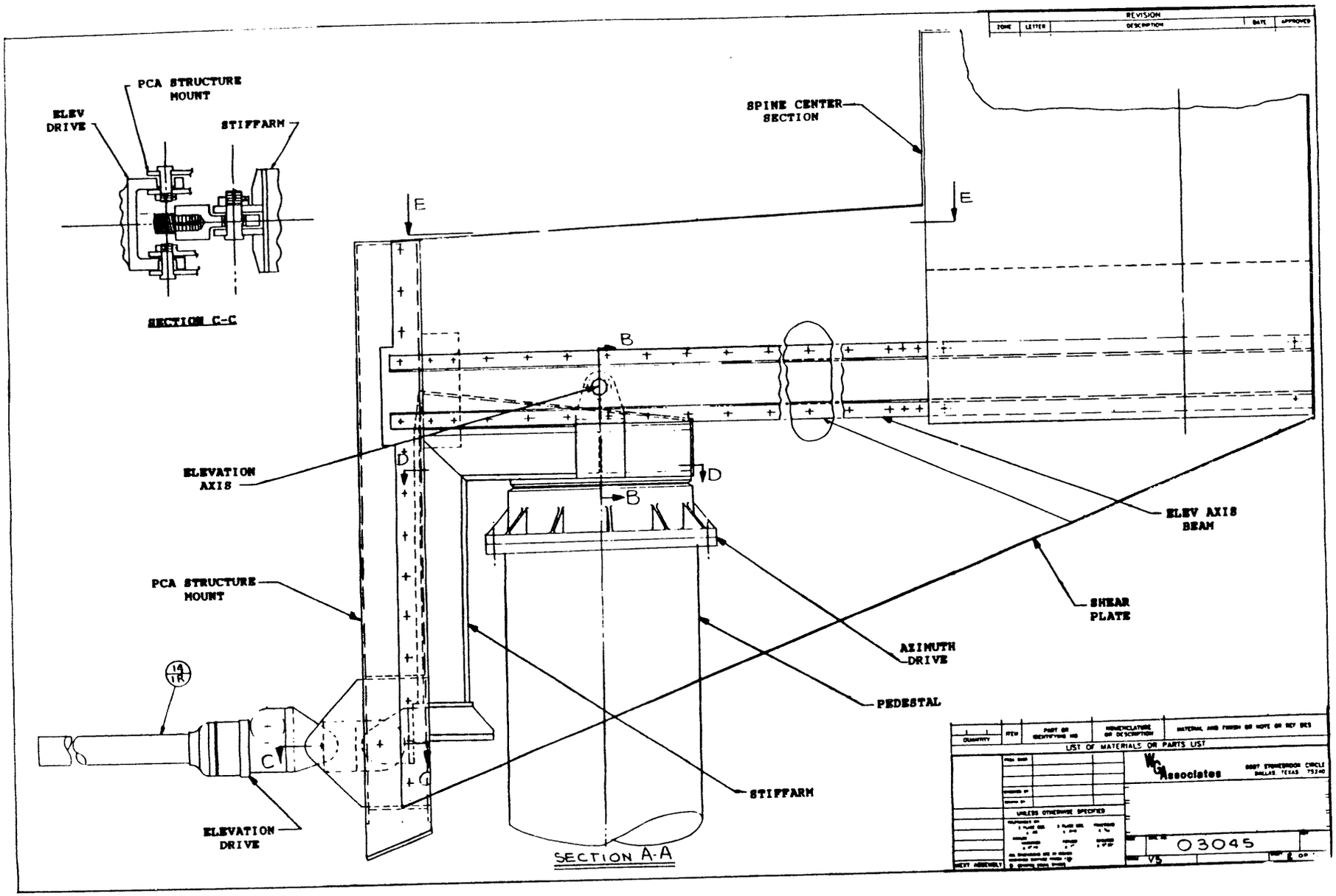

Figure 3.2-2 Transition Assembly Installation

3.3 PCA Support Structure

The PCA support structure is designed to maintain the position of the power conversion assembly relative to the facets. It is a fully triangulated, rectangular section, space frame beam, cantilever mounted to the transition assembly. As in the FSS, the PCA support structure is a deflection-driven design and, therefore, exhibits relatively low stress ratios.

The PCA support structure is shown in Figure 3.3-1. It is discontinuous, or "elbowed", so that it does not block any of the solar energy reflected from the facets. The beam is made in two sections. The inner, or root, section shown in Figure 3.3-2 contains the elbow and is of constant cross-section up to the elbow. From the elbow to the PCA mount, the structure, including the outboard section, is tapered to minimize material weight and reduce moment loading about the elevation axis. Both sections are constant width, factory-welded structures made of standard structural angle chord members and braces. Fabrication costs are minimized by the use of common parts.

The two sections are articulated at the first bay outboard of the elbow to allow lowering of the PCA to ground level for maintenance. They are hinged at the bottom with close tolerance, extra heavy-duty commercial hinges. The truss is bolted at the top to develop full structural integrity for normal operations. A machine screw linear actuator is used to lower the outboard section to the ground for engine and/or receiver maintenance. The screw jack is mounted on a pivoting trunnion outboard of the top plane of the root section. The screw jack end is pinned to a clevis on top of the outboard section. Drive power is supplied by a 1/2 HP electric drill motor with a 450 RPM output velocity. An interlock switch at the articulated joint prevents operation of the dish azimuth and elevation drive motors when the truss is in the maintenance mode. The switch is mounted at the top face of the root structure and is protected from accidental actuation. It is operated by a pin that projects from the outboard section. When the topside bolts are loosened the switch opens and cuts power to the drive motors. The interlock switch is in series

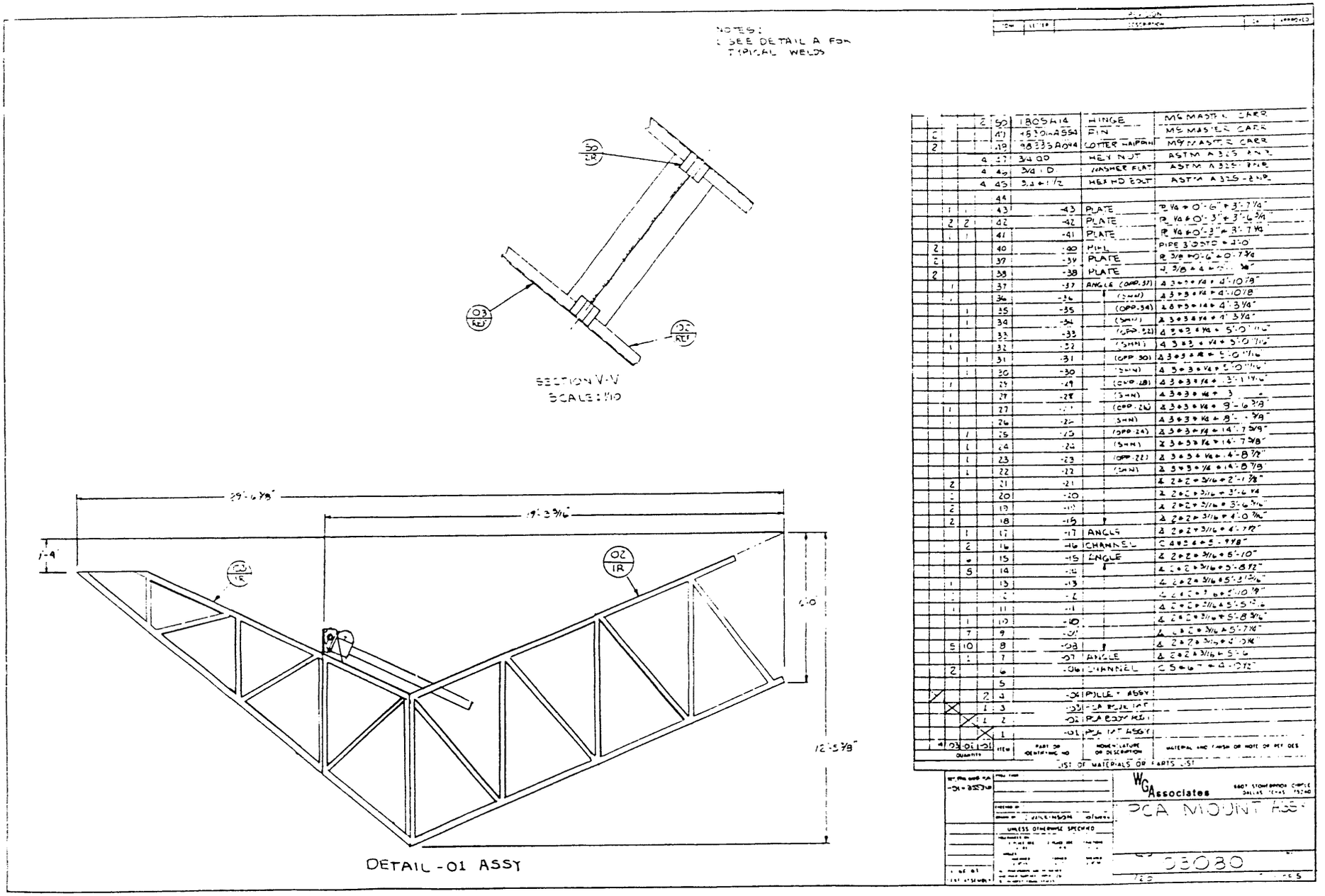

Figure 3.3-1 PCA Support Structure

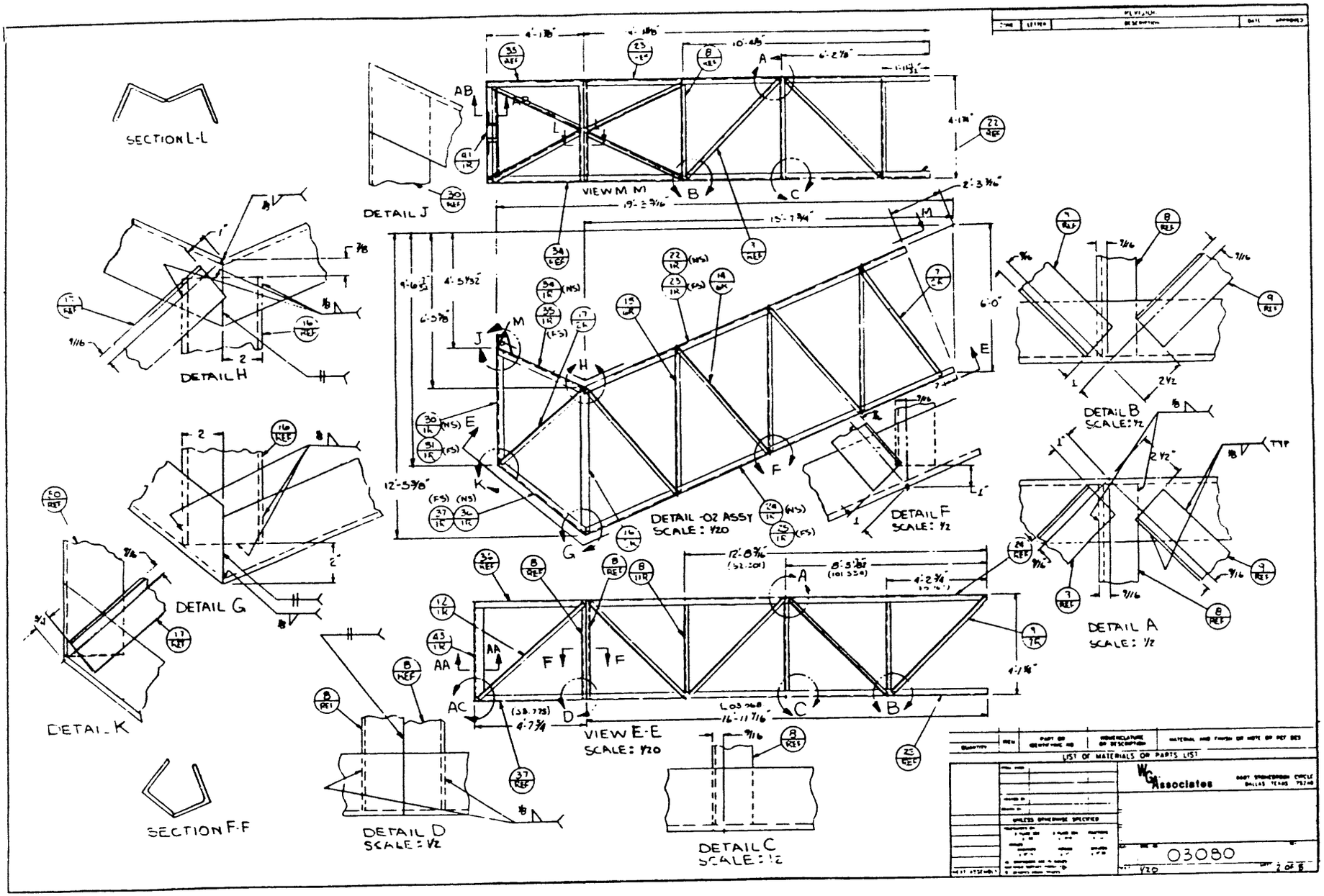

Figure 3.3-2 PCA Root Structure

with the emergency power cut-off palm switch located on the outside of the electronics housing. Both switches must be closed before the motors can be activated. An outlet for the drill motor is installed at the top of the root section. As an additional safety feature, the outlet is interlocked so that it has power available only after dish drive power is cut.

3.4 Drive System Design

The faceted dish concentrator requires a drive system that provides full hemisphere coverage for operation in near-equatorial locales. The drive system must be capable of at least 370 deg. travel in azimuth and 90 deg. in elevation. It must be compatible with operational pointing accuracy and with survival wind criteria. It must have travel rates consistent with sun acquisition, off-target tracking, and drive-to-stow requirements; it must be self-locking for stow purposes; and it must allow "bang-bang" drive control.

The drive load requirements were derived from the LTV wind tunnel test curves and from gravity load calculations. Structurally, the drive design is predicated on worst case combined loads as follows:

- Overturning moment, drive to stow - 77,000 ft-lb
- Overturning moment, stow position - 75,000 ft-lb
- Azimuth torque, drive to stow - 33,000 ft-lb
- Shear - 9,830 lb.
- Axial - 43,000 lb.

As in the structure, maximum loads and stresses occur at the drive-to-stow condition of 50 mph. However, under operating conditions (wind velocity up to 27 mph), the combined load and stress levels are relatively low. In this operating range the critical design parameters are stiffness and backlash. For initial design of the azimuth drive, it was estimated that these factors would contribute a combined 3 sigma error of 1 mr. Based on early inertia and wind calculations, this allowed for a spring rate of 1.3E08 in-lb/radian and a backlash of .018 in. on a 36-in.-diameter output gear.

The drive motors are sized using RMS wind loads since motor ratings are RMS values. The peak combined load consisting of gravity load plus the drive-to-stow RMS wind load, defines the required torque rating of the motor. The combined elevation and azimuth torque load curves for the faceted dish at the mean drive-to-stow wind of 31.25 mph are shown in Figures 3.4-1 and 3.4-2 respectively. The RMS torque loads are calculated by adding the gravity load (dead weight) to 1.06 times the mean wind moment.

3.4.1 Azimuth Drive Design

Several types of azimuth drives were considered, including those employing harmonic, planetary, spur gear, worm gear, and cycloidal reducers. On the basis of cost and other practicalities the number of candidate systems was quickly reduced to two, the Winsmith azimuth drive, and a conventional drive train consisting of a bull spur gear/ bearing and pinion final stage with multistage speed reduction.

The Winsmith drive, shown in Figure 3.4-3, is a commercially available single-bearing, self-contained unit consisting of two stages. The primary (input) stage is a planetary reducer with a 460:1 reduction. The secondary (output) stage is a planocentric reducer with a 72:1 reduction ratio. The overall ratio of this drive package is 33,120:1. In operation, free, synchronous rotation of two eccentrics in a slow-speed planet gear imparts an orbital action to the planet gear. This action, in turn, advances the output ring gear three teeth (the difference in the number of teeth of the ring gear and the planet gear) for every rotation of the synchronized eccentrics [Ref. 5].

The Winsmith azimuth drive is similar in function to a harmonic drive in that many teeth in the output ring gear are always engaged with the slow-speed driver planet gear. The mechanism is self-locking, i.e., non-backdriving, because the primary stage reduction ratio is in excess of 400:1. Planetary reducers with ratios greater than 400:1 are generally considered to be self-locking. The salient characteristics of the Winsmith azimuth drive are shown in Table 3.4-I.

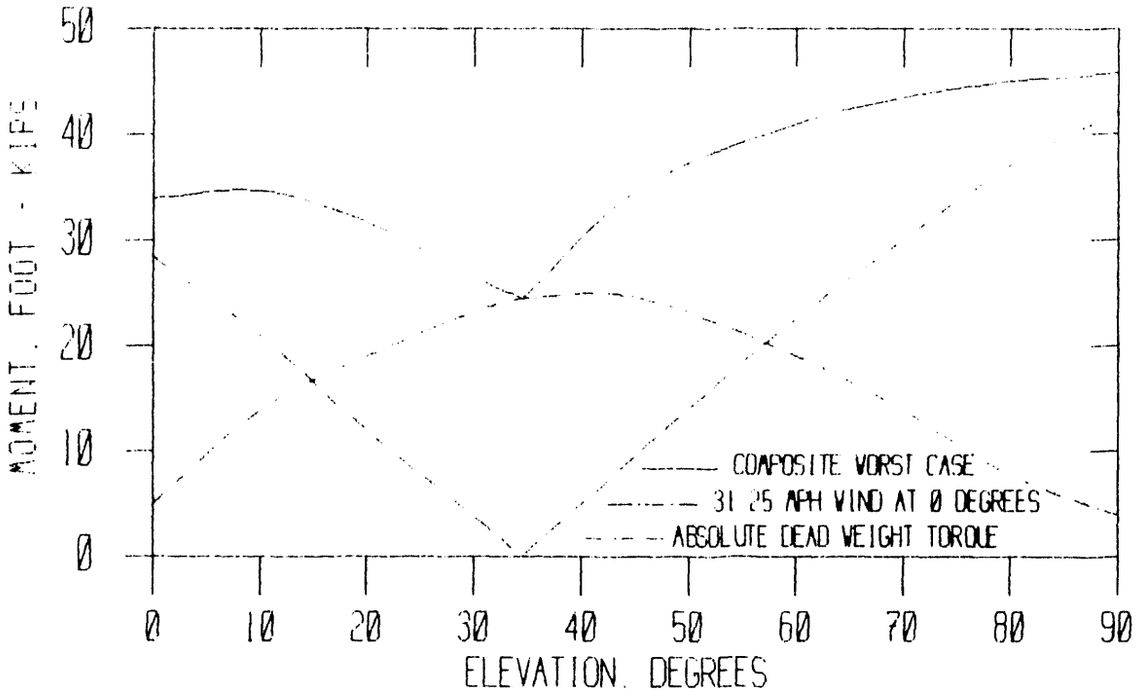

Figure 3.4-1 Elev. Torque Load w/31.25 MPH Wind

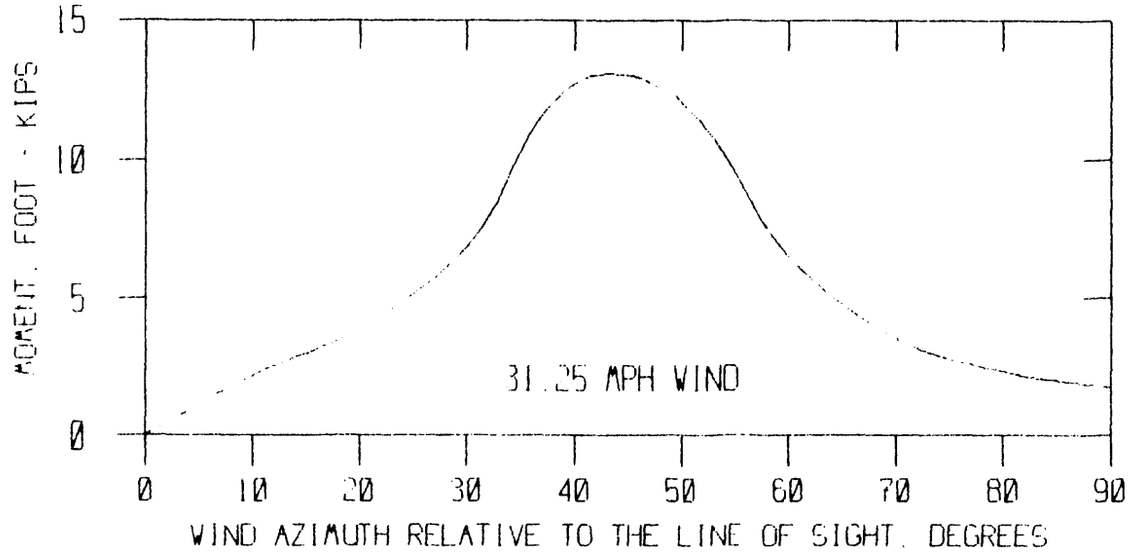

Figure 3.4-2 Azimuth Torque Load, 31.25 MPH Wind

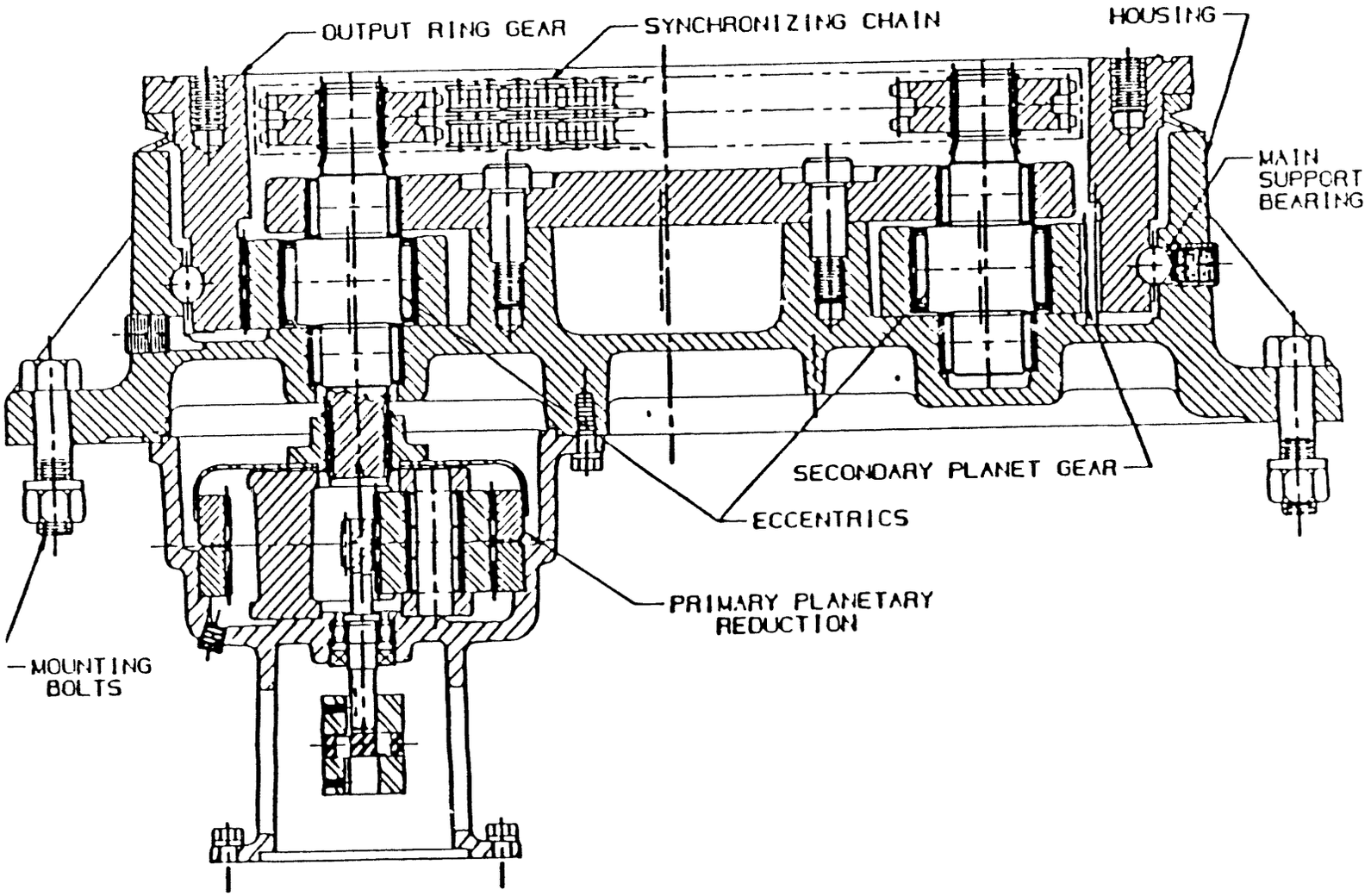

Figure 3.4-3 Azimuth Drive

Table 3.4-I Winsmith Azimuth Drive Characteristics

• Overturning Moment Capacity	-	215,000 ft-lb
• Radial Shear Capacity	-	250,000 ft-lb
• Drive Torque (Limit Load)	-	65,000 ft-lb
• Axial Load Capacity	-	250,000 ft-lb
• Backlash	-	1.38 mr
• Spring Rate	-	1.48E08 in-lb/rad
• Static Friction at Motor Shaft	-	Less than 5 in-lb

The Winsmith azimuth drive was designed under contract to Sandia National Laboratories for use on heliostats. It was fabricated and, when tested under controlled conditions, performed essentially as advertised.

The conventional spur gear train employs an output spur gear either mounted on, or integral with, a crane bearing and driven through a pinion gear by a motor and speed reducer. Two major factors drive the design of this type mechanism - tooth loading and backlash. In spur gears tooth-bending stresses are often based on the premise that only a single tooth is engaged at any time. Therefore, each tooth must be capable of carrying the total load. With a given gear pitch diameter and with a given pitch, the only remaining variable available for increased tooth capacity is face width.

It is clear that increasing the face width of the bull gear to obtain the desired load capacity has cost implications. Preliminary calculations indicated that a face width of 4 in. was required on a 36-in. pitch diameter gear. The gear would be heavy and expensive; thus this is an undesirable approach. Further, the inherent backlash causes control problems.

Manufacturing tolerances applied to factors such as runout (eccentricity), tooth-to-tooth spacing and tooth profile introduce potential for interference between mating gears. The interference can be exacerbated by a temperature differential. This condition is accommodated by increasing the center distance between the two

gears so that under the RMS of worst case conditions, no interference can exist. But this also results in considerable backlash.

Both problems are addressed by driving the bull gear with two identical motor/reducer/pinion assemblies. The two pinions distribute the torque load so that tooth loading is minimized. This allows the use of a smaller face width, hence less costly, bull gear. Backlash is eliminated by biasing the torque loop of one of the drive motors so that, in operational winds where current draw is small, they work counter to each other. At higher winds, such as drive to stow, the motors work in a torque-aiding mode. Costs are higher than with a single motor/reducer, but the difference is minimized since the dual components are each only half the rating of the single pinion drive.

Several gear reducer manufacturers were contacted, including Sumitomo and Graham, for their recommendations and costs. Different combinations of gear motors and reducers were considered in an attempt to minimize costs. However, it was concluded that the components were too expensive at this time, particularly since significant assembly and alignment time would be required.

The Winsmith drive was determined to be the prime candidate because

- it meets all load requirements,
- it has acceptable deflection characteristics,
- it is non-backdriving,
- it is compact,
- it has been built and tested, and
- it is affordable.

After close study, the only negative issue related to the Winsmith drive is that the backlash on one unit was measured at a peak of 1.38 mr. Since the manufacturer believes this is probably an anomalous measurement, a lower 3-sigma value is expected on subsequent units. In any case, it is likely that the total concentrator error budget will tolerate the 1.38 mr with the control system as designed.

In consideration of the above, the Winsmith mechanism was selected for the azimuth drive for the faceted dish concentrator.

3.4.2 Elevation Drive Design

The elevation drive assembly is shown in Figure 3.2-2. The elevation axle is part of the stiffarm assembly. The stiffarm is hard-mounted on the output gear of the azimuth drive so that it rotates with the azimuth gear. The housing of the screw jack is flange-mounted to a pivoting trunnion on the transition assembly near the PCA support structure interface. The end of the screw jack is pinned to the stiffarm assembly. The three pinned points of attachment are the apexes of a structural triangle formed by the stiffarm assembly, the transition assembly and the adjustable-length screw jack. Thus, as the screw extends, the tracking structure rotates about the elevation axis toward the zenith position, completely independent of azimuth positioning.

The stiffarm assembly is a rigid, triangulated weldment that forms the primary load path from the screw jack to the azimuth bearing. It is designed to minimize the axial loads in the screw jack by maximizing the moment arm between the elevation axis and the screw jack. The stiffarm assembly bolts directly to the top (rotating) side of the azimuth drive and transmits all moment loads directly into the azimuth bearing.

In the design of the elevation drive, consideration was given to both machine screw jacks and ball screw jacks. The machine screw is less costly and is non-backdriving. However, its low efficiency (less than 18%) must be accounted for in drive power requirements. Further, machine screws are subject to wear problems caused by sliding friction and the intrusion of foreign abrasive material on the mating surfaces. Ball screws, on the other hand, have a longer life expectancy, since they work on the principle of rolling friction. Being more efficient (on the order of 62%), ball screws require less power. But the high efficiency allows the screw to backdrive under load. Thus, if a ball screw is used, either a brake must be provided or the

efficiency of screw jack must be less than 50% if the drive is to be self-locking.

A ball screw jack has been selected for use on the faceted dish because of its longer life cycle and because its power requirements are more compatible with commercialization of the dish than is a machine screw jack. However, the backdriving problem requires special treatment. The magnetic clutch "power-off" brake approach was quickly discarded since it is considered undesirable when used in conjunction with a "bang-bang" type of control system. The frequency of on-off cycling is sufficiently high to shorten unacceptably the life of a brake.

The better solution lies in reducing the efficiency of the screw jack. This is done by providing a 70:1 primary (input) worm gear stage to drive a 1/2 inch pitch ball screw jack. The calculated efficiency of the mechanism is reduced to about 35%, causing it to be non-backdriving. This approach was used by Winsmith in the development of its drive tracking mechanism for heliostats and was successfully performance-tested on a 10-ton screw jack.

The geometry of the faceted dish places the CG of the moving structure about 18 in. above and 18 in. in front of the elevation axis when the collector is pointed toward the horizon. As the dish travels from horizon to zenith, its CG shifts from the focal point side of the elevation axis to the support structure side. The gravity load in the screw correspondingly goes from compression through a neutral point, at about 40 deg., to tension. Compression load is the limiting factor in any column, and the slenderness (L/r) ratio is the critical parameter. The elevation drive is designed so that maximum compression loads occur at 0 deg. when the screw jack is in its shortest position and the slenderness ratio is at its minimum. Therefore, the jack can easily perform to its rated capacity.

A 20-ton capacity ball screw jack was selected for the faceted dish with the screw length calculated to provide 73 in. of travel. The

input shaft is driven by a 1 HP, 1140 RPM, direct-coupled, 3-phase induction motor. The screw average travel rate of 611 deg./hr. (10.18 deg./min.) enables the concentrator to go from horizon to zenith in less than 9 minutes at rated motor speed.

To summarize, the proof-tested Winsmith planocentric drive is used to provide the azimuth motion for the faceted dish. This drive is non-backdriving and is fully compliant with the dish-loading criteria. The elevation drive is a stock 20 ton ball screw linear actuator with a customized input gear ratio of 70:1 to cause the actuator to be non-backdriving. The actuator is interfaced with the azimuth drive by a stiffarm assembly that reacts the actuator loads. At rated motor speeds the dish will slew at average rates of about 19 deg./ min. in azimuth and 10 deg./min. in elevation.

3.5 Pedestal

The solar collector pedestal is shown in Figure 3.5-1. It is a tubular structure made in two sections. The upper section provides a mounting surface on its top surface for the azimuth drive. The opposite end of the upper section bolts to the larger lower section of the pedestal that mounts to the foundation. The pedestal is symmetrical in cross-section due to the random nature of the loads. It is stepped so that it can accommodate the 90 deg. elevation movement of the tracking structure while meeting structural stiffness requirements.

Ideally, the pedestal would be lighter and stiffer, under given load conditions, if it were a constant 36-in. diameter. However, as described earlier, when the tracking structure moves up in elevation, the spine center section overlaps the pedestal. To avoid structural interference the FSS is "notched" so that it nests with the pedestal. Structural considerations require that the size of the notch be minimized; thus, the maximum pipe diameter with which the notch is compatible is 24 in. Therefore, a 24-in. constant section pedestal was evaluated. It was found that for stiffness characteristics equivalent to a 36-in. diameter, the wall thickness and weight required in a 24-in. pipe are impractical. The stepped pedestal

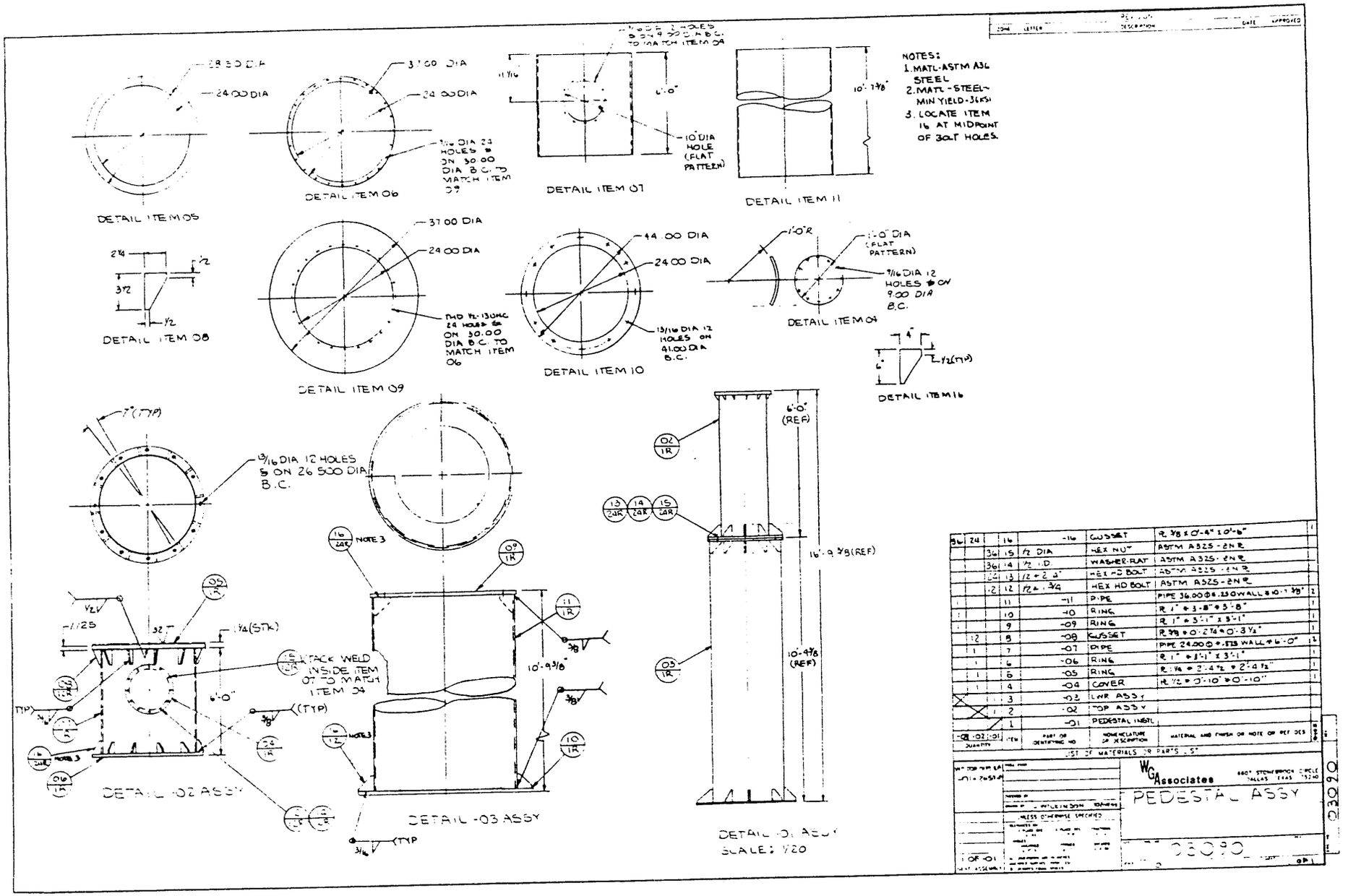

Figure 3.5-1 Pedestal

arrangement is a reasonable compromise. In this arrangement the tracking structure nests with the upper section, while the lower section provides the stiffness necessary to meet deflection requirements.

The lower section of the pedestal is a 36-in. outside diameter by .25-in. wall A36 steel pipe. It has an external flange with bolting holes at the bottom for installation on foundation studs. At its upper end the lower section is flanged internally. The underside of the flange is gusseted to the pipe to distribute the loads and reduce stresses on the relatively thin wall pipe. The internal flange has a tapped hole bolt pattern for attachment to the upper section.

The upper section of the pedestal is a 24-in. diameter standard (.375-in. wall) welded, A36 or equivalent, steel pipe. At each end it is welded to an identical flange with a bolting pattern for interfacing with the azimuth drive and the lower section of the pedestal, respectively. Both flanges are gusseted to minimize deflections. A port, with cover plate, is provided in the pipe for access to the azimuth drive motor for installation and maintenance purposes. The perimeter of the port is reinforced to restore the structural integrity of the pipe.

3.6 Structural Analysis

In the absence of any test data for faceted dish configurations, the wind loads used in the analysis of the FSS were based on LTV aerodynamic data. These data resulted from wind tunnel tests of a solid parabolic reflector structure; these tests were originally conducted in support of LTV's work in the large earth station antenna field [Ref. 6]. The LTV modeling more closely approximated the faceted dish configuration than did models tested by MIT, JPL, Andrews Corp., and others. Whereas the other tests were run on smooth parabolic shells, the LTV model included a backup structure similar to that used in the faceted dish design.

It should be noted that this the analysis does not account for the drag reduction due to spaces between facets; therefore, the analysis overpredicts loads and moments. Accordingly, it is reasonable to conclude that the analysis is conservative in this regard, i.e., design loads are greater than the dish would experience under similar wind load conditions.

The analysis was performed to insure that the structure complies not only with the functional criteria specified in the SOW but also with the requirements of the AISC code. The AISC code establishes design standards to insure the integrity of the structure. Compliance with this code is mandatory for any structure in the public domain and is invariably contractually required throughout industry. The code was meticulously followed in the design of the faceted stretched-membrane dish.

3.6.1 Discussion

Computerized finite-element techniques and classical structural analysis were used to design and evaluate the structure. The wind coefficients were taken from LTV wind tunnel data. The final specifications require the system to operate with required accuracy in a 16.7 mph wind gusting to 27 mph, and with degraded performance in winds gusting to 35 mph. The system must be able to drive to stow in winds gusting to 50 mph and survive winds gusting to 90 mph in the stowed position.

A finite-element model was constructed to represent the faceted dish structure. The model consists of a series of line members with full properties, and membrane and shell elements to simulate plate and panel sections. Ordinary rules of finite element-modeling were followed. The node intersections were chosen to best represent the elastic (centroidal) axis of intersecting members. Panels were broken into finite numbers of sub-elements to obtain low aspect ratios, thus assuring accurate computational results.

In the model, the intersections of all connecting members are assumed to be at a given node. Consideration of the member cross-section properties and the overall length ratios of structural members readily reveals that secondary bending due to elastic axis mismatch, where it might exist, produces essentially no effect on the overall strain energy of the system. Since the shear panels are capped, the finite element assumption of a series of membrane elements is legitimate for structural simulation purposes.

For dead weight deflection calculations, the structural model is assumed to be fixed in space; gravity is rotated as shown in Figure 3.6-1 to simulate varying collector elevation angles. At a particular elevation angle, the gravity vector for each structural element is resolved into orthogonal vectors with one operating parallel to the Y axis and one operating parallel to the Z axis.

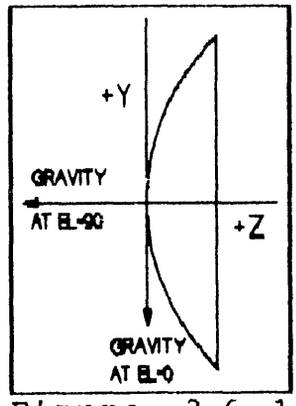

Figure 3.6-1
Gravity Vector

A finite-element program named SPACE V [Ref. 7] was used for the analysis of the stretched-membrane dish. SPACE V is a proven code that has been used in the antenna industry for 25 years. The program is applicable to the analysis and reporting of members with respect to AISC code requirements. It has excellent plotting capabilities that aid in both pre- and post-analysis, and it allows the user the freedom of interactive programming.

The faceted dish design was altered several times, using the interactive feature of SPACE V, to optimize various sections of the structure and, in the final analysis, to optimize the entire structure. The effects of even slight member or geometry changes were readily evaluated.

In the finite-element model used in this analysis, a node numbering system was selected for grouping various elements of the structure together with the same 100's series of numbers. All finite-element loading was introduced at nodal points, and member density factors

were input using data from the drawings to accurately represent the dead weight loading of the structure.

Nodal deflections were used to evaluate the dish pointing accuracy, and calculated stresses were used to size members. In order to achieve an optimal design, the process was iterative. Dish fabrication considerations were invoked at every step of the analysis to place practical limitations on the design. Maximum effort was made to establish commonality of members while remaining weight-conscious, since sizing each member as an individual component based on critical design would lead to a costly structure made from many dissimilar parts.

The elevation wind torque loads were developed using coefficients extracted from LTV wind tunnel test data. The worst-direction 50 mph wind result is shown in Figure 3.6-2.

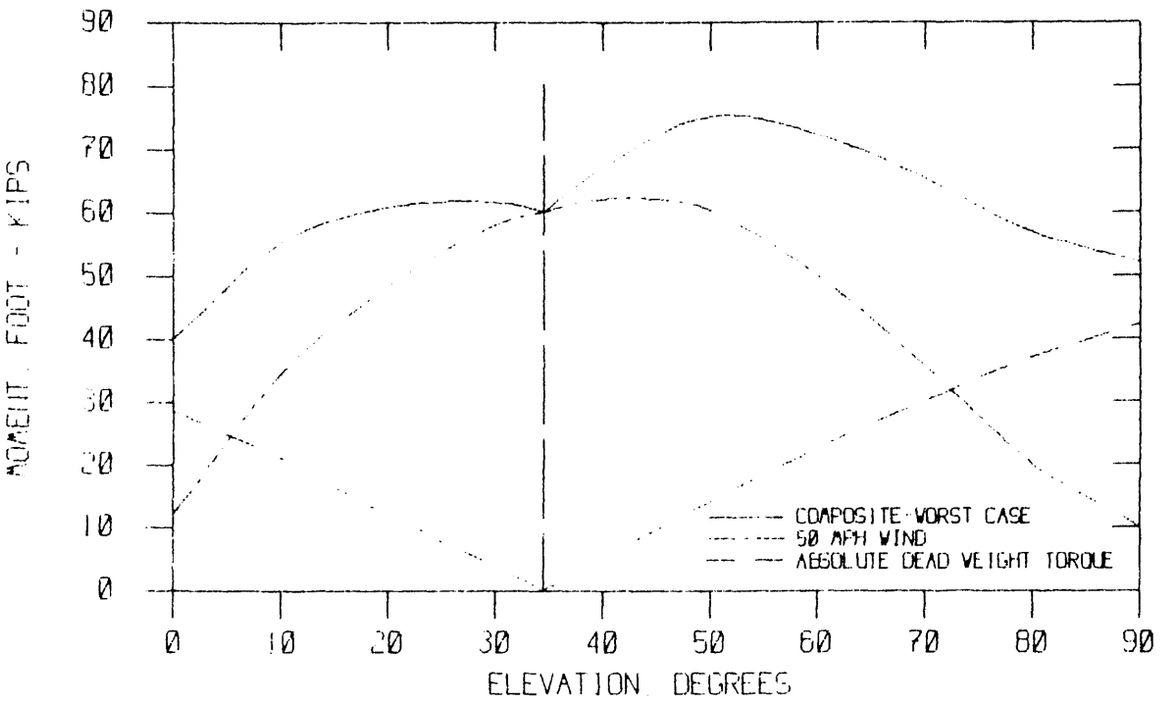

Figure 3.6-2 Elevation Torque Load, 50 MPH Wind

The absolute value of the elevation dead weight (gravity) torque loads in Figure 3.6-2 are the resultant moments from calculation of the actual element weights and moment arms acting about the elevation axis. These loads are larger than anticipated because the CG of the moving structure is not on the elevation axis. When the collector is pointed toward the horizon, the CG is above the elevation axis and on the receiver side. As a result, the gravity torque load passes through zero as the dish elevation angle increases, and the structure experiences a gravity torque load reversal. The composite elevation torque load in Figure 3.6-2 is the sum of the worst-direction wind torque and the absolute value of the gravity moment.

The azimuth torque load is the unbalanced wind torque since there is no unbalanced dead weight torque load in azimuth. The azimuth torque for a 50 mph wind as a function of wind direction relative to the azimuth pointing angle, is shown in Figure 3.6-3.

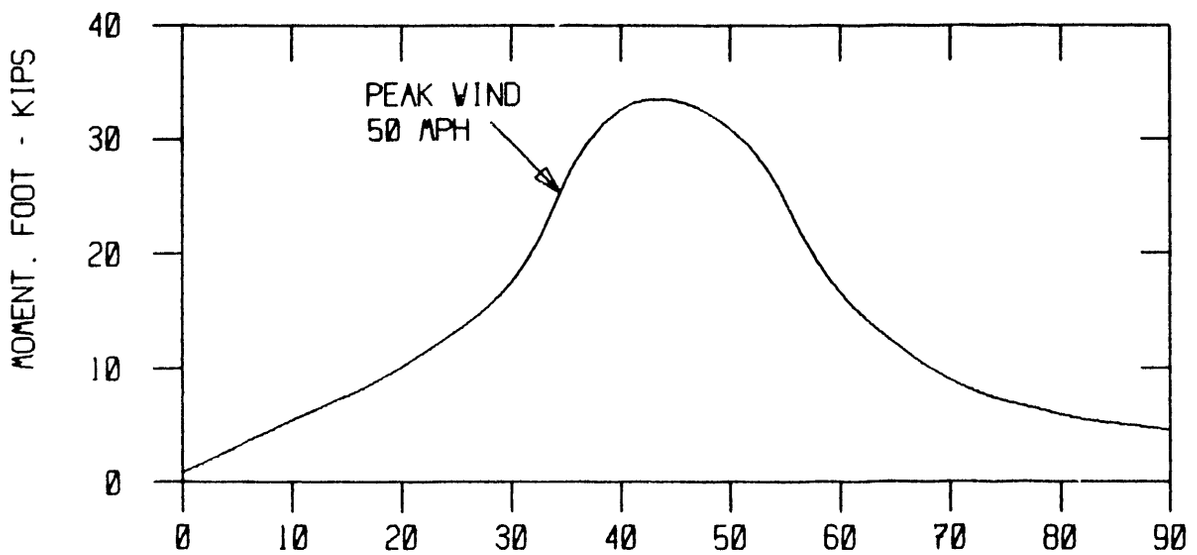

Figure 3.6-3 Azimuth Torque Load, 50 MPH Wind

The load curves in both Figures 3.6-2 and 3.6-3 represent peak loads for the worst case drive-to-stow condition, since the wind plots use the peak wind values.

The combined loads were used to calculate deflections and stresses for the pedestal, drives, and the moving structure. These data were used to determine the required compliance of the system. (Compliance is the inverse function of spring rate, usually expressed in radians/ ft-lb.) These compliances were then used to calculate the resonant frequency of the system.

The pedestal and drive elevation deflections due to the operating wind are shown in Figure 3.6-4.

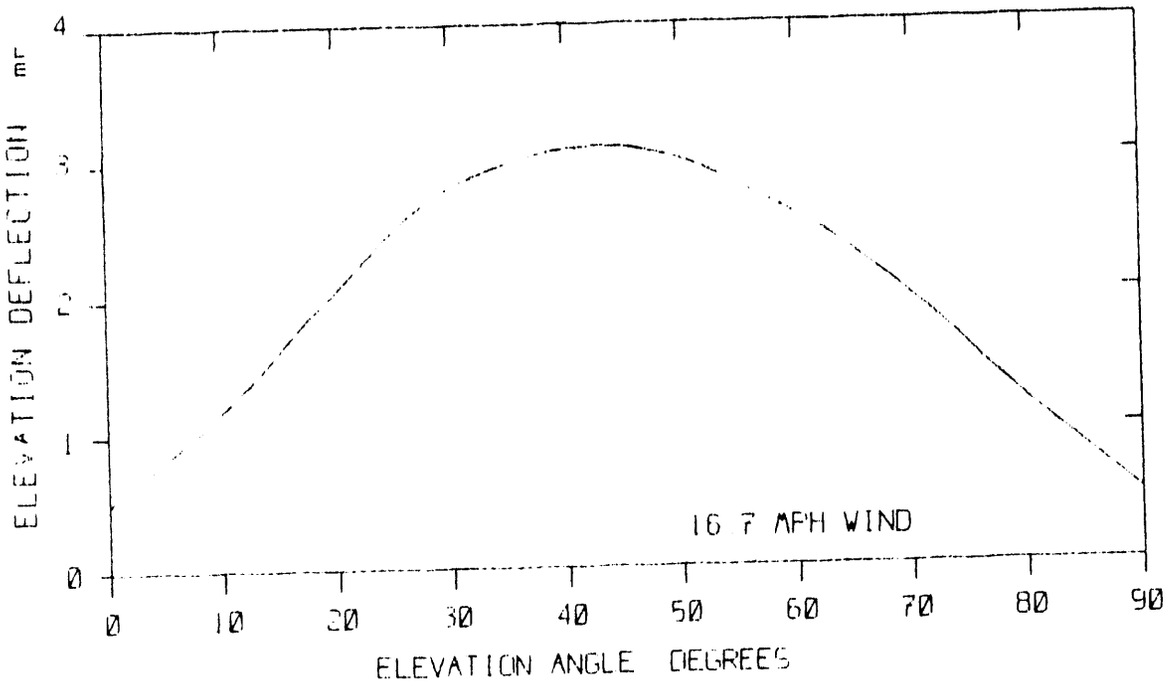

Figure 3.6-4 Pedestal and Drive Elevation Wind Deflection

The pedestal and drive azimuth deflections due to the operating wind are shown in Figure 3.6-5.

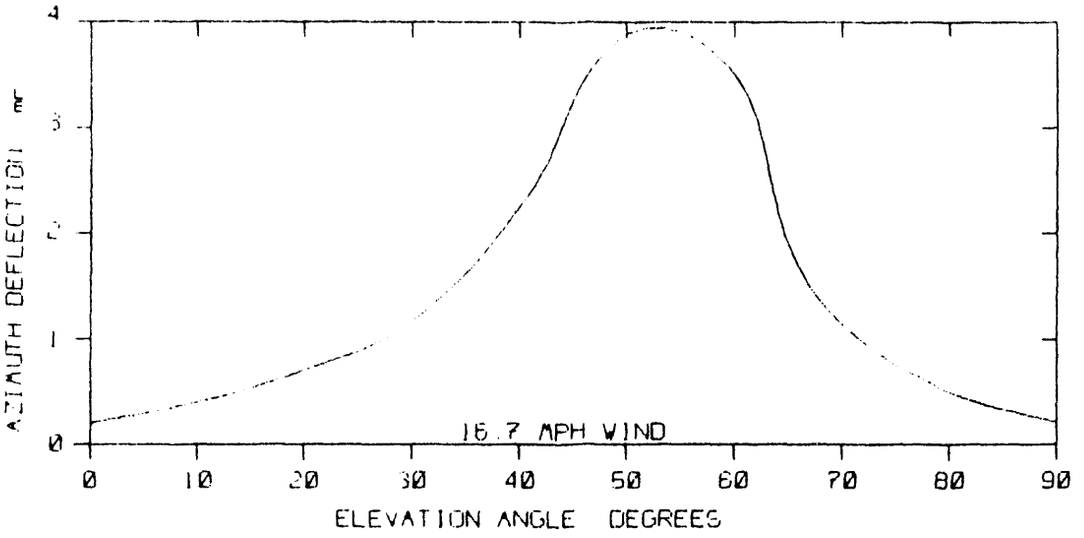

Figure 3.6-5 Pedestal and Drive Azimuth Wind Deflection

The pedestal and drive elevation deflections due to the dead weight are shown in Figure 3.6-6.

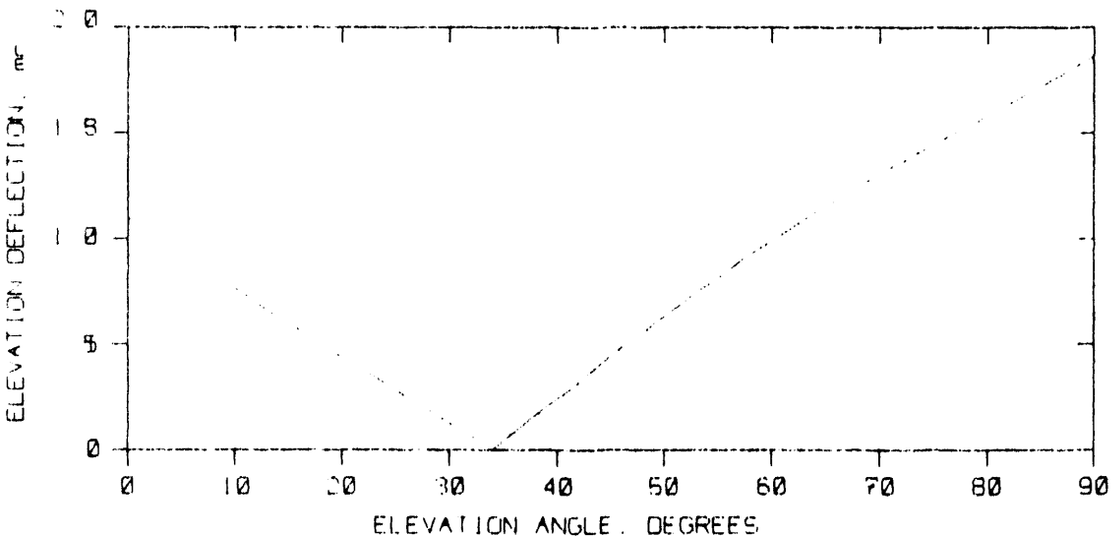

Figure 3.6-6 Pedestal and Drive Elevation Dead Weight Deflection

Finally, the deflections of the PCA support structure due to dead weight are plotted in Figure 3.6-7. These curves show the effects on error accountability when the dish is aligned at elevation angles of 45 deg. and 90 deg., respectively. The curves reveal that the deflection margins between the travel limits - 0 deg. and 90 deg. - are approximately the same for each alignment condition. However, aligning the dish at 45 deg. has the effect of dividing the deflection error around a mean of 0 deg. Thus the RMS error over the full 90 deg. of travel is significantly less than when the dish is aligned at zenith.

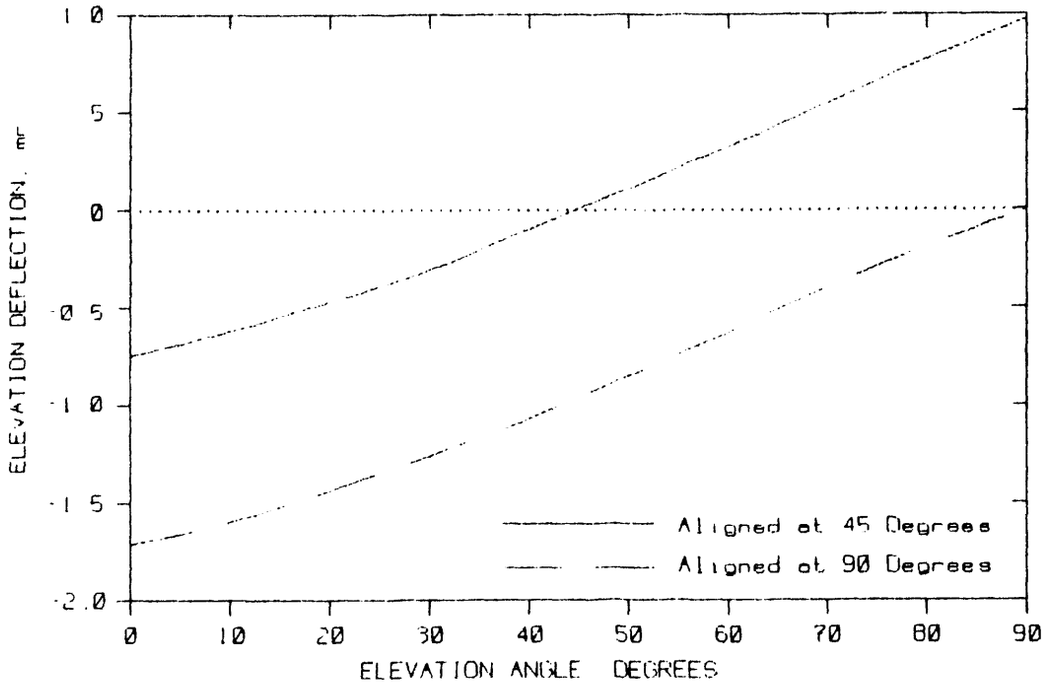

Figure 3.6-7 PCA Support Dead Weight Deflection

3.6.2 Summary

A summary of the facet pointing errors is presented in Tables 3.6-I, 3.6-II and 3.6-III. In Table 3.6-I are listed the worst-case deflections due to dead weight. These occur when the collector is pointed horizontally after it has been correctly aligned at zenith. (The facet numbering is shown in Figure 2.1-1.). The Y deflection and X deflection values are the angular deflection of the line-of-sight of the facet in

the Y and X planes, respectively. A negative value in Y indicates that the facet line-of-sight is below 0 deg. elevation. A negative value in X indicates that the line-of-sight has moved to the left when looking into the collector.

Table 3.6-I Worst Case Dead Weight Deflection Zenith Alignment

Elevation Angle = 0 deg.
Engine Deflection = -1.716 mr
Y Engine is relative to Engine Deflection
Y Diff is relative to Y Engine Average

Facet #	Y Defl. mr	Y Engine mr	Y Diff. mr	X Defl. mr
1	-1.665	.051	-.531	0.000
2	-1.405	.311	-.271	0.000
3A	-1.423	.293	-.289	.581
3B	-1.423	.293	-.289	-.581
4A	-.438	1.278	.696	-.156
4B	-.438	1.278	.696	.156
4C	-.938	.778	.196	.457
4D	-.938	.778	.196	-.457
5A	-1.309	.407	-.175	.413
5B	-1.309	.407	-.175	-.413
5C	-1.162	.554	-.028	-.630
5D	-1.162	.554	-.028	.630
Average	-1.134	.582	.000	.000
Standard Deviation		.369	.369	.436

These errors, although systematic, cannot be completely biased out of the system due to the complex gravity-caused movement of the structure. The control system can make a correction for the collector as a unit but not for individual facets. If the control system corrected for the average error in Y relative to the engine position ("Y Engine" column in the table), the residual errors would be the values in the "Y Diff." column in the table.

In Table 3.6-II, the deflections due to dead weight are listed for a collector pointed at the horizon after it has been correctly aligned at 45 deg. elevation.

Table 3.6-II Dead Weight Deflection 45 deg. Align

Elevation Angle = 0 deg.
Engine Deflection = 0.748 mr
Y Engine is relative to Engine Deflection
Y Diff is relative to Y Engine Average

Facet #	Y Defl. mr	Y Engine mr	Y Diff. mr	X Defl. mr
1	-.950	-.202	-.216	0.000
2	-.443	.305	.291	0.000
3A	-.831	-.083	-.097	.357
3B	-.831	-.083	-.097	-.357
4A	-.989	-.241	-.255	.375
4B	-.989	-.241	-.255	-.375
4C	-.609	.139	.125	-.188
4D	-.609	.139	.125	.188
5A	-.668	.080	.066	.249
5B	-.668	.080	.066	-.249
5C	-.609	.139	.125	-.510
5D	-.609	.139	.125	.510
Average	-.734	.014	.000	.000
Standard Deviation		.171	.171	.323

Comparison of Tables 3.6-I and 3.6-II shows that when the dish is aligned at 45 deg. and 90 deg. (zenith), the Y standard deviations are 0.171 mr and 0.369 mr, respectively. Thus, by aligning the collector at, or near, the middle of the operating elevation range, facet mounting point Y deflection errors are reduced by a factor of about 2. The improvement in the X deflections is approximately 35%.

In Table 3.6-III, the error encountered by each facet due to wind loads is presented. The value at degraded operational conditions is proportional to the specified wind velocities squared.

Table 3.6-III 20 MPH Wind Deflection

Wind Into the Face of Collector
Elevation Angle = 0 deg.

Facet #	Y Defl. mr	Y Diff. mr	X Defl. mr
1	-.156	-.054	0.000
2	-.118	-.016	0.000
3A	-.115	-.013	.081
3B	-.115	-.013	-.081
4A	-.112	-.010	.042
4B	-.112	-.010	-.042
4C	-.065	.037	-.074
4D	-.065	.037	.074
5A	-.104	-.002	.054
5B	-.104	-.002	-.054
5C	-.077	.025	-.082
5D	-.077	.025	.082
Average	-.102	.000	.000
Standard Deviation		.025	.063

The total collector deflection error consists of facet mount deflection errors and pedestal/drive errors resulting from wind loads and structural dead weight. The net overall, gravity-induced deflection of the line-of-sight relative to the receiver is repeatable. To the extent that gravity-induced errors can be accurately measured, they may be biased out with the control system. This is also true of errors due to structural and axis alignment. However, the wind-induced errors cannot be biased out of the system.

The structure was evaluated for compliance with the AISC code as well as stated deflection criteria. As in most large-aperture satellite earth stations, the driving criteria was stiffness of the structure rather than stress levels. When stiffness requirements were satisfied, the stress ratios were well below acceptable limits in the structure. Stresses of 5,000 to 8,000 psi at worst case conditions are typical throughout the structure. The slenderness ratio (L/R) requirement of 120:1 used for column buckling design dominates in the selection of most truss cap members rather than the allowable stress. Shear stresses within plate elements are well within the acceptable range for the thickness-to-width ratios of the

panel elements. Plate thicknesses in the transition assembly were increased beyond those indicated by calculations to provide a greater buckling safety factor in this critical element.

The maximum stress encountered in the structure is 18,000 psi; it occurs only locally in a few members at maximum loading conditions. Thus, based on minimum yield of A36 steel (36,000 psi), safety factors throughout the structure are 2:1 or greater. Individual stresses in special components such as gear teeth, support pins and bolt connections are all within the limits of the special materials used in their design and the recommendations of the manufacturers. The resonant frequency of the total structure above grade, including the mass of the facets and the PCA, is about 2 Hz in both azimuth and elevation.

3.7 Weight Summary

The weight of the faceted dish is summarized in this section. The weights were developed from the geometry inputs to the finite element analysis program. Where structure was not included in the analysis, such as brackets and fasteners, the weights of the omitted elements were manually calculated and added to the computer output. In addition, some sub-assemblies were selected for independent weight analysis to verify the accuracy of the computer data. The variance was less than 3%.

The breakdown of the faceted dish weights by major assembly and the total weight are shown in Table 3.7-I. The total unit weight of the 14.86 pounds per square foot of facet area is further analyzed below.

1. The dish structure, which includes the FSS, the transition assembly, the PCA support structure, and the hardware and brackets, weighs 15,000 pounds, or 10.24 lb/sq.ft. of facet.
2. The tracking structure, which includes the weight of the facets in addition to that of the dish structure, weighs 18,150 pounds, or 12.39 lb/sq.ft. of facet.

3. The drives and pedestal, including the stiffarm assembly, are considered the base structure. These total 3,620 pounds, or 2.45 lb/sq.ft. of facet.

Table 3.7-I Faceted Dish Weight Summary

	WEIGHT LBS.		WEIGHT PER SQ.FT. OF FACET AREA	
• Structure				
Facet Support Structure	9,700		6.62	
Transition Assembly	3,250		2.22	
PCA Support Structure	1,750		1.19	
Hardware & Brackets	300		0.20	
Stiffarm	400		0.27	
Pedestal	2,320		1.58	
Sub-total, Structure Weight		17,720		12.10
• Facets	3,150			
Sub-total, Facet Weight		3,150		2.15
• Drives				
Elevation	300			
Azimuth	600			
Sub-Total, Drives		900		0.61
Total Collector Weight		21,770		14.86

4.0 TRACKING CONTROL SYSTEM DESIGN

The tracking control system design objectives were to:

1. design a system that would provide sufficient tracking accuracy,
2. assemble the system from existing major units to the extent possible, and
3. minimize the costs consistent with the first two objectives.

As indicated in Section 2.6, several alternatives were investigated before deciding on the configuration. Based on the present perception of the accuracy required, the selected configuration satisfies all three objectives. This configuration is described below.

4.1 System Design

The tracking control system block diagram is shown in Figure 4.1-1.

The control system employs a central computer and a tracking control processor, called the front end processor (FEP), to provide passive tracking. In passive tracking, the position of the sun is calculated and this position, after transformation into the collector coordinate system, is compared to the collector position. Motor control signals then are generated to reduce the difference to zero. As will be seen later, this task is divided between the central computer and the FEP. The FEP is an existing solar collector tracking control processor, manufactured by Electronic Innovations Corp. and Advanced Thermal Systems of Englewood, CO, that is altered to meet the requirements of this project.

The FEP generates commands for the motor controllers that control the power for the motors.

The drive-motor controllers are flux-vector inverters to accommodate a "bang-bang" control that is compatible with the existing processor and yet provides sufficient accuracy. The controllers drive three-phase induction motors.

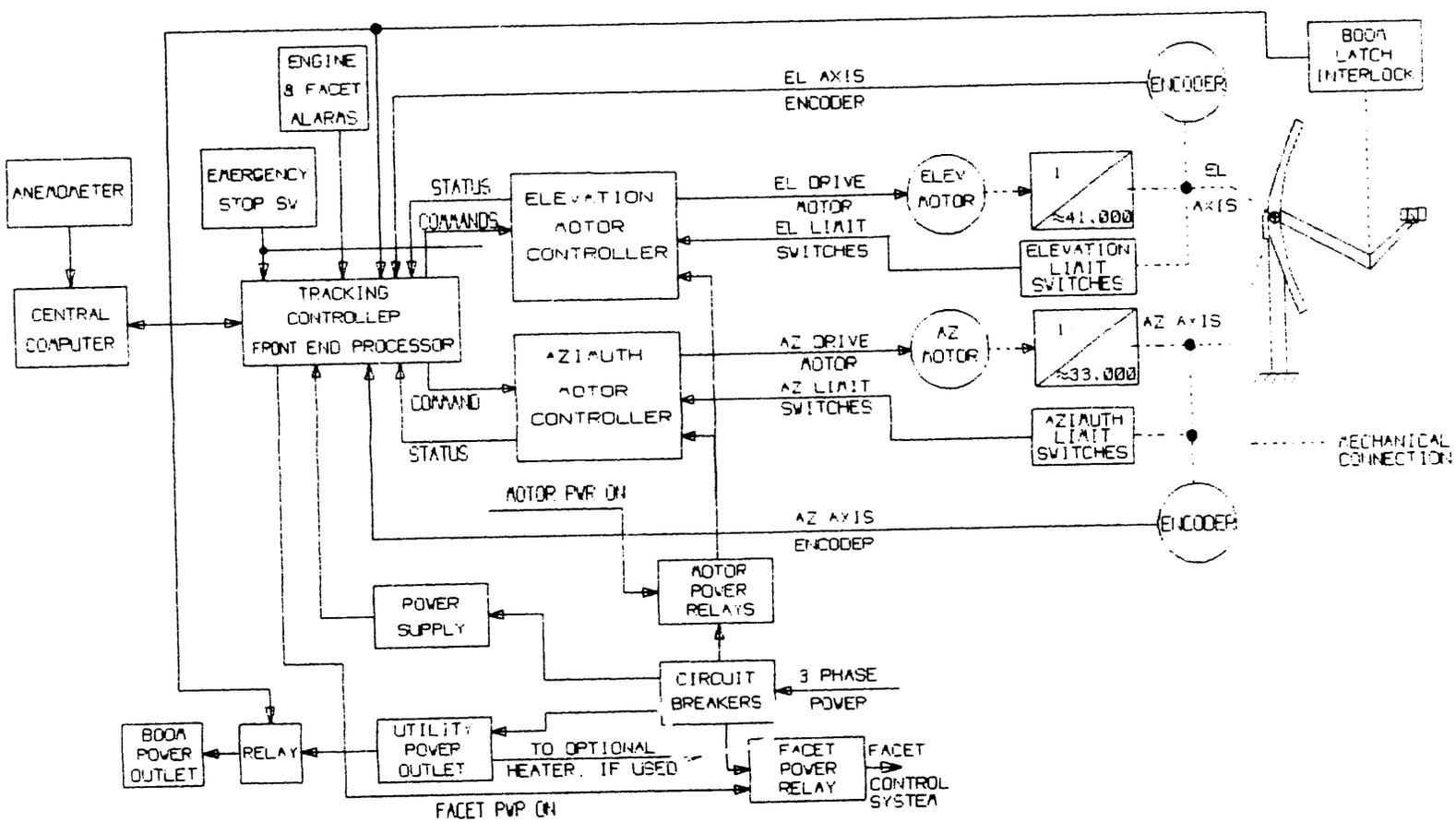

Figure 4.1-1 Tracking Control System Block Diagram

The collector is equipped with azimuth and elevation limit switches that not only interrupt the Run Direction command to the motor controllers but also provide a fault signal to the FEP. The limit-switch circuitry is arranged to inhibit the command to drive the collector further into the limit. The control system will allow the collector to be driven out of the limit position under power.

The collector position is monitored with incremental encoders coupled directly to the collector axes to provide the required accuracy. Each encoder is equipped to provide an index pulse to initialize a position counter in the FEP. If needed, limit-switch actuation can serve as a backup for the index pulses.

The PCA support structure has provisions for lowering the engine near ground level. An interlock switch prevents driving the collector except when the engine support is properly secured. When the support is not secured, this switch energizes a relay to provide power to a convenience outlet installed on the support structure. A temporary drive, such as a drill motor, may be plugged into the convenience outlet to raise and lower the engine.

Finally, provision is made to supply power under central computer control to the facet control system.

4.2 Central Computer

The central computer is compatible with an IBM Personal Computer. The division of tasks between the central computer and the FEP is a strong function of the FEP design. In the selected design, the central computer has the following functions. (For details, please see WG Associates Specification Control Drawing (SCD) number 03060.)

1. Provides the operator interface for control, status display, and capability for user-generated routines to control the collector.
2. Calculates the direction of the Sun.
3. Stores both the site and collector-specific data base items, e.g., site location, encoder initialization, etc.

4. Corrects the position commands to each collector to compensate for collector alignment and deflection errors.
5. Corrects the collector positions reported from each collector to compensate for collector alignment and deflection errors before display.
6. Provides acquisition and escape paths suitable to minimize danger of structural damage.

It is noted that items (4) and (5) above are in conflict with the requirements of the SCD, paragraph 3.1.3, which states that the corrections unique to a particular collector shall be made in the FEP. This requirement is intended to prevent overload of the communications link when a relatively large number of collectors are serviced by a single computer. This requirement was waived for the prototype system since there will only be one system for the central computer to service. Also, the central computer can easily handle more than a hundred collectors at a time. The system can be readily modified to comply with the SCD requirement.

4.3 Front End Processor (FEP)

In the selected design, the FEP has the following functions. (For details, please see WG Associates SCD number 03060.)

1. Provides for acceptance and execution of central computer control signals.
2. Transmits status data for the central computer status display. These data include internally generated status, external status (such as motor controller status and engine and facet alarms), and collector position.
3. Performs decoding of the encoder signals and updates the position counters accordingly. This includes use of the index pulses to check the position counters and update them, if necessary.
4. Generates separate commands for application of power to the motor controllers and to the facet controller.
5. Generates appropriate commands for the motor controllers. The commands for each controller include:

- a Forward command to run the motor in one direction
- a Reverse command to run the motor in the other direction and
- a command to select one of four preset output frequencies from the controller for four different motor speeds.

4.4 Motor Controllers

The motor controllers are Polyspede Electronics Corporation Model XLT solid-state, adjustable-frequency motor controllers. These controllers convert the applied 200/230 volt, three-phase, 50/60 Hz power to a fixed potential DC. This DC voltage is converted by a three-phase, sine-coded, pulse width modulated inverter to an adjustable frequency (from 1 to 120+ Hz), 200/230 volt, three-phase power.

The controllers have a two binary bit input that selects one of four frequencies that are programmable through a manual entry keyboard. A low motor speed (commanded by a low controller output frequency) is used for normal elevation tracking and for azimuth tracking at low elevation angles. An intermediate speed is used for azimuth tracking at moderate elevation angles. Rated speed is used for normal slewing and azimuth tracking at high elevation angles. Acquisition of, and escape from, the sun uses about twice the rated speed.

Each controller has a command input for forward and another for reverse. These inputs are used by the FEP to pulse the motors to produce "bang-bang" tracking. In this case the controller output frequency (analagous to velocity command) will be set to a low value to prevent excessive motor velocity while still producing the required torque. This is the "soft bang-bang" tracking drive mode described in this report. As explained in Section 2.6, this mode results in less drive error than the "bang-bang" mode where full frequency and power is used during the "on" period.

4.5 Axis Encoders

The encoders used to determine the axis positions are BEI Motion Systems Company model number H25D-SS-9000-M5-ABZ-5406-LED-

SM16-S incremental encoders. They are heavy-duty industrial units with a NEMA Type 13 enclosure rating. They produce 9000 cycles per revolution so that with quadrature decoding in the FEP, there will be 36,000 counts per revolution (resolution is 0.01 deg. or 0.175 mr). The encoder also produces one index pulse per revolution for initializing the position counter in the FEP. The encoders will be adjusted at installation to locate this index position near the wake-up position.

5.0 COLLECTOR SYSTEM POINTING ERROR BUDGET

The FSS design is deflection driven, i.e., the structure is designed for maximum stiffness at operating conditions. Characteristic of an elevation-over-azimuth axis configuration, the gravity vector changes with the elevation pointing angle. This causes proportional variations in the dead weight deflections. By limiting these deflections, system performance of the faceted dish is enhanced since changes in optical efficiency with elevation angle variations are minimized. Moreover, a stiff structure minimizes movement of the facets and unintentional superpositioning of their images, thereby reducing the possibility of receiver damage.

The error budget for the support structure and the control system is shown in Table 5.0-I. The budget incorporates the wind and dead weight deflection results of the structural analysis (Section 3.6) along with other values from the trade-off studies.

The results shown in Table 5.0-1 are slightly better (1.19 mr compared to 1.28 mr in 16.8 mph winds) than the results in Table 2.6-IV. This is due to reductions in wind deflection values from the initial estimates that more than offset increases in dead weight deflections.

Table 5.0-I includes facet-pointing errors resulting from wind and gravity-induced deflections of the facet mounting planes. Facet alignment errors, slope errors and specularity errors are not addressed in Table 5.0-I or in this report. The individual facet-pointing errors due to dead weight deflections are shown for the worst case (errors at horizon with alignment at zenith) in Table 3.6-I, where the peak deviation from the average is approximately 0.7 mr in elevation and 0.6 mr in azimuth. The standard deviations are approximately 0.37 mr and 0.44 mr, respectively. The case where alignment is performed at 45 deg. is shown in Table 3.6-II. Here the peak deviations in elevation and azimuth are 0.3 mr and 0.5 mr, respectively. The standard deviations are 0.17 mr and 0.32 mr,

respectively. Corresponding deflection values for a 20 mph wind are shown in Table 3.6-III. In this case, the peak deviations in elevation and azimuth are 0.05 mr and 0.08 mr, respectively. The standard deviations are 0.025 mr and 0.063 mr.

The budgeted error values demonstrate that the faceted dish exhibits stiffness characteristics consistent with the SOW performance specifications.

Table 5.0-I Collector System Pointing Error Budget
(Exclusive of individual facet errors)

FINAL DESIGN SYSTEM
WITH POLYSPEDE CONTROLLERS & AXIS ENCODERS

ERROR SOURCE 3 SIGMA OR PEAK VALUES	16.8 MPH WIND AZIMUTH	16.8 MPH WIND ELEVATION	27 MPH WIND AZIMUTH	27 MPH WIND ELEVATION
	Millirad	Millirad	Millirad	Millirad
Drive & Ped. Wind Def	.40	.31	1.03	.80
Facet vs Engine Wind Def	.05	.10	.13	.26
Facet vs Engine Dead Wt.	.00	.12	.00	.12
Drive & Ped Dead Wt.	.00	.38	.00	.38
Ped Lev & El Axis Align	.20	.20	.20	.20
Bang-Bang w/PolySpede	.50	.50	.50	.50
Prediction Error	.20	.20	.20	.20
Time Error (5 Seconds)	.40	.00	.40	.00
Resolver Error	.30	.30	.30	.30
RSS AXIS RESULT	.86	.83	1.29	1.13
RSS TOTAL		1.19		1.72

NOTES: All of the error source values are estimated peak values for the conditions stated except the dead weight values and Pedestal and Axis Alignment. These sources are assumed to be corrected in the control system with a residual of 20% of the peak value. The errors in each axis are combined by an RSS calculation for each axis. The values for the axis total are also the result of an RSS calculation.

Thus, it can be expected that, for a 16.8 mph wind gusting to 27 mph, the result of the 16.8 mph case represents a reasonable estimate of the probable error (one sigma). The result of the 27 mph case represents a reasonable estimate of the three sigma error for a 16.8 mph wind gusting to 27 mph.

6.0 COLLECTOR PRODUCTION AND INSTALLATION COST

The cost of production and installation of faceted stretched-membrane dish collectors is described in this section. (The costs presented do not include facet and facet control system costs; for these, please refer to references 2 and 3.) Costs are projected for collector production quantities of 50, 100 and 1,000 units per year. The processes identified and costed include: fabrication of the collector support structure, procurement of the tracking drives, procurement of the control system, procurement of miscellaneous specialty items, the shipping costs for both facets and support structures, and the installation and alignment of facets and support structures. The analysis incorporates subcontractor and vendor quotes, catalog pricing, and time and material estimates.

The three annual production quantities considered and their unit costs are summarized in Table 6.0-I.

Table 6.0-I

COLLECTOR PRODUCTION COST SUMMARY

Component/Task	Cost per Collector @ Annual Quantity of: 50	100	1,000
Collector Tracking Structure	$35,324	$32,883	$27,041
Tracking Drives	7,480	6,458	5,173
Tracking Control System	3,230	2,692	2,110
Specialty Items	1,767	1,765	1,688
Freight	1,604	1,575	1,552
Installation	13,954	13,749	13,330
Total Cost	$63,359	$59,122	$50,894

Specific ground rules and methodology used in developing these cost estimates are listed below.

1. Collector support structure fabrication - indirect cost rates factored into labor rates for each level of annual collector production, are as follows:

	50ea	100ea	1,000ea
Overhead - % of direct labor	85.00%	80.75%	76.50%
G&A - % of cost before G&A	9.00%	8.55%	8.10%
Fee - % of cost through G&A	7.00%	7.00%	5.00%

2. Depreciation of capital equipment (e.g., facet shipping racks) is calculated on a seven year - straight-line basis, with no salvage value.

3. Support structure fabrication - subcontractor budgetary time and material estimates are used for quantity of 50 units annually, with Wright Learning Curve of 93% applied for larger quantities.

4. Tracking drive costs are estimates based on vendor quotes for quantities of 1, 2, 10, and 100 per year. The cost for a quantity of 1,000 was obtained by extending the curve.

5. Shipping costs - facet loading manhours and freight rates are per facet supplier's estimates; WGA's labor-rate estimates were applied to the supplier's time estimates. Support structure loading is included in the subcontractor's estimates; freight, at $1,250 per unit, and unloading time are WGA's estimates. No time or direct cost improvements with larger quantities are factored into the estimates.

6. Installation - facet, control system, and structure installation times are per supplier estimates, with WGA labor- rate estimates. Per-unit crane rental times of: (a) truck crane, 4 hours @ $60/hr.; (b) manlift, 13 hours @ $20/hr.; (c) 25-ton crane, 48 hours @ $75/hr.; are per suppliers' estimates. Due to the one-collector-per-site scenario, no direct cost improvement with quantity

increases is factored into these estimates. A four-man installation crew is assumed , with $250/man travel cost per site, and $100.00 per man/day per diem and ground transportation. Support structure installation is estimated to require 6 days. Control system installation is based on a 95% Wright Learning Curve. Installation labor rates are factory labor rates plus 20%.

7. No costs are included for foundation and site wiring (as differentiated from collector wiring), since they are site specific. Also, no costs are included for a central computer, estimated at $1,200.00, with a capacity of up to 200 collectors at each installation site.

8. All costs are 1991 dollars, with no provision for inflation.

9. Tax (both income and sales/use) implications are ignored.

To summarize, it was assumed for all cases that only one collector would be installed on each site, with subcontractor activities and materials procurement supervised and coordinated by a general contractor/system owner. All costs included are those external to the general contractor/system owner; i.e., no general contractor's indirect cost recovery or management fee are factored into the totals. For the most part, the costs included are per vendor quotes or budgetary estimates for the various quantities required. Learning curve estimates (Wright Curve) were utilized in calculating labor hours for the support structure fabrication (93%) and control system installation (95%). The support structure estimate began with a subcontractor estimate for an order quantity of 50 units as the baseline, while the control system installation used the vendor's estimate for one unit.

The results of the cost analysis are considered to be conservative, due to several factors:

1. The use of an order quantity of 50 units as the baseline for the learning curve estimate for support structure fabrication yields a relatively small improvement factor, even at an annual production of 1,000 units.
2. The "one-collector-per-site" scenario precludes the possibility of cost savings in items such as installer's travel/per diem costs, improvement in installation time, and crane/manlift rentals. (Note: In the 1,000-collector-per-year estimate, crane and manlift rentals for one year will total over $4 million.)
3. Most significant, the analysis presumes no change of the collector design beyond that of the prototype, even for the 1,000-collectorper-year scenario.

In a market demanding hundreds of these collectors annually, the product would be redesigned to take advantage of labor-saving techniques normally associated with large-scale, automated manufacturing. As examples, extensive use could be made of castings for end fittings; truss sections could be press-formed, beaded sheet metal; and automatic welding and/or riveting, even robotics, could be employed. The result would be fewer piece parts and joints, less material handling and fixturing, and reduced linear inches of welding. It is estimated that with these methods the cost of fabricating the collector support structure in large quantities could be reduced from $27,000 to the $16,000-18,000 range.

The costs are detailed for the three annual production levels in Tables 6.0-II, 6.0-III, and 6.0-IV. Specialty items and tracking drive costs are detailed in Table 6.0-V.

Table 6.0-II Annual Production Quantity - 50 Collectors

Component/Task	Labor Hrs	Labor $	Matl/ ODC	Total
Collector Support Structure--				
Truss Fabrication	709.00	13,003	2,333	15,336
Spine Assembly	77.00	1,412	583	1,995
PCA Mount	77.00	1,412	641	2,053
Transition Structure	335.00	6,144	4,082	10,226
Hardware	N/A	N/A	816	816
Paint & Paint Supplies	N/A	N/A	1,633	1,633
Fab Facet Mounts & Tee Lugs	178.00	3,265	0	3,265
Trial Assy, Pkg, Loading	0.00	0	0	0
Coll. Supp. Struct. Totals	1,376.00	25,236	10,088	35,324
Tracking Drives--				
Azimuth Tracking Drive			4,385	4,385
Elevation Tracking Drive			3,095	3,095
Tracking Drives Totals			7,480	7,480
Control System			3,230	3,230
Specialty Items			1,767	1,767
Shipping Costs-Facets--				
Racks (Amort of Capital)			57	57
Loading/Unloading	1.80	33	0	33
Freight Cost			264	264
Total Shipping-Facets	1.80	33	321	354
Shipping Costs-Structure--				
Freight Cost			1,250	1,250
Total Shipping-Structure	0.00	0	1,250	1,250
Facets Installation--				
Install Control System	2.04	45	0	45
Install Facet	8.04	177	0	177
Align Facet	8.04	177	0	177
Focus Adjustment	8.04	177	0	177
Manlift (13 Hrs)			260	260
Crane Rental (4 Hrs)			240	240
Total Facets Installation	26.16	576	500	1,076
Structure Installation--				
Labor	192.00	4,226	0	4,226
Wiring	16.00	352		352
Crane Rental (48 Hrs)			3,600	3,600
Total Structure Inst.	208.00	4,578	3,600	8,178
Control System Inst.			1,300	1,300
Installers Travel/Per Diem--				
Airfare (4 r/t tickets)			1,000	1,000
Per Diem/Trsp(24 ManDays)			2,400	2,400
Total Travel/Per Diem			3,400	3,400
Total Costs	1,611.96	30,423	32,936	63,359

Table 6.0-III Annual Production Quantity - 100 Collectors

Component/Task	Labor Hrs	Labor $	Matl/ ODC	Total
Collector Support Structure--				
Truss Fabrication	659.37	11,766	2,323	14,089
Spine Assembly	71.61	1,278	581	1,859
PCA Mount	71.61	1,278	639	1,917
Transition Structure	311.55	5,560	4,065	9,625
Hardware	N/A	N/A	813	813
Paint & Paint Supplies	N/A	N/A	1,626	1,626
Fab Facet Mounts & Tee Lugs	165.54	2,954	0	2,954
Trial Assy, Pkg, Loading	0.00	0	0	0
Coll. Supp. Struct. Totals	1,279.68	22,836	10,047	32,883
Tracking Drives--				
Azimuth Tracking Drive			3,720	3,720
Elevation Tracking Drive			2,738	2,738
Tracking Drives Totals			6,458	6,458
Control System			2,692	2,692
Specialty Items			1,765	1,765
Shipping Costs-Facets--				
Racks (Amort of Capital)			29	29
Loading/Unloading	1.80	32	0	32
Freight Cost			264	264
Total Shipping-Facets	1.80	32	293	325
Shipping Costs-Structure--				
Freight Cost			1,250	1,250
Total Shipping-Structure	0.00	0	1,250	1,250
Facets Installation--				
Install Control System	2.04	44	0	44
Install Facet	8.04	172	0	172
Align Facet	8.04	172	0	172
Focus Adjustment	8.04	172	0	172
Manlift (13 Hrs)			260	260
Crane Rental (4 Hrs)			240	240
Total Facets Installation	26.16	560	500	1,060
Structure Installation--				
Labor	192.00	4,111	0	4,111
Wiring	16.00	343		343
Crane Rental (48 Hrs)			3,600	3,600
Total Structure Inst.	208.00	4,454	3,600	8,054
Control System Inst.			1,235	1,235
Installers Travel/Per Diem--				
Airfare (4 r/t tickets)			1,000	1,000
Per Diem/Trsp(24 ManDays)			2,400	2,400
Total Travel/Per Diem			3,400	3,400
Total Costs	1,515.64	27,882	31,240	59,122

Table 6.0-IV Annual Production Quantity - 1000 Collectors

Component/Task	Labor Hrs	Labor $	Matl/ ODC	Total
Collector Support Structure--				
Truss Fabrication	521.09	8,873	2,270	11,143
Spine Assembly	56.59	964	568	1,532
PCA Mount	56.59	964	624	1,588
Transition Structure	246.21	4,193	3,973	8,166
Hardware	N/A	N/A	795	795
Paint & Paint Supplies	N/A	N/A	1,589	1,589
Fab Facet Mounts & Tee Lugs	130.82	2,228	0	2,228
Trial Assy, Pkg, Loading	0.00	0	0	0
Coll. Supp. Struct. Totals	1,011.31	17,222	9,819	27,041
Tracking Drives--				
Azimuth Tracking Drive			2,790	2,790
Elevation Tracking Drive			2,383	2,383
Tracking Drives Totals			5,173	5,173
Control System			2,110	2,110
Specialty Items			1,688	1,688
Shipping Costs-Facets--				
Racks (Amort of Capital)			7	7
Loading/Unloading	1.80	31	0	31
Freight Cost			264	264
Total Shipping-Facets	1.80	31	271	302
Shipping Costs-Structure--				
Freight Cost			1,250	1,250
Total Shipping-Structure	0.00	0	1,250	1,250
Facets Installation--				
Install Control System	2.04	42	0	42
Install Facet	8.04	164	0	164
Align Facet	8.04	164	0	164
Focus Adjustment	8.04	164	0	164
Manlift (13 Hrs)			260	260
Crane Rental (4 Hrs)			240	240
Total Facets Installation	26.16	534	500	1,034
Structure Installation--				
Labor	192.00	3,923	0	3,923
Wiring	16.00	327		327
Crane Rental (48 Hrs)			3,600	3,600
Total Structure Inst.	208.00	4,250	3,600	7,850
Control System Inst.			1,046	1,046
Installers Travel/Per Diem--				
Airfare (4 r/t tickets)			1,000	1,000
Per Diem/Trsp(24 ManDays)			2,400	2,400
Total Travel/Per Diem			3,400	3,400
Total Costs	1,247.27	22,037	28,857	50,894

Table 6.0-IV Specialty Items

Specialty Items-- Description	Estimate Basis	Qty Per Collector	Per Collector Cost @ Qty's 1 ea	50 ea	100 ea	1,000 ea
Azimuth Drive Motor	Quote	1	165	124	124	112
Elevation Drive Motor	Quote	1	213	152	152	137
PCA Screwjack	Quote	1	382	328	328	328
Bearing	Quote	2	82	76	76	76
Bearing	Quote	1	24	24	22	22
Coupling	Quote	2	143	109	109	109
Hinges	Quote	2	282	282	282	282
Limit Switches	Quote	6	462	294	294	294
Winch Safety Switch	Quote	1	122	78	78	78
Misc Hardware	Estimate	N/A	350	300	300	250
Total Specialty Items			2,225	1,767	1,765	1,688

Tracking Drives--

Annual Qty 50 Collectors	Screw-jack	Enginrng	Patterns	Tools	Total
Azimuth Tracking Drive	4,385	incl	incl	incl	4,385
Elevation Tracking Drive	2,580	210	210	95	3,095
Tracking Drives Totals	6,965	210	210	95	7,480

Annual Qty 100 Collectors	Screw-jack	Enginrng	Patterns	Tools	Total
Azimuth Tracking Drive	3,720	incl	incl	incl	3,720
Elevation Tracking Drive	2,480	105	105	48	2,738
Tracking Drives Totals	6,200	105	105	48	6,458

Annual Qty 1,000 Collectors	Screw-jack	Enginrng	Patterns	Tools	Total
Azimuth Tracking Drive	2,790	incl	incl	incl	2,790
Elevation Tracking Drive	2,356	11	11	5	2,383
Tracking Drives Totals	5,146	11	11	5	5,173

7.0 SUMMARY

In this section of the report the results of the faceted dish concentrator design are summarized, and recommendations are made for future work. Each of the five major technical sections - Trade-off Studies, Structure Design, Control System Design, Tracking Error Budget, and Production Cost Estimates - are summarized. Recommendations are made that address both detail elements of the design and overall structure considerations.

7.1 Trade-off Studies

The configuration of the faceted dish concentrator largely reflects the results of the trade-off studies that preceded design. Each of the studies is summarized below.

7.1.1 Facet Arrangement

Selection of the 2TOP facet arrangement was based on a comparative analysis with the 4INLINE arrangement. The analysis included comparison of structural weight, wind load effects, facet-to-structure interface, PCA-to-structure interface, and ease of fabrication. Other considerations included shear loads, axial loads, facet mounting facilities, and field installation and alignment. The determination was made to use the 2TOP arrangement because it exhibits greater stiffness, leading to a higher system resonant frequency and better tracking accuracy.

7.1.2 Parabolic vs. Spherical Facet Support Structure

Prior optical studies showed that the contour of the facet support structure had little effect on dish performance. The objective of this study was to identify a structure configuration that would accommodate elastically-formed and plastically-formed facets in the same facet f/D range. A comparison between parabolic and spherical dish structures showed that both had problems. A compromise contour was selected which is within the adjustment range of plastically-formed and elastically-formed facets while having little effect on optical performance. The compromise contour allows placement of the

facets in close proximity to the backup structure, thereby minimizing mounting pad off-sets and resulting structural deflections.

7.1.3 Focal Length

Prior studies showed that at dish f/D of about 0.6, optical efficiency is almost independent of dish contour. Structural design considerations assumed potentially greater significance. The drive system, in particular, is sensitive to load changes which could occur with focal length changes. In this study the effects on the drive system of spherical and parabolic support structure configuration, each with dish f/D ratios varying from 25 ft. to 34.5 ft., were examined. In the studies the impact of changing weight, center of gravity, drive inertia and drive spring weight within the limited focal length range was analyzed. It was concluded that varying the dish focal length between 25 ft. and 34.5 ft. has little impact on the drive system.

7.1.4 Windmill Option

Wind loads on dish structures can be reduced by allowing the structure to windmill, or feather, when at the stow position. In this study the availability of the windmill option was investigated for use with the faceted dish. The windmilling option is available only on drives that can backdrive. The elevation drive, for safety reasons, must be non-backdriving. The Winsmith azimuth drive is non-backdriving due to its high reduction ratio primary stage. Therefore, the windmilling option is not available in the faceted dish design. To minimize potential problems arising from power failure in high winds, the decision was made to provide the faceted dish with an uninterruptable power source.

7.1.5 Solar Walk-Off Protection

In this study methods were investigated to protect the structure from being damaged by the concentrated solar image in times of sun acquisiton, off-axis tracking or power loss. The most critical condition occurs when emergency off-sun tracking is necessary. This requires a high-speed capability in the elevation drive since, at high elevation angles, the azimuth drive contribution is slight. Consider-

ation was given to using the articulated PCA support structure in a dual role for walk-off protection. However, in this application the drive motor is too large to be practical. It was concluded that the elevation drive can readily provide walk-off protection since it can be run at twice its rated speed for a limited time period.

7.1.6 Tracking Error Considerations

The SOW defines the tracking error requirements for the structure (less facets) in terms of deflections and control system error. These were combined into an equivalent system pointing error. Several tracking control system alternatives were evaluated, under the ground rules that they would use existing, proven equipment; have compliant accuracy; and would be reasonable in cost. The studies resulted in the decision to use passive tracking control centered around an existing heliostat controller. A modified "bang-bang" motor drive configuration with axis-position sensor feedback was selected. This configuration yielded tracking errors somewhat greater than originally specified, but well within the modified requirements developed during the project.

7.2 Structure Design

The faceted dish concentrator is a kingpost type, elevation-over-azimuth tracking structure in which the facet support structure and the receiver-engine-generator assembly are balanced about the elevation axis. It is configured in compliance with the results of the trade-off studies made early in the project. The tracking structure employs triangulated space-frame technology to develop high stiffness-to-weight characteristics and acceptable pointing accuracies. After meeting deflection requirements, the design was checked for compliance with AISC codes for buckling and stress. Since the design is deflection-driven, stress levels throughout the structure are low.

The faceted dish structure is designed to comply with the requirement for a low-risk, near-term solar concentrator. It is made from standard structural steel shapes and is designed for ease of fabri-

cation and installation. Within shipping and field handling practicalities, parts are factory-assembled to reduce installation time. Field assembly of the structure requires only conventional material-handling equipment. A small truck crane (5-10 ton capacity) is adequate for placement of all parts with the possible exception of the transition section. If the transition can be shipped assembled, considerable field time will be saved. However, the present design requires a wide load permit for shipping and possibly a 15-20 ton crane for installing it. Facet mounts are readily accessed for ease of facet installation and alignment of the facets.

The drive system uses a proven azimuth drive built by Winsmith. It is a planocentric reducer with non-backdriving characteristics. It has adequate margin in overturning moment and torque limit loads for the faceted dish application. The elevation drive is a conventional linear ball screw actuator that has been customized to make it non-backdriving. Both the azimuth and elevation drives use one HP (rated) motors for input power. The drive pedestal is a stepped tubular kingpost designed to minimize deflections. The pedestal and azimuth drive can be conveniently factory-assembled and shipped to save field installation time.

The tracking structure, the drives and the pedestal (less facets and PCA) weigh about 12 pounds per square foot of facet area. The total collector, including facets and power conversion unit, weighs less than 16 pounds per square foot.

7.3 Tracking Control System

The tracking control system is designed to provide the specified system pointing accuracy at minimum cost using existing equipment wherever possible. The system consists of a central computer, a front end processor, drive motors and controllers for each axis, axis position encoders, and ancillary components including switches, alarm circuitry, etc. In a multiple collector field, the system components

are replicated on each collector with the exception of the central computer.

The control system employs passive tracking with modified "bang-bang" motor control and direct axis feedback. The drive control uses controllable frequency inverters to permit more accurate tracking than can be achieved with conventional methods.

7.4 Tracking Error Budget

Wind and dead-weight deflections as well as other values from the trade-off studies were used to develop the pointing error budget for the faceted dish structure. The estimated error, based on the final control system design using Polyspede controllers with axis encoders for position feedback, is about 1.19 mr, one sigma, in operating winds of 16.8 mph winds gusting to 27 mph. This is compatible with the accuracy requirements established during the project.

7.5 Cost Estimates

The estimated cost of the installed faceted dish (less facets and facet controls) in small quantity production (100 per year) is in the order of $2,300 per kW (electric). This estimate is conservative since it is based on installing only a single dish at each site. Installation costs would be significantly reduced as a result of installing multiple dishes on a given site. Also, the estimates are made on a prototype design and do not take into account any redesign for quantity manufacturing. It is reasonable to conclude that, with generational improvements and design for true production, the costs will be substantially reduced.

7.6 Recommendations

The design of the faceted dish solar concentrator meets the requirements and specifications of the SOW. However, some further effort on specific elements of the structure design could improve both the performance and the cost of the prototype as well as subsequent models. The general level of effort on each of the affected elements with recommended action is described below.

7.6.1 Transition

In the present design the center of gravity of the tracking structure is about 18 in. in front of, and 18 in. above, the elevation axis. This static imbalance causes a continuous change in gravity moment as a function of elevation angle with a gravity load reversal occurring at about 40 deg. elevation. The result is higher drive loads than originally anticipated. Although the drives are designed to comfortably handle these loads, it is possible that less costly drives could be used if the imbalance were eliminated. The present design of the transition will not accommodate any further improvement in the location of the center of gravity.

- **It is recommended that the transition design be reviewed and the design modified with the objective of reducing the static imbalance.**

- **Once this has been done, it is recommended that the drive requirements be re-evaluated.**

7.6.2 Tubes vs. Structural Shapes

The facet support structure is configured to be stiff and relatively lightweight using standard structural steel shapes. Nevertheless, the material content and the attendant cost of the structure may be greater than it has to be. Tubes are more efficient in cross section than equivalent structural shapes; thus, lighter weight tubes can supplant structural shapes, resulting in significant weight savings. The design decision was made to use shapes because the labor content in tube fabrication was believed too great to justify the weight savings.

- **With the better knowledge of the specific structure resulting from a completed design effort, it is recommended that the issue of tubes vs. structural shapes be re-examined for potential long-range cost savings in large quantity production.**

7.6.3 Pedestal

The initial pedestal design used a one-piece, 24-in. diameter standard pipe, flanged at each end for interfacing with the azimuth drive and the foundation, respectively. This approach was relatively inexpensive because it had a relatively small labor content; its stiffness-to-weight ratio was less than desired. In the present design, the pedestal is incrementally stepped from a 36-in. diameter base section to a 24-in. upper section. This configuration exhibits a significant increase in stiffness and reduction in weight, but its cost is high due to a substantial escalation in the labor content. Although the present design is satisfactory for the prototype dish, the mass production design must be simplified to reduce cost. One of the most promising configurations, considering function, cost and manufacturability, would employ a tapered tube similar to those used in light standards. This approach offers the labor cost saving advantages of the one-piece pedestal and the stiffness-to-weight ratio advantage of the stepped configuration.

- **It is recommended that the pedestal design be reviewed, and revised as applicable, with the objective of achieving production quantity cost savings.**

7.6.4 Elevation Drive

In the present design the elevation drive is a non-backdriving ball screw jack linear actuator. For compatibility with the "bang-bang" control system, a commercial screw jack has been customized to include a high-reduction input worm gear stage to develop the non-backdriving characteristics. The one-time costs for engineering, patterns and tools for the customized screw jack are high and have a significant impact on production quantity costs of the screw jack. The cost of the elevation drive could possibly be reduced by changing the elevation drive control to linear instead of "bang-bang". This would allow use of a power-off brake in conjunction with an off-the-shelf ball screw jack for the non-backdriving capability and thereby eliminate the customizing costs. This approach potentially has the additional advantages of reducing tracking control system error,

increasing elevation drive efficiency and reducing the size of the drive motor.

- **It is recommended that the elevation drive design be reviewed and redesigned, in conjunction with its control system, with the objective of reducing costs and improving system performance.**

7.6.5 Wind Test Data

The faceted dish was designed using wind tunnel data developed on solid-surface parabolic reflector models. No test data exists for faceted dishes nor for any solid-surface reflector with large voids in its surface. Any wind load reductions used in the design of the faceted dish attributable to the spaces between facets would be nothing more than a guess. Therefore, no credit was taken in the design for the voids. As a result, the design is conservative. If the faceted dish is to become a commercial reality, every effort must be made to reduce the loads since that is the best way to reduce the weight and cost of the structure.

- **It is recommended that the faceted dish be modeled in a wind tunnel to determine drag coefficients specifically applicable to this configuration.**

- **It is further recommended that the prototype dish, after construction, be instrumented to verify the wind tunnel data.**

7.7 Conclusions

The faceted dish concentrator structure is conservatively designed to ensure meeting or exceeding the performance specifications of the SOW. The design is in conformance with construction industry codes and with good commercial practice. It makes maximum use of off-the-shelf components and is readily fabricated with conventional tools and fixturing. The result is a low-risk, first-generation dish

structure that will first provide proof of performance of the concept and then serve as the building block for generational progress.

8.0 GLOSSARY

2TOP	A facet arrangement (see Figure 2.1-1)
4INLINE	A facet arrangement (see Figure 2.1-1)
10E08	Ten to the eighth power
AISC	American Institute of Steel Construction
bang-bang	A control system drive mode where full power is applied for short pulses to provide tracking motion
C	Celsius
CG	Center of gravity
DC	Direct Current
f/D	Focal length divided by diameter
FEP	Front End Processor, control system processor unit at the individual collector
FSS	Facet Support Structure
Ft-Lb	Foot Pounds
Hz	Hertz, cycles per second
In-Lb	Inch Pounds
JPL	Jet Propulsion Laboratory
ksi	Kips (1000 pounds) per square inch
kW	KiloWatts
L/r	Length divided by radius of gyration
Lb/sq. ft.	Pounds per square foot

LTV	Ling Temco Vought
m	Meters
MIT	Massachusetts Institute of Technology
mr	Milliradians
OS	Over Shoot
PCA	Power Conversion Assembly
psf	Pounds per square foot
RH	Relative Humidity
RMS	Root Mean Square
RPM	Revolutions per minute
RSS	Root Sum Square
SAIC	Science Applications International Corporation
SCD	Specification Control Drawing
SKI	Solar Kinetics, Inc.
SOW	Statement of Work
SPACE V	Structural Preprogrammed Analysis Capability for Engineers, a linear finite element analysis program
Winsmith	Peerless-Winsmith, Inc.
WGA	WG Associates

9.0 BIBLIOGRAPHY

1. T. R. Mancini, *Optical and Thermal Performance of a Faceted, Stretched-Membrane Dish Concentrator*, Dec. 1989.

2. *Stretched Membrane Facet Development by SAIC*, Scientific Applications International Corporation, San Diego, CA, SAND91-7008, Contract 42-9814A, June 1991.

3. P. T. Schertz, D. C. Brown, A. Connerth, *Stretched Membrane Facet Development by SKI*, Solar Kinetics, Inc., Dallas, TX, SAND91-7009, Contract 42-9814B, June 1991.

4. T. R. Mancini, "Faceted Dish Pointing Error Budget", Memorandum, April 13, 1990.

5. Werner H. Heller and Joseph S. Peters, *Development of a Low-Cost Drive Tracking Mechanism for Solar Heliostats*, Peerless-Winsmith, Inc., Feb. 1989.

6. *Wind Loading of Parabolic Antennas*, LTV Electrosystems, R&D Report G-3705.18.04A, Sept. 1970.

7. *SPACE V Users Manual*, Digital Analysis Consultants, Inc., 1983.

UNLIMITED DISTRIBUTION
INITIAL DISTRIBUTION

U.S. Department of Energy (5)
Forrestal Building
Code CE-314
1000 Independence Avenue, SW
Washington, DC 20585
Attn: M. Scheve
S. Gronich

U.S. Department of Energy (2)
Forrestal Building
Code CE-33
1000 Independence Avenue, SW
Washington, DC 20585
Attn: B. Annan

U.S. Department of Energy (3)
Albuquerque Operations Office
P.O. Box 5400
Albuquerque, NM 87115
Attn: C. Garcia
G. Tennyson
N. Lackey

U.S. Department of Energy
San Francisco Operations Office
1333 Broadway
Oakland, CA 94612
Attn: R. Hughey

AAI Corporation
P. O. Box 6787
Baltimore, MD 21204

Acurex Corporation (2)
555 Clyde Avenue
Mountain View, CA 94039
Attn: J. Schaefer
H. Dehne

Advanced Thermal Systems
7600 East Arapahoe
Suite 319
Englewood, CO 80112
Attn: D. Gorman

Arizona Public Service Company
P.O. Box 21666
Phoenix, AZ 85036
Attn: J. McGuirk

Arizona Solar Energy Office
Dept. of Commerce
1700 W. Washington, 5th Floor
Phoenix, AZ 85007
Attn: F. Mancini

Australian National University
Department of Engineering Physics
P. O. Box 4
Canberra ACT 2600 AUSTRALIA
Attn: S. Kaneff

Barber-Nichols Engineering
6325 West 55th Avenue
Arvada, CO 80002
Attn: R. Barber

Battelle Pacific Northwest
Laboratory (2)
P.O. Box 999
Richland, WA 99352
Attn: T. A. Williams
D. Brown

BDM Coporation
1801 Randolph Street
Albuquerque, NM 87106
Attn: W. Schwinkendorf

Bechtel National, Inc.
50 Beale Street
50/15 D8
P. O. Box 3965
San Francisco, CA 94106
Attn: P. DeLaquil

Black & Veatch Consulting
Engineers
P.O. Box 8405
Kansas City, MO 64114
Attn: J. C. Grosskreutz

Tom Brumleve
1512 Northgate Road
Walnut Creek, CA 94598

California Energy Commission
1516 Ninth Street, M-S 43
Sacramento, CA 95814
Attn: A. Jenkins

California Polytechnic University
Dept. of Mechanical Engineering
Pomona, CA 91768
Attn: W. Stine

California Public Utilities Com.
Resource Branch, Room 5198
455 Golden Gate Avenue
San Francisco, CA 94102
Attn: T. Thompson

Cummins Engine Co.
MC 60125
P. O. Box 3005
Columbus, IN 47202-3005
Attn: R. Kubo

Dan Ka
3905 South Mariposa
Englewood, CO 80110
Attn: D. Sallis

DLR
Pfaffenwaldring 38-40
7000 Stuttgart 80 WEST GERMANY
Attn: R. Buck

DSET
P. O. Box 1850
Black Canyon Stage I
Phoenix, AZ 85029
Attn: G. Zerlaut

Electric Power Research
Institute
P.O. Box 10412
Palo Alto, C[illegible] 94303
Attn: J. Sc[illegible]ffer

Engineering Perspectives
20 19th Avenue
San Francisco, CA 94121
Attn: John Doyle

Energy Technology Engr. Center
Rockwell International Corp.
P. O. Box 1449
Canoga Park, CA 91304
Attn: W. Bigelow

ENTECH, Inc.
P. O. Box 612246
DFW Airport, TX 75261
Attn: R. Walters

Florida Solar Energy Center
300 State Road 401
Cape Canaveral, FL 32920
Attn: Library

Ford Aerospace
Ford Road
Newport Beach, CA 92663
Attn: R. Babbe

Foster Wheeler Solar Development
Corporation (2)
12 Peach Tree Hill Road
Livingston, NJ 07039
Attn: M. Garber
R. Zoschak

Garrett Turbine Engine Co.
111 South 34th Street
P. O. Box 5217
Phoenix, AZ 85010
Attn: E. Strain

Georgia Power (2)
7 Solar Circle
Shenandoah, GA 30265
Attn: W. King

Harris Corporation (2)
Government and Aerospace
Systems Division
P. O. Box 9400
Melbourne, FL 32902
Attn: K. Schumacher

Industrial Solar Technologies
5775 West 52nd Avenue
Denver, CO 80212
Attn: R. Gee

Institute of Gas Technology
34245 State Street
Chicago, IL 60616
Attn: Library

ISEIR
951 Pershing Drive
Silver Spring, MD 20910
Attn: A. Frank

Jet Propulsion Laboratory
4800 Oak Grove Drive
Pasadena, CA 91109
Attn: M. Alper

LaJet Energy Company
P. O. Box 3599
Abilene, TX 79604
Attn: M. McGlaun

L'Garde, Inc. (2)
1555 Placentia Avenue
Newport Beach, CA 92663
Attn: M. Thomas
J. Williams

Lawrence Berkeley Laboratory
MS 90-2024
One Cyclotron Road
Berkeley, CA 94720
Attn: A. Hunt

Luz International (2)
924 Westwood Blvd.
Los Angeles, CA 90024
Attn: D. Kearney

3M-Energy Control Products (2)
207-1W 3M Center
St. Paul, MN 55144
Attn: R. Dahlen

Mechanical Technology, Inc. (2)
968 Albany Shaker Road
Latham, NY 12110
Attn: G. Dochat
J. Wagner

Meridian Corporation
4300 King Street
Alexandria, VA 22302
Attn: D. Kumar

NASA Lewis Research Center (4)
21000 Brook Park Road
Cleveland, OH 44135
Attn: R. Beremand 500-215
R. Evans 500-210
J. Savino 301-5
R. Corrigan 500-316

Nevada Power Co.
P. O. Box 230
Las Vegas, NV 89151
Attn: Mark Shank

Pacific Gas and Electric Company (2)
3400 Crow Canyon Road
San Ramon, CA 94526
Attn: G. Braun
J. Iannucci

Polydyne, Inc.
1900 S. Norfolk Street, Suite 209
San Mateo, CA 94403
Attn: P. Bos

Power Kinetics, Inc.
415 River Street
Troy, NY 12180-2822
Attn: W. Rogers

Renewable Energy Institute
1001 Connecticut Ave. NW
Suite 719
Washington, DC 20036
Attn: K. Porter

Rocketdyne Division
6633 Canoga Park Ave.
Canoga Park, CA 91304
Attn: W. Marlatt

San Diego Gas and Electric Company
P.O. Box 1831
San Diego, CA 92112
Attn: R. Figueroa

SCE
P. O. Box 800
Rosemead, CA 91770
Attn: P. Skvarna

Schlaich, Bergermann & Partner
Hohenzollernstr. 1
D - 7000 Stuttgart 1
West Germany
Attn: W. Schiel

Sci-Tech International
Advanced Alternative Energy
5673 W. Las Positas Blvd.,Suite 205
P.O. Box 5246
Pleasanton, CA 84566
Attn: U. Ortabasi

Science Applications International
Corporation (2)
10343 Roselle Street, Suite G
San Diego, CA 92121
Attn: K. Beninga

Solar Energy Research Institute (5)
1617 Cole Boulevard
Golden, CO 80401
Attn: B. Gupta
L. M. Murphy
G. Jorgensen
T. Wendelin
A. Lewandowski

Solar Kinetics, Inc. (2)
P.O. Box 540636
Dallas, TX 75354-0636
Attn: J. A. Hutchison
P. Schertz
D. Konnerth

Solar Power Engineering Company
P.O. Box 91
Morrison, CO 80465
Attn: H. Wroton

Solar Steam
P. O. Box 32
Fox Island, WA 98333
Attn: D. Wood

SPECO
P. O. Box 91
Morrison, CO 80465
Attn: W. Hart

SRS Technologies
990 Explorer Blvd., NW
Huntsville, AL 35806
Attn: R. Bradford

Stearns Catalytic Corporation
P.O. Box 5888
Denver, CO 80217
Attn: T. E. Olson

Stirling Thermal Motors
2841 Boardwalk
Ann Arbor, MI 48104
Attn: B. Ziph

Sun Power, Inc.
6 Byard Street
Athens, OH 45701
Attn: W. Beale

Tom Tracey
6922 South Adams Way
Littleton, CO 80122

United Solar Tech, Inc.
3434 Martin Way
Olympia, WA 98506
Attn: R. Kelley

University of Chicago
Enrico Fermi Institute
5640 Ellis Avenue
Chicago, IL 60637
Attn: J. O'Gallagher

University of Houston
Solar Energy Laboratory
4800 Calhoun
Houston, TX 77704
Attn: L. Vant-Hull

University of Utah
Mechanical and Industrial
Engineering
Salt Lake City, UT 84112
Attn: B. Boehm

Eric Weber
302 Caribbean Lane
Phoenix, AZ 85022

WG Associates
6607 Stonebrook Circle
Dallas, TX 75240
Attn: V. Goldberg

1840	R. E. Lochman
1846	D. H. Doughty
1846	C. S. Ashley
3141	S. A. Landenberger (5)
3145	Document Processing (8) For DOE/OSTI
3151	G. C. Claycomb
6000	V. L. Dugan, Actg.
6200	B. W. Marshall, Actg.
6210	J. T. Holmes, Actg.
6215	C. P. Cameron
6215	R. M. Houser
6216	C. E. Tyner
6216	L. Yellowhorse
6216	D. J. Alpert
6216	J. W. Grossman
6216	T. R. Mancini (30)
6216	J. E. Pacheco
6217	P. C. Klimas
6217	K. L. Linker
6217	R. B. Diver
6220	D. G. Schueler
6221	E. C. Boes
6223	G. J. Jones
6224	A. R. Mahoney
7470	J. L. Ledman
7476	F. P. Gerstle
7476	S. T. Reed
8523	R. C. Christman